UNIVERSITÀ DEGLI STUDI DI PADOVA

UNIVERSITA' DEGLI STUDI DI PADOVA

Dipartimento di Ingegneria Industriale DII

Corso di Laurea Magistrale in Ingegneria Energetica

Optimization of a heat pump for utilization of geothermal energy in district heating

Relatore: Prof.ssa Anna Stoppato

Laureando: Fabio Lucchetta

Matricola: 1154535

Anno Accademico 2018/2019

Project information

Danish title: Optimering af varmepumpe for udnyttelse af geotermisk energy i fjernvarme
English title: Optimization of a heat pump for utilization of geothermal energy in district heating

Author:

Fabio Lucchetta – student number 181847

Supervisors:

Brian Elmegaard, Head of Thermal Energy Section, Professor, Department of Mechanical Engineering

Torben Schmidt Ommen, Researcher, Section of Themral Energy, Department of Mechanical Engineering

Pernille Hartmund Jørgensen, Ph.D. Student, Section of Thermal Energy, Department of Mechanical Engineering

Cooperative companies: HOFOR

ECTS Points: 30

Project period: September 2018- February 2019

Acknowledgements

This project was prepared during a five months exchange semester in the context of the Erasmus Project thanks to an agreement between the Technical University of Denmark (DTU) and the Universitá degli Studi di Padova. It was carried out at DTU campus in Lyngby and it constitutes the final exam to achieve the MSc degree in Energy Engineering at the University of Padua. This project is worth 30 ECTS at DTU and counts for 18 CFU at the University of Padua.

I would like to thank my supervisor at DTU Brian Elmegaard, for his support and help throughout the development of this thesis and for the guidance in studying with accuracy and enthusiasm this exciting topic. I would also like to thank my co-supervisor Torben Ommen Schmidt for his presence and help in identifying the various goals of this project and keep pushing toward their achievement. Most of all I would like to thank co-supervisor Pernille Hartmund Jørgensen for her patience in listening to my numerous questions and for always being able to provide useful and targeted answers and suggestions that really fuelled my activity in this months.

I would like to thank my supervisor at the University of Padova Anna Stoppato for giving me the opportunity of living this great educational experience.

I must thank and dedicate this project to Eleonora, for being such an inspiration and source of strength in my life and in this difficult months and for always listening to me even when I had no right to ask for help. I thank my sister Silvia for being an incredible and irreplaceable presence and my parents for sustaining my efforts here in Copenhagen and being the best foundation of my life. I thank my grandma for being a reference and model in my whole life. I thank my aunt Wilma for obvious reasons.

I finally thank so much my roommate Andrea, for always being more than a true friend, Nicola, Sandro, Antonio e Alessandro for everything; I'm eventually grateful for the opportunity to meet incredible people here like Flo, Mitchell, Morgan, Iñaki, Lotte,Fredrik, Matthew.

Abstract

The aim of this thesis is to find the thermodynamically optimal configuration for a 5 MW heat pump using geothermal water available at 73°C as a heat source.
This heat pump is hence a relevant application in the context of utilization of geothermal energy for the district heating of Copenhagen.
The geothermal resource is located in Amager, south of Copenhagen, and that is the place in which this system is supposed to be built.

To study this energy system, different mathematical models of the system were developed using EES (Engineering Equation Solver). In the first part of the project, various 1-stage HPs configurations were analysed to get familiar with the modelling and to understand deeply how different types of components and their positioning in the system influence the performance of the system itself.
These configurations include different refrigerants (ammonia, propane and HFO's) and different compressors (screw and piston type); the performance of these alternative solutions were compared to identify the best one.
Real data for screw compressors were obtained from GEA's compressors selection software RTselect.

In the second part of the project more advanced 2-stages cycles were modelled with EES to see how much the system could be improved.
In order to find the best thermodynamic configuration the Pinch Method was applied. This method allows to realize the maximum internal heat recovery by integrating the heat streams that are present in the system.
Therefore, in the final part of the project, the Pinch Analysis was applied to the most performing configurations to see how far the improvement could be pushed and finally to find the thermodynamic upper limits of the system.

The results show that the best solution consists in using a direct heat exchanger followed by the series of two 2-stages HPs using ammonia as refrigerant. The COP that is achieved with this solution is 6.39. Encouraging results are also obtained with the same configuration using HFO's, as the highest COP with R-1243zf is 6.29. These results will be compared also considering the different compressors that are used and all the assumptions on which the results are based.
Finally, the results will be discussed to understand more clearly which is the winning technology and to analyse the efficiency of the pinch method on these kinds of system.

Contents

List of Figures

List of Tables

Nomenclature

Abbreviations

DH	District heating
HP	Heat pump
HFC	Hydrofluorocarbons
HFO	Hydrofluoroolefins
CHP	Combined heat and power plants
COP	Coefficient of performance
LFL	Lower flammability limit
hc	Heat of combustion
PEL	Permissible exposure limit
GWP	Global warming potential
ODP	Ozone depletion potential
GCA	Greater Copenhagen Area
SVAF	Experimental development of electric HPs in the Greater Copenhagen district heating
EUDP	Energy Technology Development and Demonstration Programme

TEWI	Total equivalent warming impact
DHEX	Direct heat exchanger
HEX	Heat exchanger
HEN	Heat exchanger network
HGS	Greater Copenhagen Geothermal Cooperation
PP	Pinch Point
GCC	Grand Composite Curve
CC	Composite curves

Symbols

$\dot{Q}$	Heat flowrate	$[kW]$
$\dot{W}$	Work	$[kW]$
T	Temperature	$[°C]$
p	Pressure	$[bar]$
h	Specific enthalpy	$\left[\frac{kJ}{kg}\right]$
$\dot{V}$	Volumetric flowrate	$\left[\frac{m^3}{s}\right]$

$\dot{m}$	Mass flowrate	$\left[\frac{kg}{s}\right]$
ρ	Density	$\left[\frac{kg}{m^3}\right]$
cp	Specific heat capacity	$\left[\frac{kJ}{kg * K}\right]$
$\dot{CP}$	Heating capacity flowrate	$\left[\frac{kW}{K}\right]$
η	Efficiency	$[-]$
k	Polytropic exponent	$[-]$
v	Built-in volume ratio	$[-]$
π	Built-in pressure ratio	$[-]$
r_p	Pressure ratio	$[-]$
x	Refrigerant quality	$[-]$
Δ	Difference	$[-]$

Chapter 1 Introduction

1.1 Project background

In the past years Denmark approved ambitious climate policies aimed at reducing the overall emissions of the energy sector by pursuing a sustainable energy supply based on renewable energies and on the extended utilization of electricity also in the heating sector.
To achieve these targets, the Danish energy sector will rely heavily on renewable energies (mainly wind, solar and biomass) to achieve a 100% renewable energy supply by 2050 [1].
In this scenario, electrically-driven large scale heat HPs are considered a winning technology to complete the transition to a carbon free heat supply system, in which the heat for the DH will not be provided by fossil fuel-based plants but by these electrically-driven systems.
These systems present some important advantages: they allow to utilize the power from renewable sources and at the same time they can be able to balance the electrical grid through a smart management of electricity and heat production; moreover, they can use waste heat and other low temperature heat sources that otherwise won't find any meaningful application.
With this in mind many projects related to large scale heat pumps were started in the recent years, like for example the SVAF project which initially aims to study the possibility to implement two 5 MW heat pumps using different heat sources (sea water and sewage water for one and geothermal water for the other). The heat pump using geothermal energy is the subject of my project, in which an analysis of this system will be conducted in order to find an optimal solution for the heat pump itself.
To achieve this target, a mathematical model will be created to describe the system and to find out the best choices regarding components and operating conditions of the HP; my personal expectation is to be able to provide results that will help to design a performing and effective system that will find a real application in the following years.
The opportunity to study a project of this size and relevance makes me feel really motivated to do my best and to give my contribution.

1.1.1 The District Heating System of Copenhagen

The District heating system of the city of Copenhagen has been developed for nearly the past 100 years, and today it provides heat for more than half a million inhabitants of the city.
It is part of the Greater Copenhagen district heating system, which supplies the metropolitan area with heat coming from four combined heat and power plants (CHP), three waste management plants and 40 back up boiler plants in the region [2].
A district heating system is a very environmentally-friendly way to provide heat, giving the possibility to substitute the individual domestic heating systems with a centralized system in which it's much easier to control the emission of pollutants.
The main companies that operate in the Greater Copenhagen Area are VEKS, CTR, Vestforbrænding and HOFOR and the area that they cover is distributed as indicated in the following figure.
The first three own the 180 km of hot water transport system while HOFOR controls a steam system that will be replaced by hot water DH before 2022 [3].
The system supplies a total area of 75 milions m^2, providing 30000 TJ per year.
Another interesting fact is that 99% of the buildings belonging to the two largest municipalities (Copenhagen and Frederiksberg) are heated by the district heating, making the city one of the most sustainable cities in the world [3].

Figure 1.1– The district heating in Greater Copenhagen [1]

The biggest input for the development of the system came from the oil crisis in the 1970s, which gave life to a smart and far-sighted energy plan made by municipalities and energy companies.
This plan began in Denmark with the Heat Supply Act that was approved in 1979. As for the city of Copenhagen, the official step toward this efficient and sustainable direction came with the Heat Plan Copenhagen in 1984 [1].
Therefore, following these acts, the expansion of the system was fueled by many positive factors and more recently, the conservation of the environment has become one of the most important.
The hints related to the damage produced by human activities toward the environment have become more and more evident and nowadays all the most advanced countries in the world have already started many actions in order to delay as much as possible the negative effects of the ill-advised treatment of the environment.
Denmark was already one of the leading countries in this process, but the government together with the energy companies keeps pushing toward sustainability; as a proof of that, Copenhagen municipality has set the goal of reaching a CO_2 free district heating system by 2025 [1].
This means that all the fossil fuels that are used in CHP plants and incinerators have to be somehow replaced.
A big part in this transition process will rely on biomass, but later on it is expected that large scale HPs together with geothermal energy and solar heat will complete this transition.
This is the reason why a lot of research has been carried on about the integration of large scale heat pumps in the district heating system.
Considering the topic of this project, the most important study related to HPs using geothermal water as heat source is the SVAF project.

1.1.2 The geothermal resource

Before introducing the SVAF project, it is interesting to describe briefly the geothermal energy source that will be used for this application and that already has been used for the district heating in Copenhagen.
The geothermal resource is located in Amager, south of Copenhagen, where in 2000 HGS made a seismic survey both on and offshore [4].
As a result of this survey in the following years two 2.6 km deep geothermal wells were drilled and a geothermal demonstration plant was commissioned in 2005 [4].
The plant is located near the Amager CHP. It produces geothermal energy from these wells, where the water is available at 73 °C and is pumped by a 700 kW electrical submersible pump. The water is then cooled down to 17 °C in the heat exchanging section of the plant and then injected back by another pump [4].
The existing plant provides up to 27 MW of DH, of which 14 are coming from the geothermal reserve and 13 from the steam that serves the absorption heat pumps [4].

Figure 1.2– The geothermal plant in Amager [4]

Considering all the licensed area where the reserves are situated, three large reservoirs have been individuated.
The total amount of geothermal energy that was estimated in 2008 is more than 60000 PJ, which means that if the district heating system will proceed with an usage rate of 30-40 PJ per year from the area, the reserves could last thousands of years [4].
This numbers confirm that this natural heat source could be profitably used also to fuel the integration of large scale HPs in the DH of the city.

1.1.3 The SVAF project

The SVAF (in Danish Store Varmepumper Til Fjernvarme) is a project funded by EUDP whose goal is to study first and realize secondly the possibility of using large electric heat pumps for district heating to speed up the sustainable transition that was mentioned above.
This project, that sees the collaboration of different energy companies and universities, is going to be carried out in 3 phases [5]:

- Phase 1 (until 2016): two different large scale heat pumps (5 MW each) have been studied as far as designing concepts and development of test programs. One HP will use a geothermal energy source situated at Amager, while the second one will use low temperature heat sources (sea and sewage water).
- Phase 2 (2016-2021) : the results will be analyzed and used for the detailed design and construction of two prototypes to verify the real behavior and operation of the two systems.
- Phase 3 (2021-future): Actual operation of large scale HPs in the GCA.

These systems will be useful to investigate the possibility of upscaling the size of the HPs to reach facilities able to provide heat in the order of 50-100 MW.
For the purposes of this project the most relevant part of the phase 1 SVAF final report that was submitted at the beginning of 2016 is the one related to the design and analysis of the configuration for the HP situated at Amager and using geothermal water as heat source.

For this system a two-stage hybrid configuration had been designed and analyzed; this kind of system uses a mixture of ammonia and water that is carried through an absorption cycle in order to operate with lower differential pressures and consequently better energy efficiency [6].
Two traditional ammonia compressors are also part of the configuration as seen in the scheme below.
A direct water/water heat exchanger is used in the initial part of the system to take advantage of the hot geothermal water that is available at 73° C to preheat the water returning back from the DH at 50 °C.
This systems allows to reach a high overall COP of equal to 6.3 while providing 7.1 MW of Heating capacity, of which around 5 are obtained at the absorber while the remaining 2 at the direct heat exchanger [6].

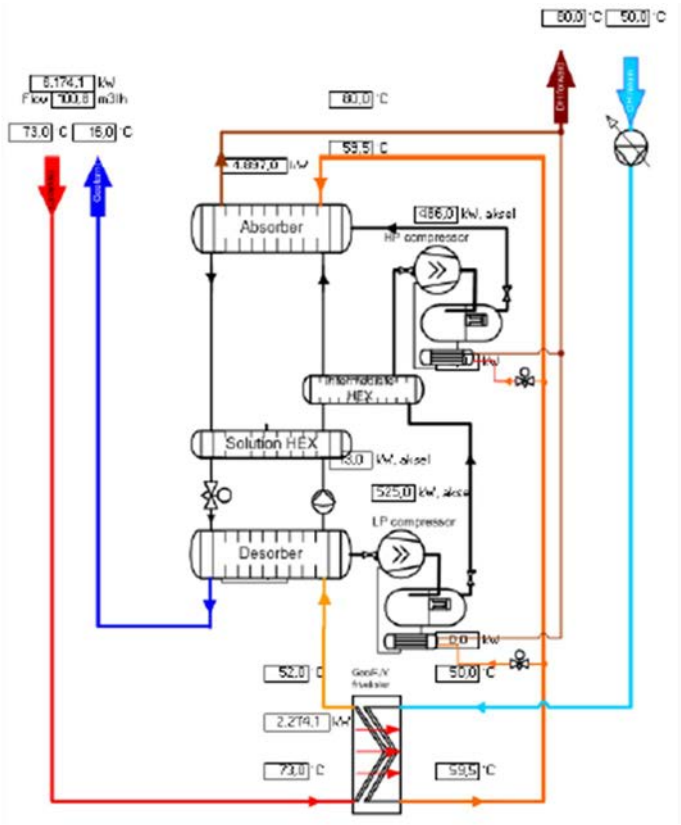

Figure 1.3– Hybrid HP configuration [6]

This choice was justified by various advantages [6]:

- The high efficiency of the system, theoretically higher than a traditional HP solution.
- An easier implementation in the system due to the absence of fixed intermediate pressures as it would be in a system with multiple HPs,
- The lower operating pressures that give more flexibility in the components selection and operation.
- The possibility of increasing the temperatures of the DH water.

However also some disadvantages were considered, like:

- The bigger dimensions of the system
- Higher investment costs
- The fact that this technology is exclusively owned by a Norwegian company and also that the heat exchanger must be designed in a precise way that could make the system more complicated or expensive.

Even if the expectation was that the hybrid configuration could be more efficient and attractive, further test programs showed results that were worse than expected, making it meaningful to investigate again the traditional solutions.
Because of that, in the phase 2 of the SVAF project an alternative solution was presented; this design consists of a multiple HPs system with a direct heat exchanger that operates with a COP of 6.1 with the two HPs having respectively COP equal to 4.4 and 4.6. [7]

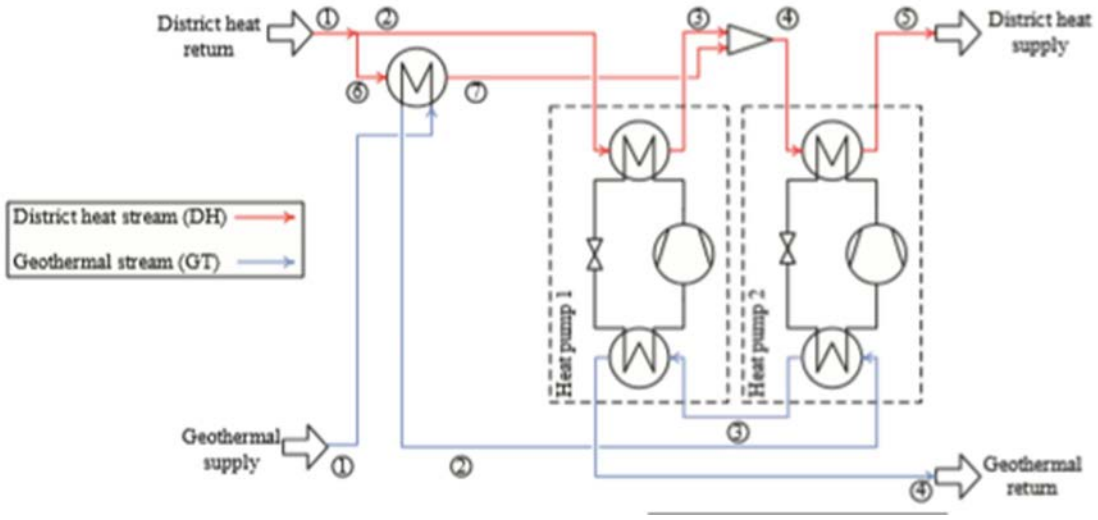

Figure 1.4– Multiple HPs with DHEX configuration [7].

In this project in fact I will present the results obtained with traditional vapour compression cycles, and possibly a useful comparison will emerge from this work.

1.2 Problem statement

This project corresponds to an optimization problem, in which as mentioned above the target is to find out the optimal design options and operating conditions for a heat pump system that is meant to provide 5 MW of heat supply to the DH of Greater Copenhagen. That's exactly the main point of this project: Which is the optimal heat pump configuration in order to connect the energy of the geothermal water to the demand of the district heating system? Which refrigerant should be used as the best operating fluid for this application? Which components will be the most suitable for the chosen

configuration? Which COP (Coefficient Of Performance) can be obtained for this system using the Pinch Analysis method to identify the most performing HEN (heat exchanger network)? So, in other words, will this method be proved to be an effective way of analyzing such systems?

1.3 Task and Methods

This project is based on the software EES (Engineer Equation Solver) which allows to study these kinds of energy systems in a simple and yet very effective way.
The main concept and technical method that is used to analyse the case study is the pinch analysis method. This well-established method permits to study a thermodynamic system in order to reach the best possible integration of the heat streams that exist in the system.
Another useful tool is the RTselect (GEA's compressors selection software) which gives the possibility to collect data related to the working conditions of real compressors so that they can be used in EES to produce a more accurate model.
Basically, this heat pump system will have to provide the heat required to increase the temperature of the DH water from 50°C to 80°C. Since this temperature glide and the power of the system are quite large, the system will need a certain degree of complexity, so it will include various hot and cold streams at different temperature levels and the related heat exchangers that can be integrated to improve the overall performance of the system.
When the system is complex, it's not immediate to identify the best HEN, but this is possible by applying a rigorous pinch analysis to the system.
Therefore, the main tasks that I faced step by step are the following:

- Acquire a good confidence with the modelling of heat pump systems through EES
- Re-establish a deep knowledge of the concepts related to the pinch analysis method
- Learn to implement the pinch analysis method with EES
- Apply the method to the actual system that is being studied
- Study and analyse through EES different and more advanced configurations to look for possible improvements of the system itself
- Simulate the operation of the system with EES to obtain and discuss the results that will provide the final solution of this optimization problem
- Identify and build the HEN (Heat Exchanger Network) reaching the highest COP
- Consider and discuss in a proper way the implications of the obtained solution to verify the effectiveness of the method and to investigate the possible application of it in the new actual system.

Chapter 2 Heat pumps

2.1 Heat pump

A heat pump is a machine that is able to transfer heat from a hot source at a certain temperature T_1 to a heat sink at a higher temperature T_2 by means of an external work usually provided by an electrically driven compressor.
This is of course accordingly to the second law of thermodynamics, for which Clausius' formulation states that heat cannot be transferred from a colder to a warmer place without some additional external work [8].

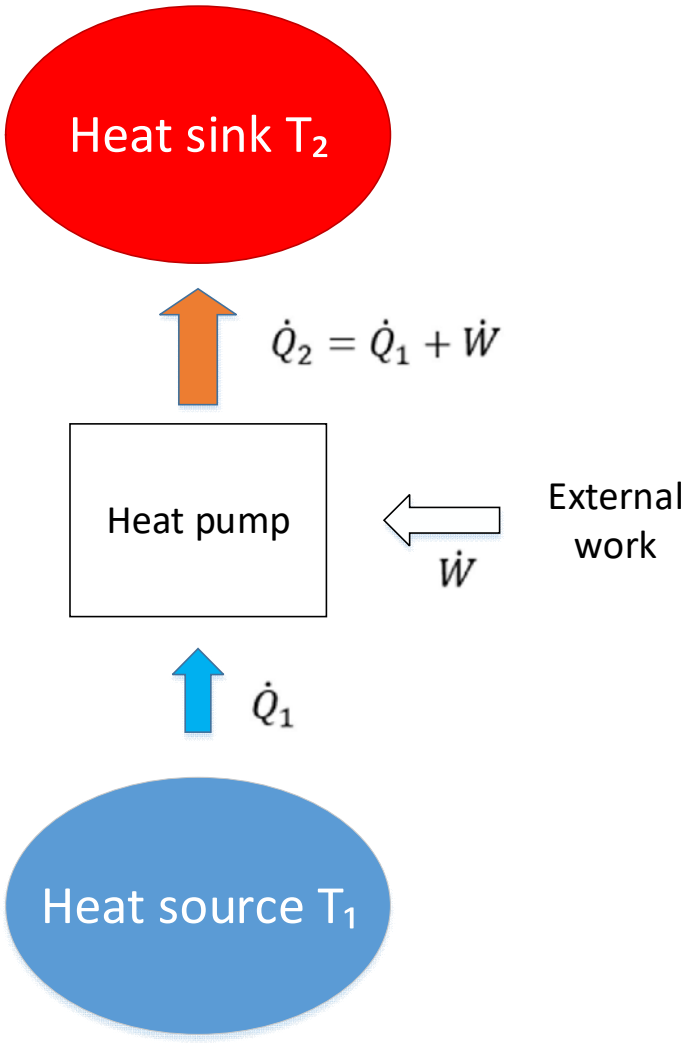

Figure 2.1– HP thermodynamic operating principle

As seen in the above picture, the useful effect is the heat obtained at high temperature $\dot{Q}_2$, while the required work is $\dot{W}$ and usually corresponds to the electricity used to drive a compressor or to the mechanical power delivered by the compressor shaft. In this thesis the required work will always refer to the mechanical power of the compressor shaft.
Having said this, it is possible to understand that the efficiency of such a machine would be defined as the ratio between the desired effect and the required work; and that is in fact the definition of the *COP* (Coefficient of Performance), which is the common indicator of this efficiency:

$$COP = \frac{\dot{Q}_2}{\dot{W}} \tag{2.1}$$

In the most basic heat pump applications the attainable COP is usually between 3 and 4.
It is very interesting though to compare this coefficient with the "thermodynamic limit" related to the HP application, that corresponds to the efficiency of a Carnot inversed cycle operating between the temperatures T_2 and T_1, and is a function of only the two temperatures:

$$COP_{Carnot} = \frac{T_2}{T_2 - T_1} \tag{2.2}$$

Where, as mentioned before, T_2 is the absolute temperature of the heat sink while T_1 is the absolute temperature of the heat source.
It is already easy to understand that the closer the two temperatures are, the higher the resulting COP will be, so it is easier to design an efficient HP if the heat source is at a high temperature.
The consequence of this is that a Carnot efficiency can be defined to compare the two previously defined efficiencies:

$$\eta_{Carnot} = \frac{COP}{COP_{Carnot}} \tag{2.3}$$

Another relevant parameter that can be used to characterize the performance of a heat pump is the SPF (seasonal performance factor), that is defined as follows [9]:

$$SPF = \frac{\sum Q_2}{\sum W} \tag{2.4}$$

In which $\sum Q_2$ is the sum of all the heat that has been obtained in a certain time, for example one year, and $\sum W$ is the sum of all the energy consumption associated with the operation of the heat pump for the same period of time.
This parameter can be useful to evaluate the overall performance of a heat pump in a certain period of time and it allows to take into account all the energy expenses connected to the operation of the whole system.

In this project the objective is to maximize the COP to obtain the best design conditions for the system so this parameter won't be used. It would become more interesting in a second phase of the design of the heat pump when economic evaluations can be made.

2.2 The vapour compression cycle

The traditional technology used for a HP is the vapour compression cycle.

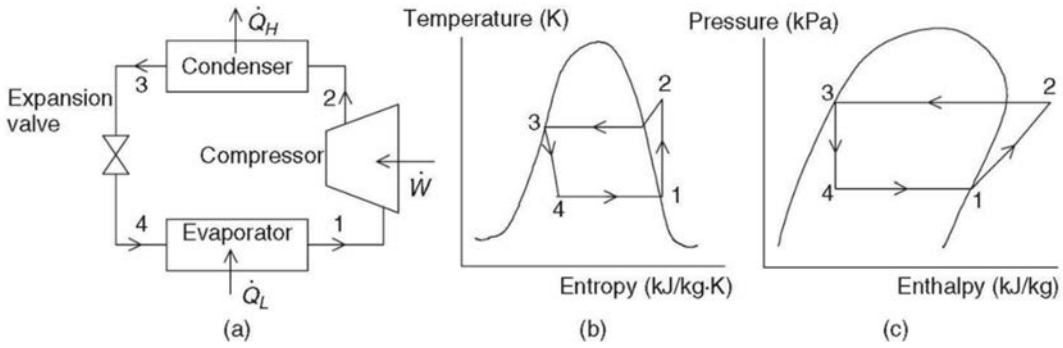

Figure 2.2– HP cycle and components [10]

As it can be seen in the figure above, in this ideal thermodynamic cycle the "refrigerant" fluid is carried through a closed cycle in which it undergoes four transformations delivered by the four main components of the cycle.

From point 1 the gas refrigerant enters the compressor and it is isentropically compressed to the high pressure of the cycle whose value is related to the condensing temperature of the same.

Subsequently the hot and compressed gas rejects heat at constant pressure at the condenser going through a phase changing process that ends when it becomes saturated liquid (point 3).

Then the liquid refrigerant expands at constant enthalpy in an expansion device to go back at the low pressure section of the cycle, where it is heated up by the heat source and it evaporates at constant temperature to reach point 1.

The COP of the cycle is calculated by:

$$COP = \frac{\dot{Q}_H}{\dot{W}} = \frac{h_2 - h_3}{h_2 - h_1} \tag{2.5}$$

2.3 The real cycle and possible improvements

Below a *p-h* diagram related to a basic HP cycle is presented.
The main difference between a real cycle and an ideal one is in the compression process; in fact the compressor is unable to produce an isentropic compression; so the inefficiencies of the compression process will be evaluated with an indicator, the isentropic efficiency.

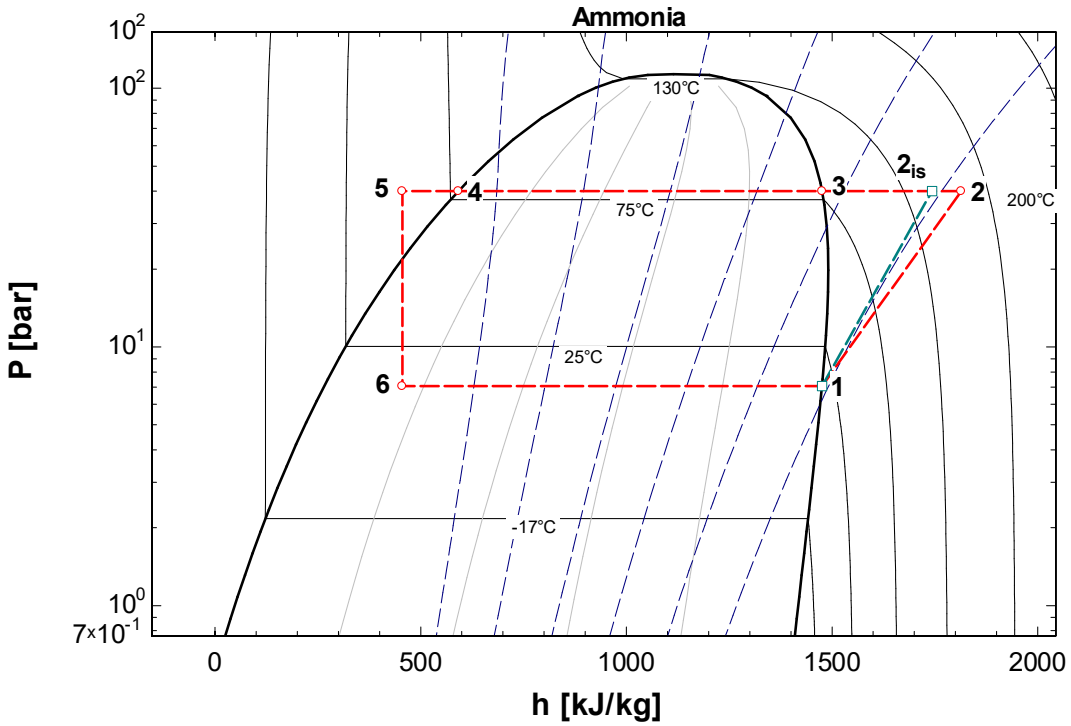

Figure 2.3– p-h diagram for a 1-stage real HP cycle

The isentropic efficiency indicates the ratio between the ideal work required for the compression and the real one, that will be larger, causing a decrease in the COP of the cycle.

$$\eta_{is} = \frac{\dot{W}_{ideal}}{\dot{W}} = \frac{h_{2is} - h_1}{h_2 - h_1} \tag{2.6}$$

The isentropic efficiency depends on the type of compressor that is used and on its operating conditions, as it will be understood more clearly in the next chapter.
So one first measure to have a high COP is to use compressors operating with high isentropic efficiency; however, other actions can be taken to obtain the same goal.
For HP cycles, in which the positive effect is the heating rejection at the condenser, a method to increase it is to cool down the saturated liquid after the condenser.

In this way some heat at lower temperature can be used, bringing some benefit to the overall performance of the cycle.
In particular the improvement can be calculated as follows (expressed in %/ °C of subcooling) [11]:

$$y = \left(\frac{h_2 - h_5}{h_2 - h_4} - 1\right) * \frac{100}{t_3 - t_5} \tag{2.7}$$

When the temperature lift, and subsequently the pressure lift, is large enough (indicatively when $T_{cond} - T_{ev} > 50°C$) it is interesting to consider the possibility of designing a two-stage cycle, in which the compression work is splitted between two smaller compressors [12].
A 2-stage cycle is presented below; it´s important to notice that this cycle includes additional components that will be explained in detail in the next chapter like the oil separators after the compressors, the open intercooler between the stages and the low stage desuperheater.

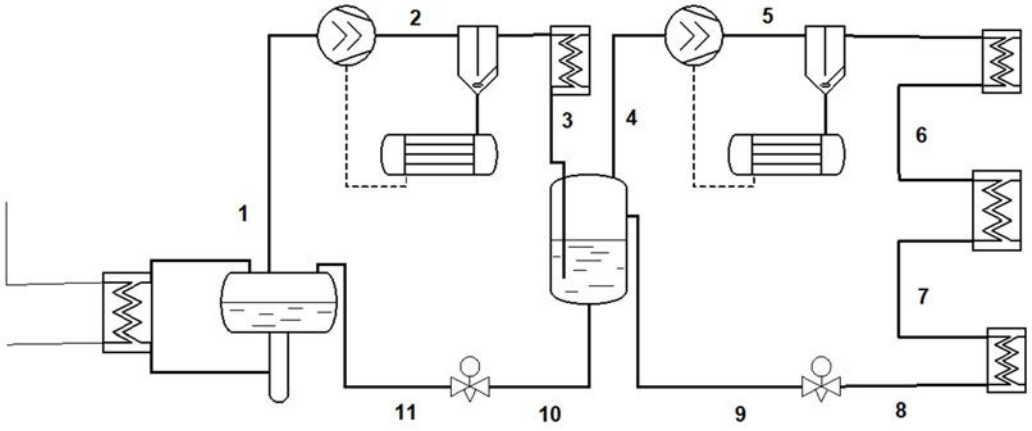

Figure 2.4– HP 2-stage cycle configuration

If only one compressor is used to obtain this pressure lift there will be two undesired effects:

- A degradation of the isentropic efficiency as it will be clear from the equations of the isentropic efficiency in the next chapter
- A consequent high discharge temperature of the refrigerant that causes troubles with the compressor cooling, which is necessary to avoid big thermal and mechanical stresses to the components.

These effects emerge clearly from the p-h diagram for the 2-stage ammonia heat pump cycle that is presented below.

Considering how the compressor efficiency influences the line of the compression process, the benefit that is given by this design is bigger than it could be guessed from the ideal case.

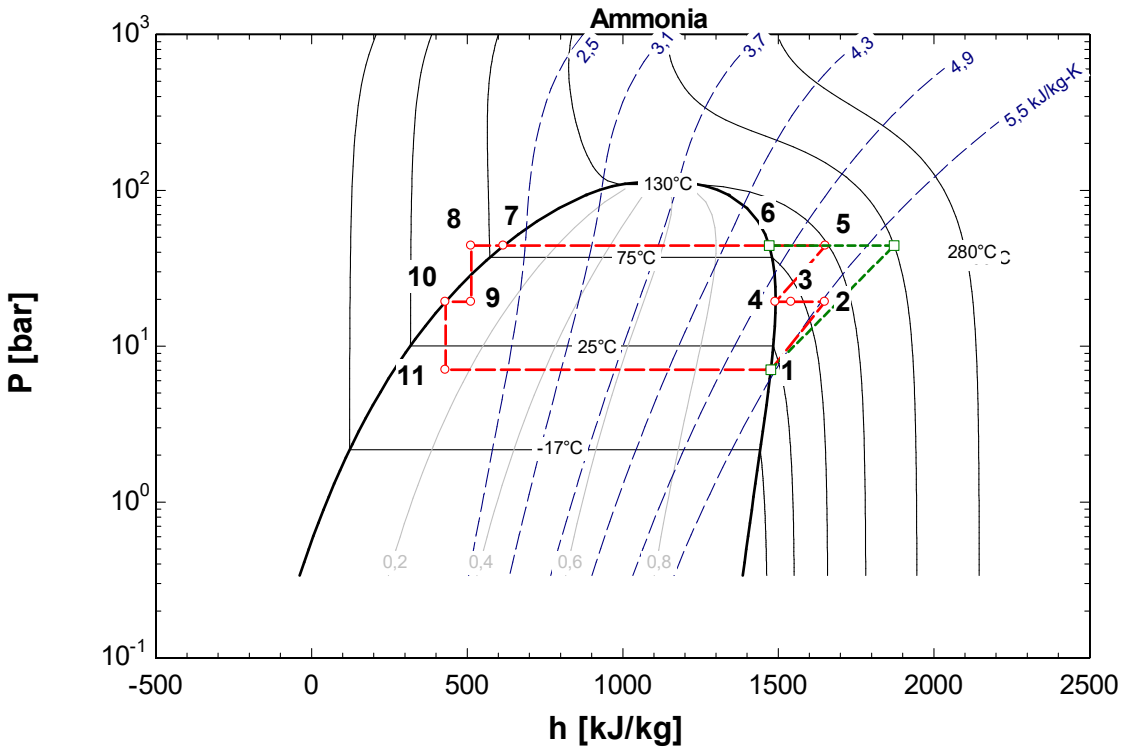

Figure 2.5– p-h diagram for a 2-stage ammonia cycle

Instead, using this solution is possible to divide the compression work and reduce the disadvantages related to the large pressure lift.
The COP for this configuration is given by:

$$COP = \frac{\dot{Q}_1}{\dot{W}_1 + \dot{W}_2} = \frac{h_5 - h_8}{(h_2 - h_1) + (h_5 - h_4)} \tag{2.8}$$

Chapter 3 Components

3.1 Refrigerants

The selection of the working fluid of the cycle is always an important part of the design of an inversed cycle.
The requirements that a refrigerant must fulfill are many and are related not only to chemical and thermal properties but also to health, safety and environmental characteristics; the relevance of these last aspects has increased a lot in the past thirty years because of the threats of global warming and ozone layer depletion.
Many refrigerants with high GWP (Global Warming Potential) and ODP (Ozone Depletion Potential) like the CFCs and HCFCs have been indeed banned in the past years and to substitute them the two main solutions that are being studied are natural refrigerants (NH_3 CO_2) and new synthetic low GWP refrigerants like HFOs.
In general, a refrigerant should be stable and inert in the system, in order to avoid any kind of reactions and modifications of its structure; besides that it should have favorable thermodynamic and transport properties and more importantly these properties must be suitable for the desired application [11]. For example when dealing with a heat pump system that delivers heat at 80 °C, the condensing temperature will be somewhere close to this value, so a refrigerant should have a critical temperature that is higher, so that is it possible to operate with a subcritical cycle.
Other characteristics that can make one refrigerant preferable are, among others, the cost, the mixing properties with the oils that are used in the compressors, the ease in detecting leakages.
However, as mentioned before, safety and environmental characteristics are becoming more and more relevant, so the focus will now be put in describing the indicators that allow to classify the refrigerants according to these properties.
The safety classification of refrigerants that was defined by the ASHRAE Standard 34 distinguish four classes based on flammability properties and two classes based on toxicity properties [13], as indicated in the next table.

Table 3.1 – Safety classification of refrigerants

	A: Low toxicity Permissible Exposure Limit PEL > 400 ppm	**B: High toxicity Permissible Exposure Limit PEL < 400 ppm**
1: Non flammable No flame propagation	A1: CFC, HCFC, most HFCs	B1: rarely used
2L: Mildly flammable Same as class 2 but with burning velocity < 10 cm/s	A2L: Most low GWP HFC	B2L: Ammonia
2: Lower flammability LFL>010kg/m^3 hc < 19MJ/kg	A2: R152a	B2: rarely used
3: Higher flammability LFL<010kg/m^3 hc > 19MJ/kg	A3: Hydrocarbons	B3: /

As far as the impact of a refrigerant to global warming, an indicator called TEWI was developed to take into account both the direct effect of the release of these products into the atmosphere and the indirect effect of the production of the electricity that is consumed in the systems that use refrigerants [13].
This parameter can be calculated as follows:

$$TEWI = X * GWP + \alpha_{CO_2} * L * E \quad (3.1)$$

Where:

- X is the quantity of refrigerant that is released into the atmosphere [kg]
- GWP is the global warming potential associated to the refrigerant
- α_{CO_2} is the mass of carbon dioxide that is emitted for kJ of energy produced
- L is the operation time of the system
- E is the energy per unit of time that is consumed by the system

3.1.1 History of refrigerants

Refrigerants have existed since the beginning of mechanical refrigeration, more than 150 years ago; at that point the only criteria that was used to select a fluid was that it was able to produce cooling, so no interest was put into efficiency and safety properties. The second generation started when the chemical industry became able to synthesize stable and safe substances with good thermodynamic properties as the CFC´s (Chlorofluorocarbons) and HCFC´s (Hydrochlorofluorocarbons) [14].
The problems with these substances were related to the high values of GWP but most of all of ODP; when the scientists discovered that these substances containing chlorine enhanced the ozone layer destruction, a new protocol was designed and agreed in Montreal in 1987 to determine the phase out first and the ban after of CFCs and HCFCs [15].
Therefore, these refrigerants were substituted by HFC´s (Hydrofluorocarbons) that don't contain Cl and consequently produce no damage to the ozone layer.

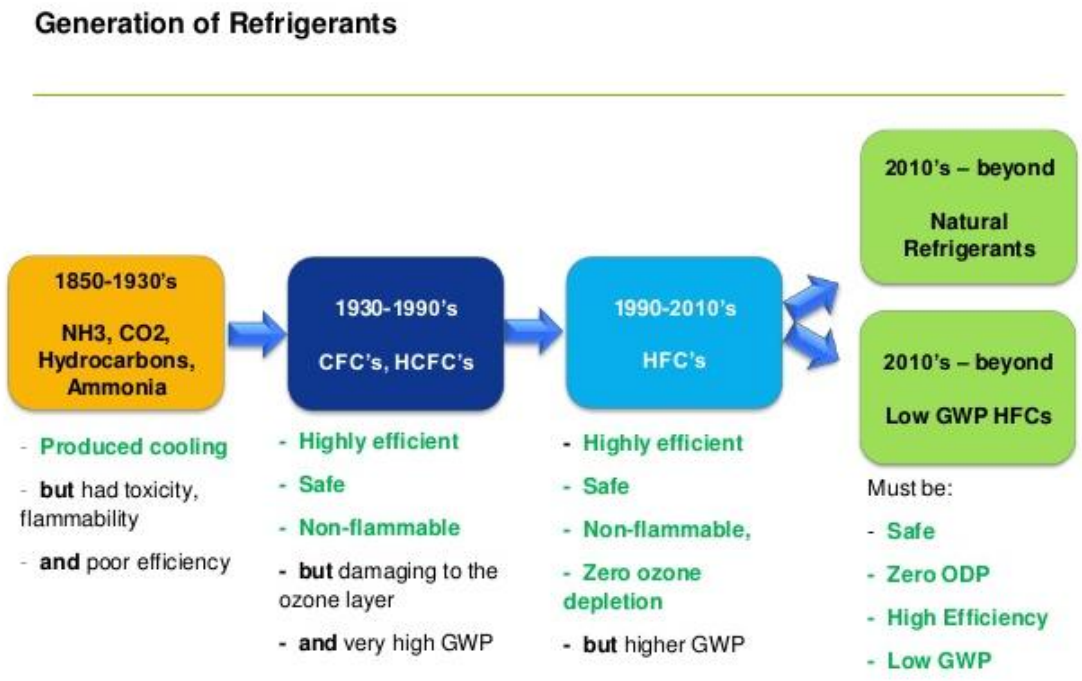

Figure 3.1– Generations of refrigerants [16]

However, more recently a lot of attention was pointed at the GWP of refrigerants, since the limitation of the global warming has become one of the most important environmental challenge of the modern era. Because of that, new international treaties like the Kyoto protocol, the EU F-gas Regulation and the Kigali Amendment of the Montreal protocol were signed to start the phase out of HFC's in the following years.

These new regulations have forced companies to study and test new low GWP refrigerants, like the HFOs or to investigate the possibility of using natural refrigerants, like ammonia, carbon dioxide or hydrocarbons to substitute the HFCs.

Consequently, great attention is now put into trying to identify the best solutions to respect the new regulations, and also in this project different alternatives are studied to verify which paths could be the more successful in the following years.
Now a deeper description of the main groups and types of refrigerant will be conducted, keeping in mind the application for which they are required, that is the considered heat pump system.

3.1.2 Ammonia

Ammonia (NH_3) is a natural refrigerant, hence with zero GWP or ODP.
However, it is toxic in low concentrations and flammable so it brings some risks that make it difficult to use it in places where it could get in contact with many people. Fortunately, its smell is really strong and recognizable so it has a kind of intrinsic alarm system that can prevent people from breathing it without realizing the danger.
Moreover, it must be noticed that ammonia is not compatible with copper, so the structure of the system has to be built considering this [13].
Nonetheless it has good thermodynamic properties like a high critical temperature (132.3°C at a pressure of 113.3 bar), large heat of vaporization, a high volumetric refrigerating effect and an effective heat transfer so its use is very interesting for safer and closed applications like for example large heat pumps.
It is a high-pressure working fluid so the components also have to withstand this aspect.

3.1.3 HFCs

HFC's are halogenated hydrocarbons that have successfully replaced great part of the CFCs and HCFC's like R12, R11 and R22 that were the most used at the beginning of the 90s. In particular for heat pumps R22 ($\mathbf{CHClF_2}$) was used but it has been nearly completely replaced by mixtures like R-404A, R-407C and R-410A and by R134a, that is a pure fluid.
R-410A is a mixture of R-32 and R-125 that has zero ODP and is not flammable or toxic but it displays a high value of GWP (2088), so it is going to be phased out in the near future **[17]**. It is used mainly in small to medium heat pump applications with low desired temperatures **[**18**]**.
The best candidates for replacing it are low GWP fluids like natural refrigerants, HFO's and R-32 that is a component of R-410 A but has a lower GWP. R134a is used for medium to large heat pump systems; it has a very high efficiency but lower compared to ammonia [18].

3.1.4 Hydrocarbons

HCs can be used as refrigerants and have small ODP and GWP so they could be used as replacements for HFCs. In particular, propane (R-290), butane (R-600) and isobutene (R600a) could find application instead of R134a in heat pump systems at high temperature.
One barrier to the use of these fluids is that they are really flammable and explosive [18].

3.1.5 HFOs

The hydrofluoroolefins are quite a recent class of refrigerants that could substitute the HFC due to their much lower GWP (<1).
This characteristic comes from the fact that these molecules are unsaturated, which means that they have at least one double bond [19].
They are however quite new and expensive so there is some resistance in using them largely and some of them are still in the development stage.
The most known are R-1234yf, R-1234ze(E), R-1234ye(Z), R-1243zf.
R-1234yf has shown similar performances when compared to R-410A, but it requires much bigger units to achieve this target.
It is also suitable as a drop-in refrigerant for R-134a.
HFO-1234ze(E) and HFO-1233zd(E) are used in chillers while HFO-1336mzz could be interesting for high temperature heat pumps [17].

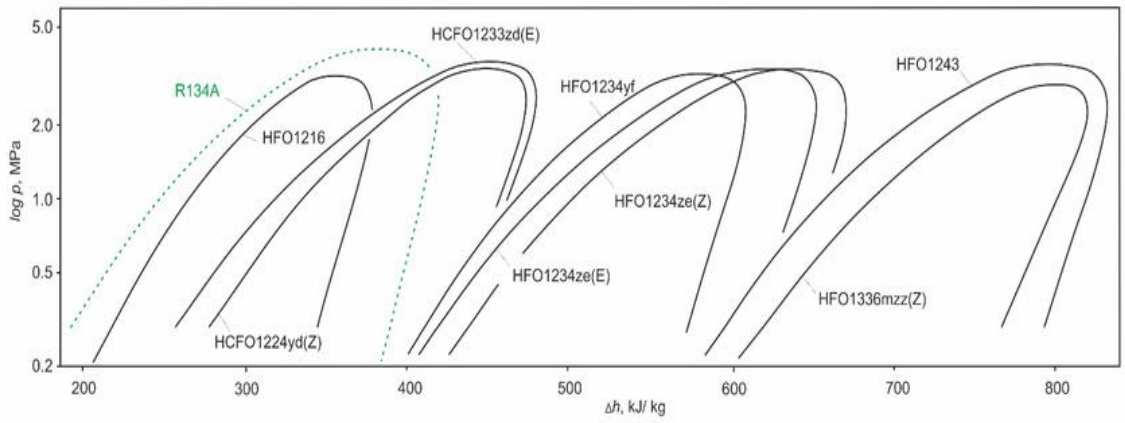

Figure 3.2– Comparison between p-h curves of R-134a and different HFOs [20].

3.2 Compressors

Compressors are crucial components in the operation of inverse cycles, as their behavior can importantly affect the efficiency of the whole system.
They can be of classified in two main categories depending on the working principle [11]:

- Positive displacement compressors like the piston type compressors, the screw compressors, the scroll compressors and the rotary compressors in which the compression work is obtained by a gradually decreasing volume.
- Dynamic compressors that are represented by the turbo compressors, in which the compression work derives from the change of the gas speed performed in the rotating impeller and in the diffuser

The choice of the compressor depends on many characteristics of the system, first its size. Some compressors like the scroll or rotary are used in small size applications, while screw, reciprocating and turbo compressors find application in larger systems.
As a consequence of that, these last three will be described more in detail.
Compressor can be classified based on the design of the drive motor arrangement in "open" or "hermetic": the first type requires a shaft seal, while for hermetic and semihermetic compressors the drive motor and the compressor are built in the same closed cage, thus avoiding the problems related to the design of the shaft seal, but making it more difficult to cool down the motor windings [11].
For positive displacement compressors, the concept of swept volume ($V_s\left[\frac{m^3}{revolution}\right]$) is quite relevant; it is defined as the volume that is supposed to be filled by the gas at the inlet of the compressor.
In practice the swept volume flow is usually used (indicating with n the speed in revolutions per minute):

$$\dot{V}_s = V_s * \frac{n}{60} \tag{3.2}$$

This volume will not be completely filled, so it is necessary to introduce the concept of volumetric efficiency η_s ($\dot{V}_2$ is the volumetric flowrate in the compressor $\left[\frac{m^3}{s}\right]$) :

$$\dot{V}_2 = \dot{V}_s * \eta_s \tag{3.3}$$

So, considering that the compression work for an adiabatic reversible process is equal to the enthalpy difference between the outlet and inlet gas conditions, the ideal compressor power for a given mass flowrate $\left(\dot{m}\left[\frac{kg}{s}\right]\right)$ is:

$$\dot{E}_{is} = \dot{m} * \Delta h_{is} \tag{3.4}$$

However in reality the compressor work will always be larger, because of different losses that are included in a parameter called “isentropic efficiency”, that was already introduced in chapter 2, and that allows to write the expression for the real work:

$$\dot{E} = \dot{m} * \frac{\Delta h_{is}}{\eta_{is}} \tag{3.5}$$

Finally, considering that for a compressor with known swept volume flow the mass flowrate is:

$$\dot{m} = \frac{\dot{V}_s}{v_{in}} * \eta_s \tag{3.6}$$

The work can be expressed as:

$$\dot{E} = \frac{\Delta h_{is}}{v_{in}} \frac{\dot{V}_s}{\eta_{is}} * \eta_s \tag{3.7}$$

This expression marks the importance of volumetric and isentropic efficiencies for a compressor; in particular the isentropic efficiency is affected by four types of losses [21]:

1. Fluid friction
2. Mechanical friction
3. Heat transfer
4. Sealing defects

3.2.1 Screw compressors

The operating principle of this kind of compressor is quite simple, as two screws rotating toward each other gradually reduce the volume of the gas that exit the discharge port at the desired pressure. The suction and discharge ports are fixed, so no valves are required for its operation.

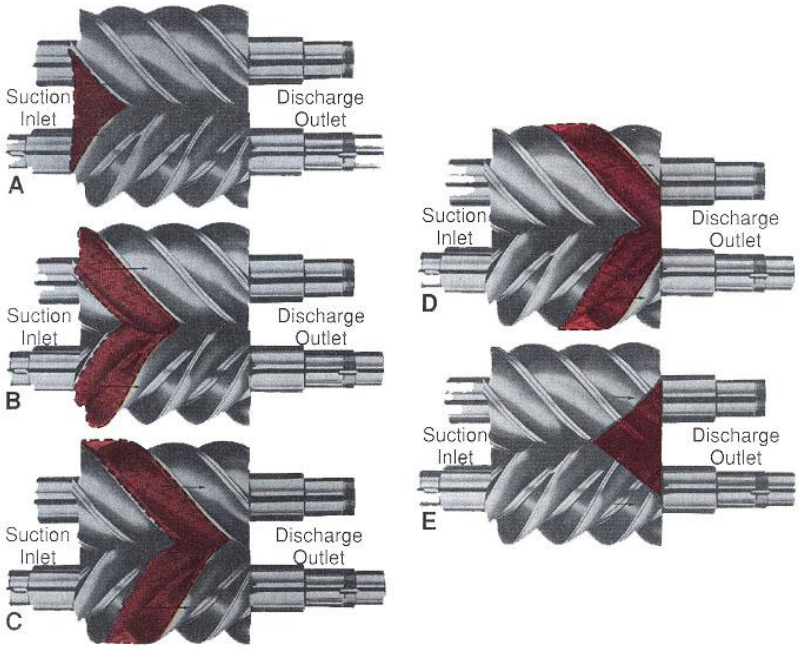

Figure 3.3– Principle of operation for a screw compressor [22].

The ratio between the volume at the inlet and the volume at the outlet is a very important parameter for a screw compressor and its efficiency. It is called built-in volume ratio (v_i) and can be used to define a built-in pressure ratio (π_i):

$$v_i = \frac{V_s}{V_i} \qquad \pi_i = v_i^k \tag{3.8}$$

with k being the polytropic exponent for the isentropic compression process.
It is important that the compressor is selected for an application in which the required pressure ratio is close to the built-in pressure ratio, to avoid a decrease in the isoentropic efficiency as expressed by Granryd (1964) [11]:

$$\eta_{is} = \frac{\left(\frac{p_2}{p_1}\right)^{\frac{(k-1)}{k}} - 1}{\pi_i^{\frac{k-1}{k}} - \frac{k-1}{k} * \pi_i^{\frac{-1}{k}} * \left(\pi_i - \frac{p_2}{p_1}\right) - 1} \tag{3.9}$$

Screw compressors are usually operated with oil injection in order to seal and lubricate the mechanical structure and to cool down the hot gas; as a rule of thumb a compressor of 200 m^3/h has an amount of injected oil of 30/50 liters/minute [11].
The oil must be separated from the refrigerant after the compression, so the presence of an oil separator is required.
Also "dry" screw compressor exist and are used for special applications; the specifically designed mechanical structure of these compressors make them more expensive than oil injected screws, so the cost constitutes a downside of the advantages related to the absence of oil in the system.
Screw compressors are used for very large capacities, above 180 m^3/h to 6000 m^3/h, corresponding to 50 kW to 1,7 MW of power [11].
This kind of compressor is not sensitive to the presence of liquid droplets at the suction, so superheating of the inlet gas is not necessarily required; it is quite reliable and offers the possibility of reaching high pressure ratio even in a single stage compression.

3.2.2 Reciprocating compressors

In this type of compressors, also called piston compressor, a piston that moves in a cylinder does the compression work.

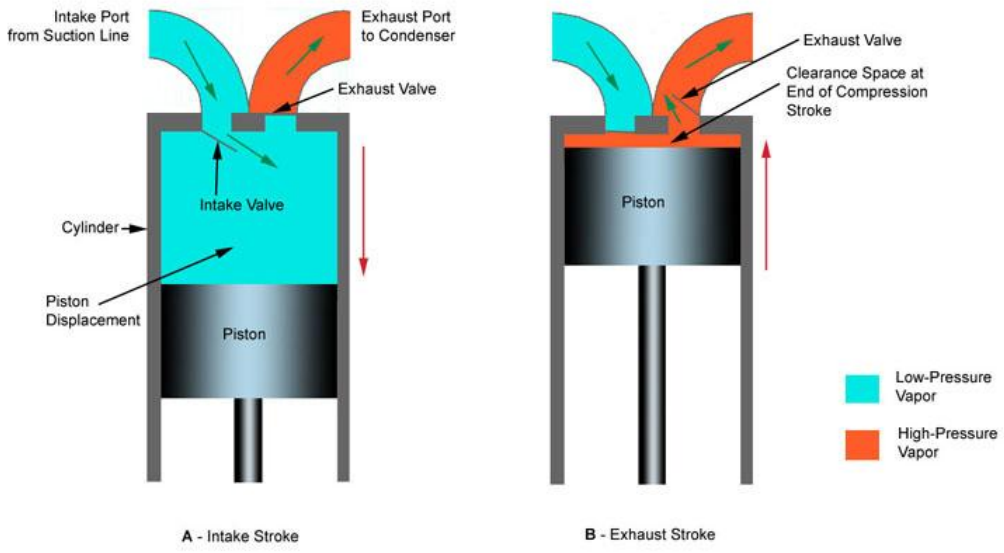

Figure 3.4– Principle of operation for a piston compressor [22].

These compressors have an intrinsic source of irreversibility in their structure, as the volume of the cylinder is not filled entirely by the movement of the piston, so there is a dead space that is one of the causes of a decrease of the volumetric efficiency of the compressor. This theoretical efficiency that considers only the effect of the dead space gives an idea on how much of the cylinder volume is used for the gas compression, and it decreases with the increase of the pressure ratio, as it derives from the following equations [11].

$$\eta_{sth} = 1 - \frac{V_0}{V_s}\left(\left(\frac{p_2}{p_1}\right)^{\frac{1}{k}} - 1\right) \quad (3.10)$$

Where V_0 is the dead space, V_s the swept volume and $\frac{p_1}{p_2}$ the pressure ratio.

For reciprocating compressors Pierre (1982) found two empirical equations for the volumetric efficiency and the ratio between the volumetric efficiency and the isentropic one that are reported below:

$$\eta_s = k_1 * \left(1 + k_s * \frac{t_{1k} - 18}{100}\right) * \exp\left(k_2 * \frac{p_2}{p_1}\right) \quad (3.11)$$

$$\frac{\eta_s}{\eta_{is}} = \left(1 + k_e * \frac{t_{1k} - 18}{100}\right) * \exp\left(a * \frac{T_2}{T_1} + b\right) \quad (3.12)$$

where $k_s k_1 k_2 k_e a b$ are all constants depending on the refrigerant and t_{1k} is the temperature at the inlet (in °C) and $\frac{T_2}{T_1}$ is the ratio of the condensing and evaporating temperatures (in K).

Piston type compressors are used for applications that go from small sizes to very large ones (up to 500 m^3/h) [21].

3.2.3 Turbo compressors

As mentioned at the beginning of this section, these compressors are dynamic because the compression work derives by the change on the speed of the fluid that is given by the rotating compressor and it is proportional to the square of the tangential velocity of the impeller wheels at the outlet.

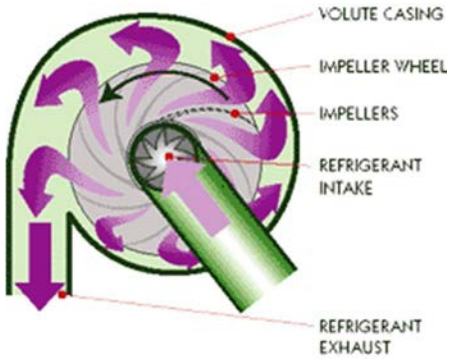

Figure 3.5– Principle of operation for a piston compressor [23].

These compressors are used only for large capacities with a quite constant pressure ratio, as the volumetric flowrate is importantly affected by the pressure ratio. Besides

that, many stages are required to obtain certain pressure ratios, most of all for refrigerants with a low molecular weight.

3.3 Condensers

3.3.1 The condensing section

The condenser is the heat exchanging section in which the refrigerant rejects heat in a phase changing process at constant pressure.
As said before, this heat is the useful effect of a heat pump cycle, so it has to be maximized.
In order to do that, the heat rejection takes place in three steps that correspond to three different heat exchangers:

- The desuperheater, in which the compressed refrigerant releases heat at high temperature until it reaches the condition of saturated vapor.
- The condenser, where the majority of the heat transfer happens at constant temperature.
- The subcooler, in which the saturated liquid refrigerant is cooled down further to use also the less valuable heat at lower temperature.

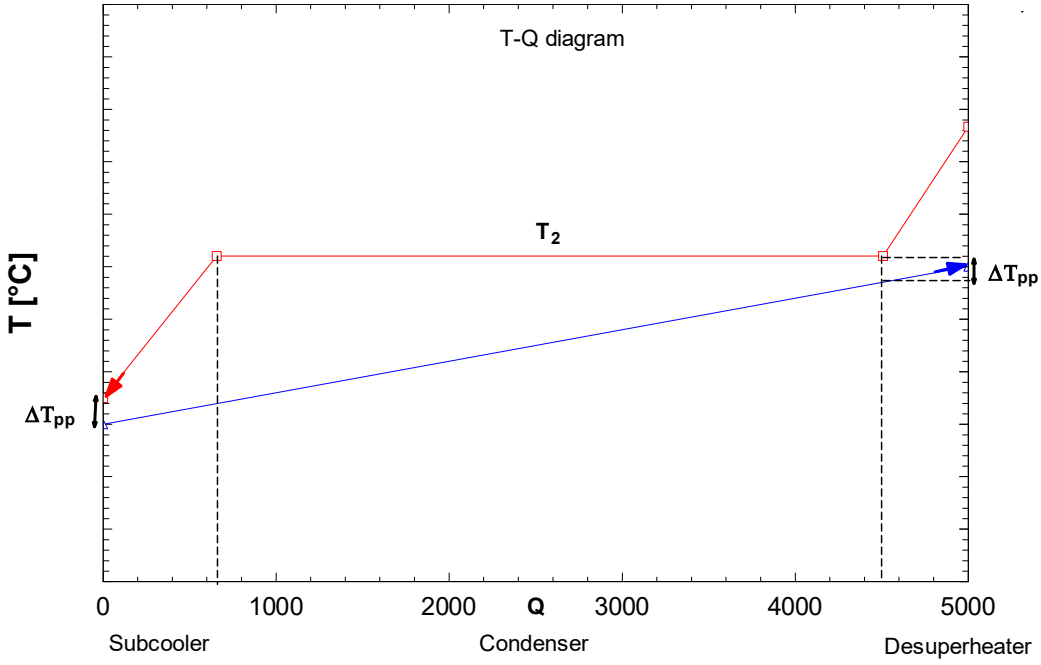

Figure 3.6 Q-T diagram for the condensation process.

To increase the COP of the heat pump, the condensing process should happen at the lowest possible temperature, as a decrease of 1 K in condensing temperatures allows to save around 2-3 % of compression work [24].

The compression process is also relevant for the heat rejection at the condenser; in fact if the isentropic efficiency of the compressor is low, the temperature of the superheated refrigerant will be very high, so the heat transfer in the desuperheater will be larger.

3.3.2 The technologies

Depending on the application, the choice of the right kind of condenser is fundamental to increase as much as possible the efficiency of the heat transfer.

The parameter that marks the difference in this regard is the overall heat transfer coefficient U $\left[\frac{W}{m^2K}\right]$ that depends on the type of condenser,on the fluid that is used to extract the heat from the refrigerants and on the type of condensation that takes place in the condenser.
For water cooled condensers, as it is in the application that is being studied, some typical values of U are the ones reported below.

Table 3.2 – Overall heat transfer coefficient for some kinds of condensers [24]

Type of condensers	U $\left[\frac{W}{m^2K}\right]$
Tube in tube type	600-800
Tube and shell (horizontal)	900-1200
Tube and shell (vertical)	600-1500

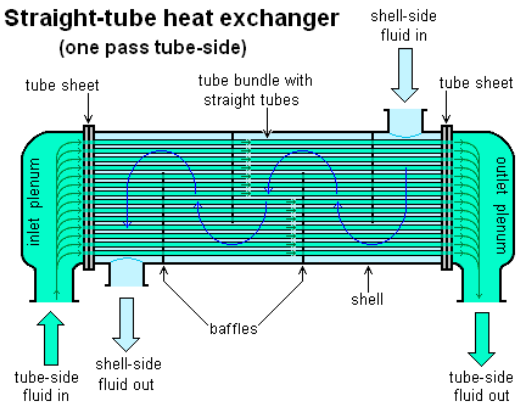

Figure 3.7– Example of shell and tube condenser [25].

3.4 Expansion valves

The expansion valve is a device whose purpose is to maintain the pressure differential between condenser and evaporator and when needed to regulate the refrigerant flow accordingly to the heat flux in the evaporator. The expansion of the refrigerant in the expansion valve takes place at constant enthalpy, so no work is produced in the device. There are many kinds of expansion valves:

1. Hand expansion valve
2. Capillary tube
3. Automatic expansion valve
4. Thermostatic expansion valve
5. Electronic expansion valve
6. Low-pressure float valve
7. High-pressure float valve
8. Constant level regulator

In large systems, where often a flooded evaporator is used, is common to find float type expansion valves. They are situated in the low-pressure receiver that precedes the evaporator and thanks to floating devices and sensors are able to react to the changes of the level of liquid in the receiver that is related to the change of the load in the evaporator.
When the load of the system increases, more refrigerant evaporates, lowering the level in the receiver; when this happens the float valve opens letting more refrigerant inside the evaporator and re-establishing the level in the receiver. When the opposite situation occurs, they close decreasing the amount of refrigerant that arrives in the evaporator. [26]

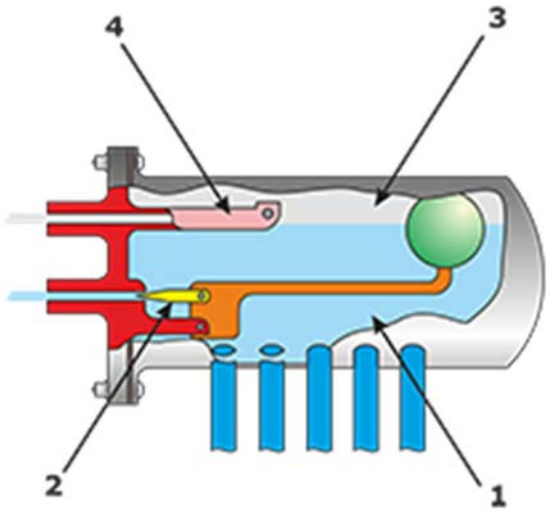

Figure 3.8– Sketch of a low-side float valve [27]

3.5 The evaporator

The evaporator is the component after the expansion valve, in which the refrigerant receives the heat from the heat source and vaporizes completely before reaching the compressor.
There are two big categories of evaporators:

- The direct expansion evaporators
- The flooded evaporator

In a direct expansion evaporator the refrigerant undergoes phase change in a single circuit connecting the expansion valve to the compressor.
In this way usually, some degrees (2-5 K) of superheat is required at the end of the evaporator, because the dynamics of the phase changing fluid could allow some droplets of refrigerant to reach the suction of the compressor, causing problems in its operation.
In a flooded evaporator, instead, the liquid refrigerant is kept in a low pressure receiver from which it reaches the evaporator and then it comes back to the receiver where the separation between the gas and the residual liquid ensures that no liquid refrigerant is entering the compressor.
In this way the superheat is not necessarily required.
Usually the right level of liquid refrigerant in the receiver is maintained by a low pressure float valve.

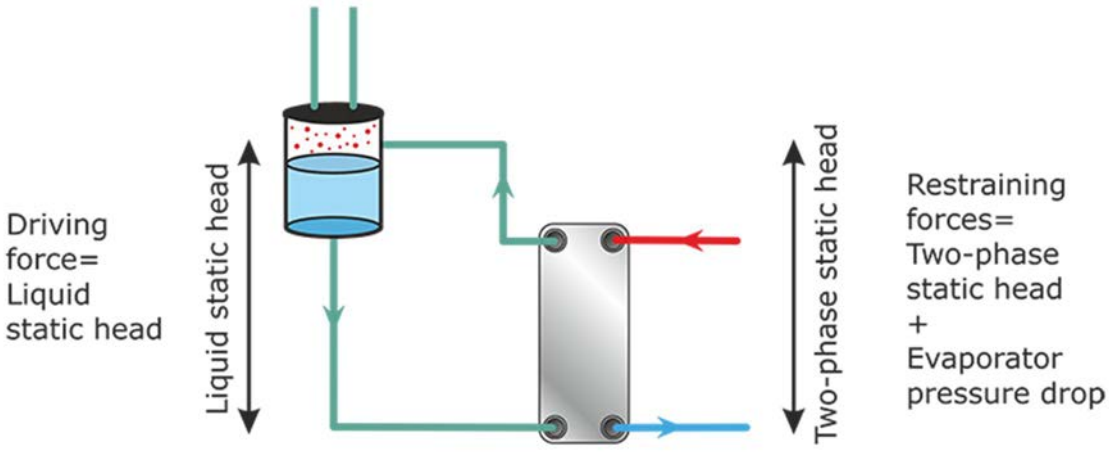

Figure 3.9– Scheme of a flooded evaporator with balances of forces [28].

The choice between these two types of evaporators depends on different factors: usually for larger sizes of the system the advantages of having a flooded evaporator justify the higher costs and complexity of this solution while for smaller systems a simple dry expansion evaporator can used.

The advantages of flooded evaporators include a higher COP, the absence of problems related to maldistribution of the flow, because at the inlet of the evaporator the refrigerant is completely in liquid phase, a better use of the plate area due to the absence of the superheating zone and the self-regulating property of the evaporator; the disadvantages are related to the higher costs of the equipment, the higher amount of refrigerant required to avoid superheating, the sensitivity of the system to variations of the designed flow. [28]

3.6 The open intercooler (Flash tank)

In a 2-stage cycle there is an additional component, the open intercooler (or flash tank), that is a vessel that operates at an intermediate temperature and pressure between the evaporating and condensing temperatures and pressures.
It allows to maintain the right separation of the different mass flowrates of the refrigerant in the two stages of the cycle.
This vessel receives the hot gas from the low stage compressor and the liquid refrigerant coming from the expansion device of the high-pressure stage; at the same time saturated vapor refrigerant leaves the intercooler and reaches the high-pressure compressor and saturated liquid leaves the intercooler and goes to the expansion device of the low stage cycle.

Chapter 4 The mathematical model

4.1 Introduction to the model

The mathematical model has been developed in EES, that is a quite effective tool when analyzing energy systems because it contains all the thermophysical properties of most of the fluids that are used in these applications.
The solver doesn't require the equations to be written in order because it solves them "simultaneously".
The model was built writing energy and mass balances for each component, starting from some assumptions:

- The mass flowrates are supposed to be stationary
- Pressure losses are not considered in any component
- Kinetic and potential energy are neglected in the energy balances

In this way for each component the conservation of mass allows to write:

$$\sum_i \dot{m}_i = \sum_e \dot{m}_e \tag{4.1}$$

With *i* and *e* indicating the inlet and the outlet of the control volume of the considered component.

Furthermore, in accordance to the First Law of Thermodynamics the energy balance for each component becomes:

$$0 = \dot{Q}_{cv} - \dot{W}_{cv} + \sum_i \dot{m}_i * h_i - \sum_e \dot{m}_e * h_e \tag{4.2}$$

Where $\dot{Q}_{cv}$ is the heat and $\dot{W}_{cv}$ the work exchanged in the control volume.
Having set this hypothesis it's possible to describe the equations related to each component.

4.2 Compressors

To find the best configuration of the system different solutions have been studied, including configurations with different compressors; in particular screw and piston compressors are the ones that have been used in the cycle to compare the resulting COP and select the most appropriate one.
These two compressors operate according to different principles, so the set of equations that are used are not all the same, and both of them will be presented below.
Before doing that though, it's convenient to introduce the expression of the isentropic efficiency, that is the same and is the starting point for the model of the compressors:

$$\eta_{is} = \frac{h_{2is} - h_1}{h_{2w} - h_1} \qquad h_{2w} = \frac{h_{2is} - h_1}{\eta_{is}} + h_1 \tag{4.3}$$

where h_1 is the enthalpy of the refrigerant at the inlet of the compressor and h_{2is} is the enthalpy at the outlet in the case of ideal compression, while in the real case the value of the enthalpy is h_{2w} .

4.2.1 The oil-cooled screw compressor

In the operation of screw compressors, in particular when ammonia is the refrigerant, high discharge temperatures are commonly reached, so the oil cooling of the compressor becomes necessary.

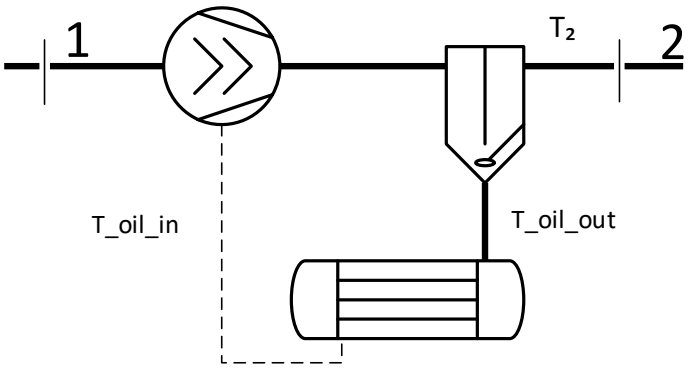

Figure 4.1– schematic of the oil cooled screw-compressor.

The oil injected in the compressor cools down the gas from the maximum temperature T_{2w} to the temperature T_2, resulting in a final enthalpy h_2 that will be at the same pressure but, depending on the quantity of oil that is injected, at a temperature that is acceptable for the compressor.

The volumetric flowrate of the oil $\left(\dot{V}_{oil}\left[\frac{m^3}{s}\right]\right)$ is chosen in such a way that the discharge temperature of the gas is lower than the maximum temperature tolerated by the compressor $(T_{max} = 110℃)$.

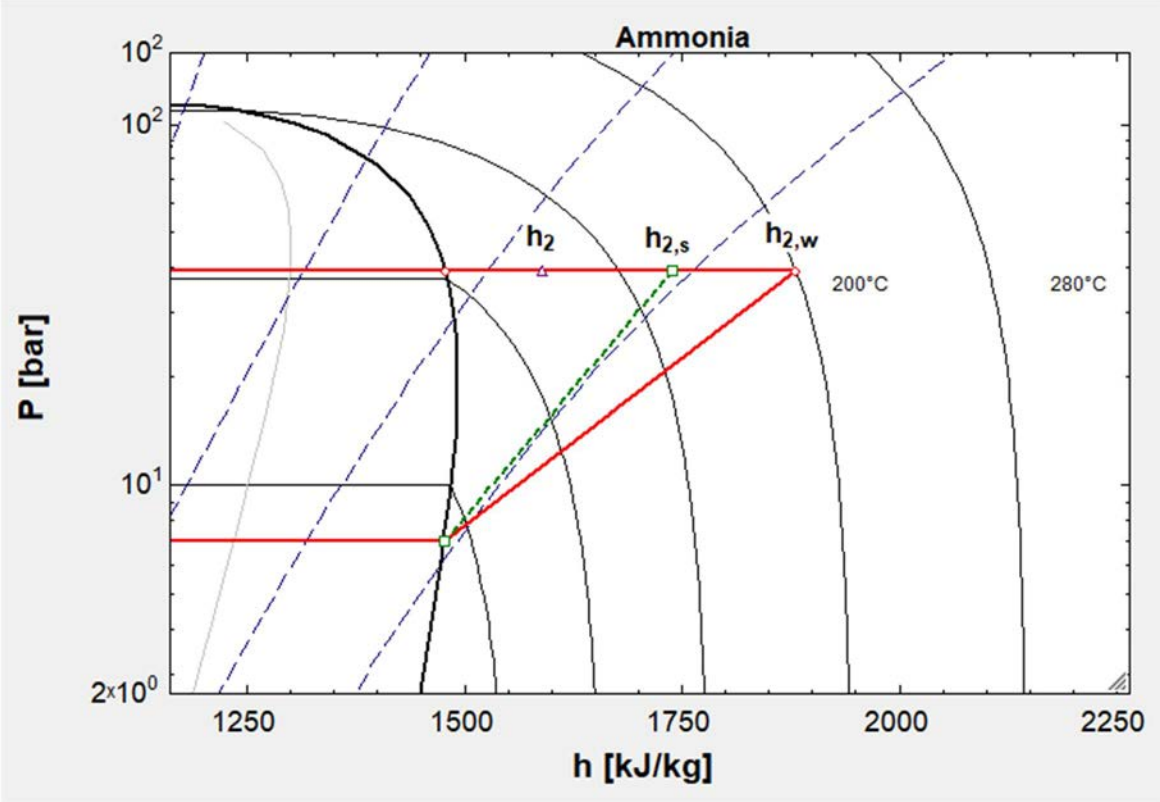

Figure 4.2– p-h diagram with detail on the compression work

The compression process is modelled according to the following assumptions:

- The oil enters the compressor at a fixed temperature $T_{oil_{in}} = 70℃$
- The oil and the refrigerant exit the compressor at the same temperature $(T_2 = T_{oil_{out}})$
- The properties of the oil are calculated at the average temperature of the oil

$$T_{avg} = \frac{T_{oil_{in}} + T_{oil_{out}}}{2} \tag{4.4}$$

In this way the heat absorbed by the oil will be:

$$\dot{Q}_{oil} = cp_{avg} * \rho_{avg} * \dot{V}_{oil} * (T_{oil_{out}} - T_{oil_{in}}) \tag{4.5}$$

where $cp_{avg}\left[\frac{kJ}{kg*K}\right]$ is the specific heat of the oil at the average temperature and $\rho_{avg}\left[\frac{kg}{m^3}\right]$ is the density of the oil at the average temperature.
The properties of the oil are inserted in the thermophysical properties of an incompressible fluid called "Engine_oil_10W" that is included in the libraries of EES.

Therefore, this heat will be the same as the heat released by the refrigerant:

$$\dot{Q}_{oil} = \dot{m}_{ref} * (h_{2w} - h_2) \tag{4.6}$$

In this way, it is possible to determine the enthalpy and temperature of the refrigerant at the discharge.

It is important to notice though that the work of compression will be:

$$\dot{W}_{comp} = \dot{m}_{ref} * (h_{2w} - h_1) \tag{4.7}$$

4.2.2 The piston type compressor

For the piston compressor usually, oil cooling is not present also because the structure of the compressor makes it release some percentage points (5-10 %) of the heat of the hot refrigerant, so the high discharge temperature typical of the screw compressors are not reached.

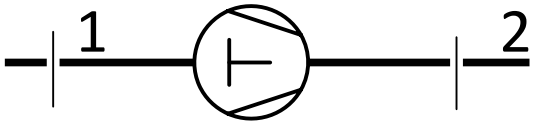

Figure 4.3– Block diagram of the piston compressor.

So this heat loss has to be taken into account as described below.
If the compression ends at h_{2w}, the work done by the compressor is:

$$\dot{W}_{comp} = \dot{m}_{ref} * (h_{2w} - h_1) \tag{4.8}$$

But considering a 5 % heat loss it can be written:

$$\dot{Q}_{comp} = \dot{W}_{comp} - 0{,}95 * \left(\dot{m}_{ref} * (h_{2w} - h_1)\right) = \dot{m}_{ref} * (h_{2w} - h_2) \tag{4.9}$$

In this way the final state point of the compression process is found.

4.3 Condenser

The condensing section of the cycle includes three heat exchangers:

- The desuperheater (2-3)
- The condenser (3-4)
- The subcooler (4-5)

The hot superheated gas exits the compressor at the condition in point 2 and heats up the district heating water in counter-flow configuration along the series of heat exchangers.

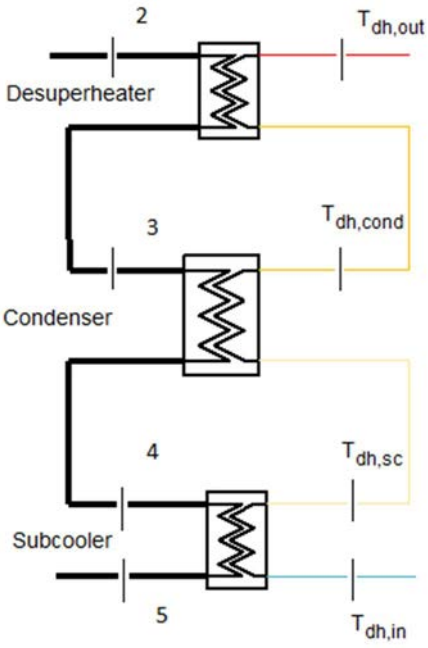

Figure 4.4– Scheme of the condensing section.

So the total heat capacity will be the sum of these terms:

$$\dot{Q}_{tot} = \dot{Q}_{dsh} + \dot{Q}_{cond} + \dot{Q}_{sc} \tag{4.10}$$

Following the numeration given in the figure above it can also be written:

$$\dot{Q}_{tot} = \dot{m}_{ref} * (h_2 - h_3) + \dot{m}_{ref} * (h_3 - h_4) + \dot{m}_{ref} * (h_4 - h_5) \tag{4.11}$$

$$\dot{Q}_{tot} = \dot{m}_{dh} * (h_{dh,out} - h_{dh,in})$$

Defining these values attention must be paid on the heat-temperature diagram, because a minimum temperature difference must be kept along the heat transfer profile.
In the model a fixed ΔT_{cond} and a fixed $\Delta T_{subcooling}$ where set in the following way:

$$T_3 - T_{dh,cond} = \Delta T_{cond} \quad (4.12)$$

$$T_5 - T_{dh,in} = \Delta T_{sub} \quad (4.13)$$

where $T_{dh,cond}$ is the temperature of the district heating water at the end of the condenser while $T_{dh,in}$ is the inlet temperature of the DH water.
These temperature differences are usually between 3 and 5 °C but can be optimized to reach the best overall efficiency in a system with many different heat fluxes through the pinch method that will be explained in the following chapter.

4.4 The expansion valve

The subcooled liquid refrigerant passes through the expansion valve expanding at constant enthalpy down to the evaporating pressure. The quality of the refrigerant is somewhat bigger than zero.

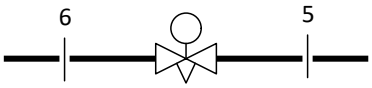

Figure 4.5– Scheme of the expansion valve.

$$h_6 = h_5 \quad (4.14)$$

4.5 The evaporator

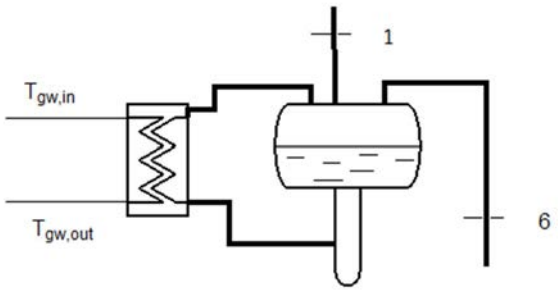

Figure 4.6– Scheme of the flooded evaporator.

In the flooded evaporator the geothermal water releases heat decreasing its temperature from $T_{gw,in} = 73°C$ (or another value depending on the configuration) to $T_{gw,out} = 16°C$ while the refrigerant evaporates at constant temperature:

$$T_1 = T_{gw,out} - \Delta T_{ev} \tag{4.15}$$

where a pinch temperature difference ΔT_{ev} is kept at the outlet of the evaporator. In this project this difference has been assumed equal to 2°C.

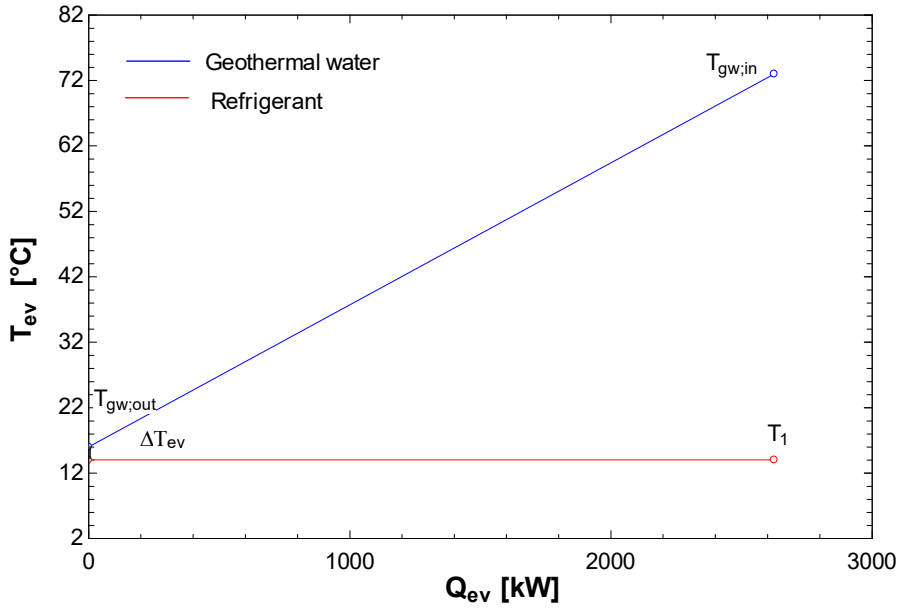

Figure 4.7– Q-T diagram for the evaporation process.

So the enthalpy difference in the refrigerant side is:

$$\dot{Q}_{ev} = m_{ref} * (h_1 - h_6) = \dot{m}_{dh} * (h_{gw,in} - h_{gw,out}) \tag{4.16}$$

4.6 The 2-stages cycle components

4.6.1 The open intercooler

The intercooler is a relevant component in 2-stages cycles; it operates at an intermediate pressure and temperature between the condensing and evaporating ones.
Two flowrates of refrigerants come into it while two other leave it.

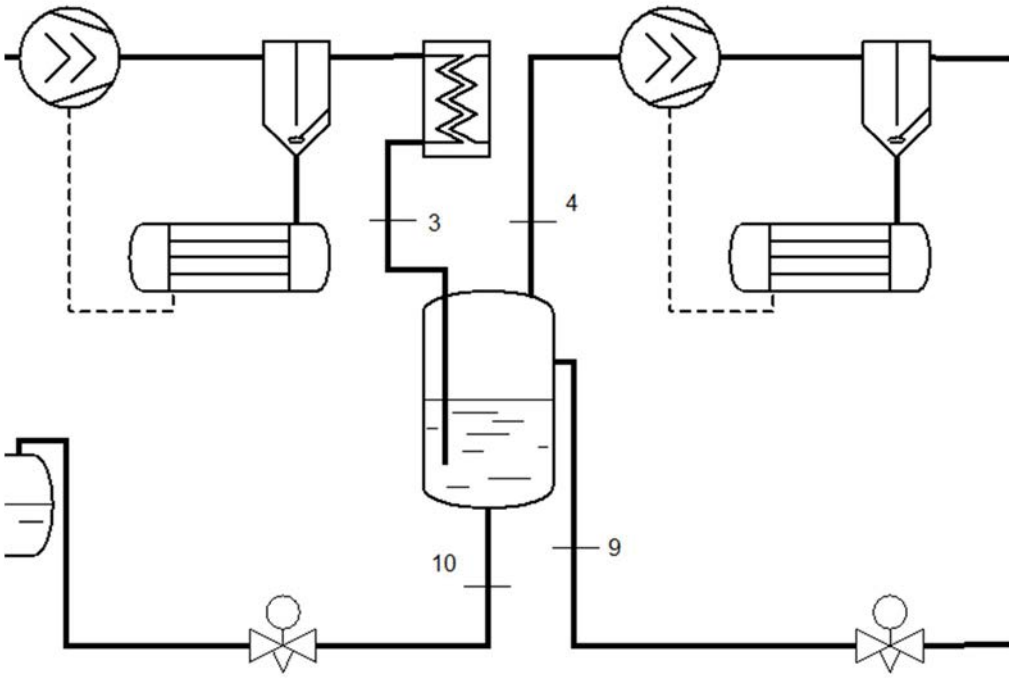

Figure 4.8– Scheme of the intercooler section.

The conservation of energy inside this control volume gives:

$$m_3 * h_3 + m_9 * h_9 = m_{10} * h_{10} + m_4 * h_4 \quad (4.17)$$

All these state points are at the same pressure but at point 3 the vapor is superheated.

$$p_3 = p_4 = p_9 = p_{10} \quad (4.18)$$

$$T_4 = T_9 = T_{10} \tag{4.19}$$

The intermediate temperature T_4 was chosen in order to maximize the COP using parametric tables in EES to find the optimal one.

4.6.2 The low-stage desuperheater

The low-stage desuperheater is an heat exchanger that is situated between the low-stage compressor and the intercooler to recover part of the heat of the superheated vapor, that otherwise would be lost in the intercooler.

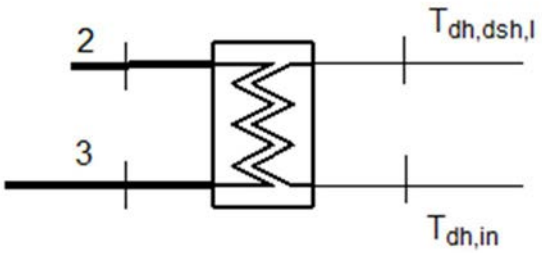

Figure 4.9– Scheme of the low stage desuperheater.

$$\dot{Q}_{dshl} = m_{ref} * (h_2 - h_3) = m_{dh} * (h_{dh,dshl} - h_{dh,in}) \tag{4.20}$$

Chapter 5 The pinch method

5.1 Process integration

In many industrial systems, there are hot streams that need to be cooled and/or cold streams that need to be heated.
In most cases to fulfill the energy requirements of the system it´s necessary to use external utilities, that corresponds to high costs and less energy efficiency of the system itself.
Nonetheless process integration can help reduce this external requirements increasing the overall performance of the systems.
Process integration consists in identifying the energy streams that exist in a systems and trying to integrate them to recover internally as much energy as possible to reduce the external requirements.
In the ideal case, all the heat that is needed for the cold streams can be recovered from the hot streams and vice versa; but this situation almost never applies to real cases.
Furthermore in complex systems is not always easy to identify the streams and the temperature intervals in which they are situated which makes the heat recovery a very difficult task, so a rigorous methodology needs to be used.
The pinch method has been developed by Bodo Linnhoff at the end of the 70s and has become since a very used, known and reliable method to perform heat recovery and obtain energy savings in processes and industrial systems. [29]

The pinch method is performed following three main actions [30]:

- Identification of the heat load of the streams and of the temperature intervals in which they are located
- Application of the Pinch analysis principles
- Design of a Heat Exchangers Network (HEN) that realizes the heat recovery suggested by the pinch analysis.

The first step seems the easiest one but sometimes for very complex systems not all the required data may be available and so it could become a very long process to be done.

5.2 Streams data identification

This step consists in making a table in which for each stream are displayed all the useful information.
To do so, for each stream the equation that gives the heat load should be written as follows:

$$\dot{Q}_i = \dot{m}_i * cp_i * |T_{in} - T_{out}| = \dot{C}P * |T_{in} - T_{out}| \quad (5.1)$$

where $\dot{C}P$ is the heat capacity flow rate (kW/°C), given by the product of the mass flowrate (kg/sec) and the specific heat capacity (kJ/°C kg).
The resulting table will be something similar to the one below.

Table 5.1 – Example of a streams data table

Stream number and type	**Initial temperature [°C]**	**Final temperature [°C]**	**Heat capacity flowrate [kW/°C]**	**Heat load [kW]**
1 Cold	20	140	2	240
2 Hot	160	60	3	300
3 Cold	80	120	4	160
4 Hot	150	30	1.5	180

5.3 The composite curves

At this point a graphical representation of the hot and cold streams has to be done.
To do so, the temperature interval in which the hot streams are contained must be discretized in smaller temperature intervals that can be larger or smaller depending on the accuracy that is required.
Then for each temperature interval the heat capacities flowrates of the hot streams are summed, giving a single hot composite curve in the T-Q diagram, like it is shown below.

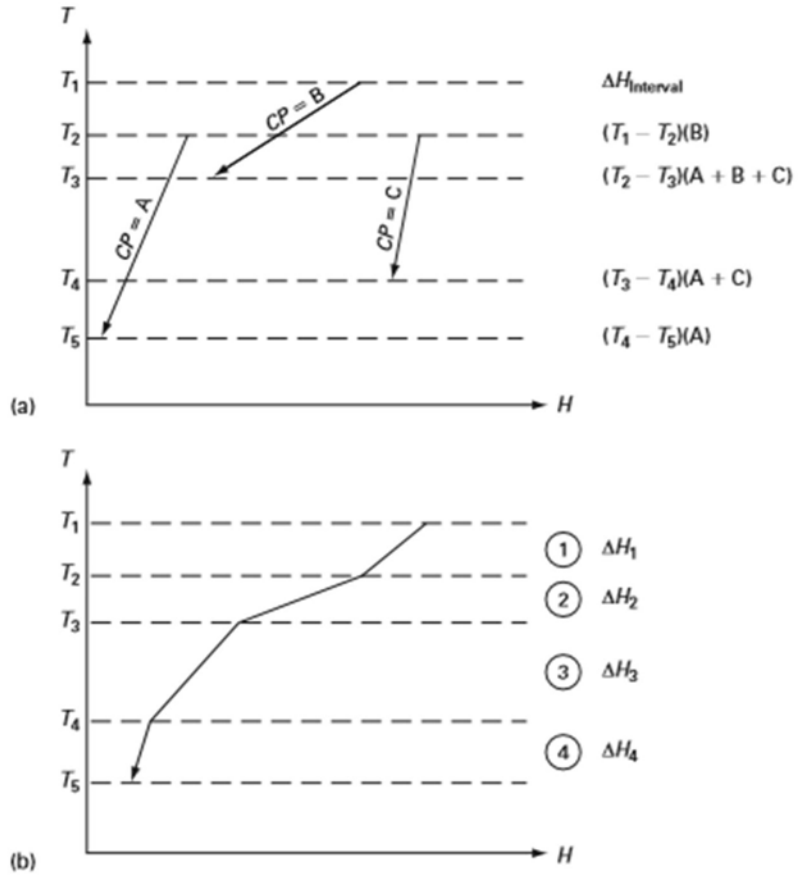

Figure 5.1– Formation of the hot composite curve [31]

The same procedure is used to build the cold composite curve, so that the problem can be handled like a two streams problem [31].
The resulting graph will display the hot and the cold composite curves and it can be used to visually identify the potential for heat recovery; as indicated in the figure, the overlapping of the two curves shows the maximum heat that can be exchanged by the two total streams for a given minimum temperature difference at the pinch point.

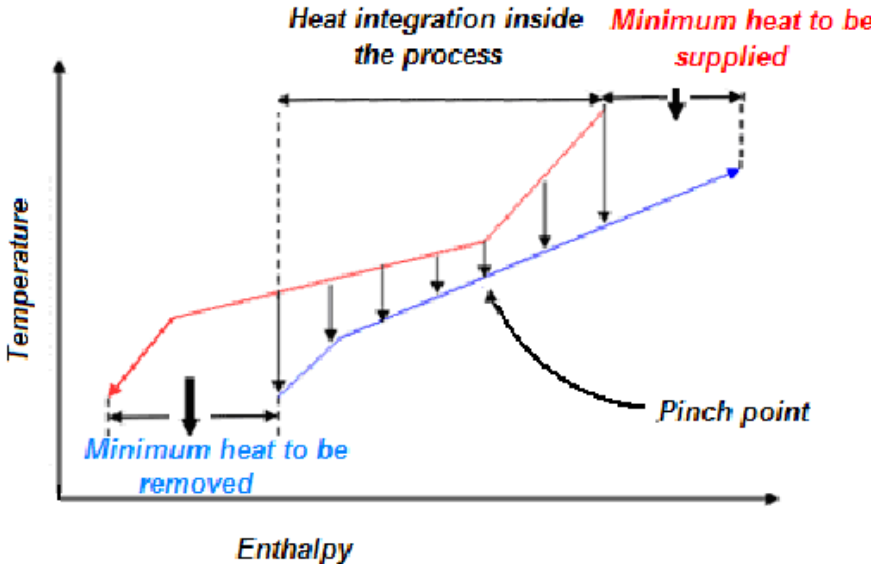

Figure 5.2– Meaning of the composite curves [32]

Also, at the top of the hot composite curve the minimum external heat requirement can be seen as the difference between the last value of heat load of the cold composite curve and the first value of the hot composite curve. The same is valid for the external cooling requirement.

The pinch point represents a very important parameter of the system, as it´s the point in which the minimum temperature difference ($\Delta T_{\min}$) occurs.

Practically $\Delta T_{\min}$ will be the minimum temperature difference that will exists in the heat transfer section of the system.

5.4 The problem table

Of course the graphical representation gives quite a good idea about the external requirements, but an algebraic method is necessary to calculate them in a rigorous way; this method is called the "problem table" approach [31].

If the minimum external requirements have to refer to a case with a minimum temperature difference $\Delta T_{\min}$, the temperature intervals have to be adjusted; practically, to ensure that the $\Delta T_{\min}$ is everywhere respected, the temperatures of the hot streams are decreased by $\frac{\Delta T_{\min}}{2}$ while the temperatures of the cold streams are increased by $\frac{\Delta T_{\min}}{2}$, so that is possible to write enthalpy balances for every temperature interval obtaining a net surplus or a net deficit of heat [31].

In this way the external requirement is calculated as follows [30]:

- Performing an energy balance for every interval using the simple equation:

$$\Delta H_i = (T_i - T_{i+1}) * \left(\sum \dot{CP}_H - \sum \dot{CP}_C\right)_i \tag{5.2}$$

where T_i and T_{i+1} are two consecutive shifted temperatures and $C\dot{P}_H$ and $C\dot{P}_C$ are the heating capacities flowrates for every interval.

- Summing all the results from the energy balance of an interval to the following interval with the right sign so that it is possible to identify the smallest value of net cooling demand as the minimum external heating utility that is required to make the problem feasible. That value will exists at a temperature that is called the pinch temperature.
- If that value of minimum external heating is summed to every energy balance the value of the final one will correspond to the minimum external cooling utility.

5.5 The Grand composite curve

Another useful tool used to evaluate the external utilities requirements is the Grand composite curve (GCC), which is obtained from the shifted composite curves; the shifted composite curves are made adjusting the temperatures that describe the temperature intervals for the composite curves. The shifted temperatures will be on the y-axis while the values obtained at the last step of the problem table procedure will be on the x-axis, giving the Grand composite curve, as the one shown below.

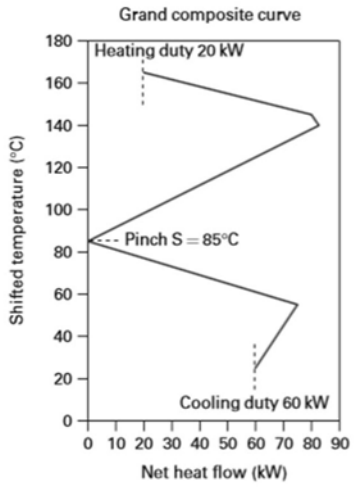

Figure 5.3– Formation of the GCC [31]

5.6 The meaning of the pinch point

Once the pinch point has been found the system can be considered as two separate systems, because at this point is clear that any heat that is transferred from the zone above the pinch to the zone below will increase external cooling utility and vice versa if cooling is inserted in the zone above the pinch.

These observations result in the three rules of pinch analysis [31]:

- Heat must not be transferred across the pinch
- Cold utilities must not be used above the pinch
- Hot utilities must not be used below the pinch

5.7 The MER exchanger network

The MER design is a HEN design that provides minimum energy requirement or maximum energy recovery.

To do so the procedure as illustrated by Linnhoff can be summarized as follows [31]:

- After the identification of the pinch point the two parts that are separated by it should be designed independently from each other
- The design should begin at the pinch and moving toward the extreme points of the system
- Close to the pinch point two rules must be respected:
  $\dot{C}P_{hot} \leq \dot{C}P_{cold}$ (above the pinch)
  $\dot{C}P_{hot} \geq \dot{C}P_{cold}$ (below the pinch)
- Maximixing the heat exchanged between the streams to reduce the number of units of the system.
- Using hot utilities only above the PP and cold utilities only below it.

5.8 The pinch method for HPs

The application of the Pinch method for HPs presents some differences with the traditional method presented above.
In fact the traditional method is used to find and minimize the external utilities, but for a HP external utilities are not even existing [33], because the system is a closed one, in which all the heat is recovered internally by the district heating water (in this application).
For this reason also the composite curves will have a different aspect, as they overlap each other completely.
What is interesting though, is that when the HP system is modelled, some minimum temperature differences are set in some points where it is expected or desired to have the heat transfer happening with some minimum ΔT.
Designing the network in this way it should be possible to obtain two curves that are close enough to a HEN that operates near the maximum thermodynamic efficiency.
What emerges instead when applying the pinch analysis is that the pinch points of the system can be situated in different places and that the HEN design should be started from this new pinch points, with the optimal temperatures given by an optimization process that applies the rules of the pinch analysis.

5.9 The pinch method in EES

The procedure that has been implemented in EES to use the pinch analysis method will be now explained in detail.
To create all the necessary arrays a ***Procedure*** has been used inside the code.
A simple 1-stage model will be used to make the explanation more efficient.
The selected configuration is the most simple: the district heating water is divided into 2 streams, one being heated by the condensing section of the HP and the other, the smaller one, by the oil cooler heat exchanger. Both streams are heated from 50 to 80 °C and the total heating capacity of the system is 5 MW.
First of all the model was created and simulated to check the number and types of the hot streams, that are the black and red ones in the Q-T diagram below, respectively indicating the oil cooler and the condensing section heat exchangers.

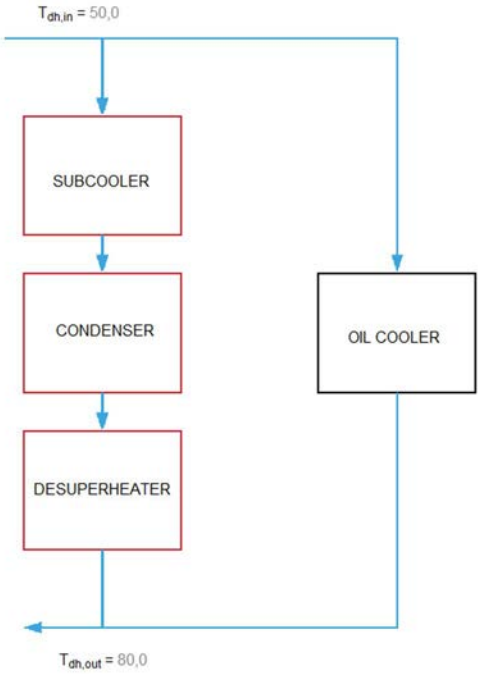

Figure 5.4– Block diagram for the example model.

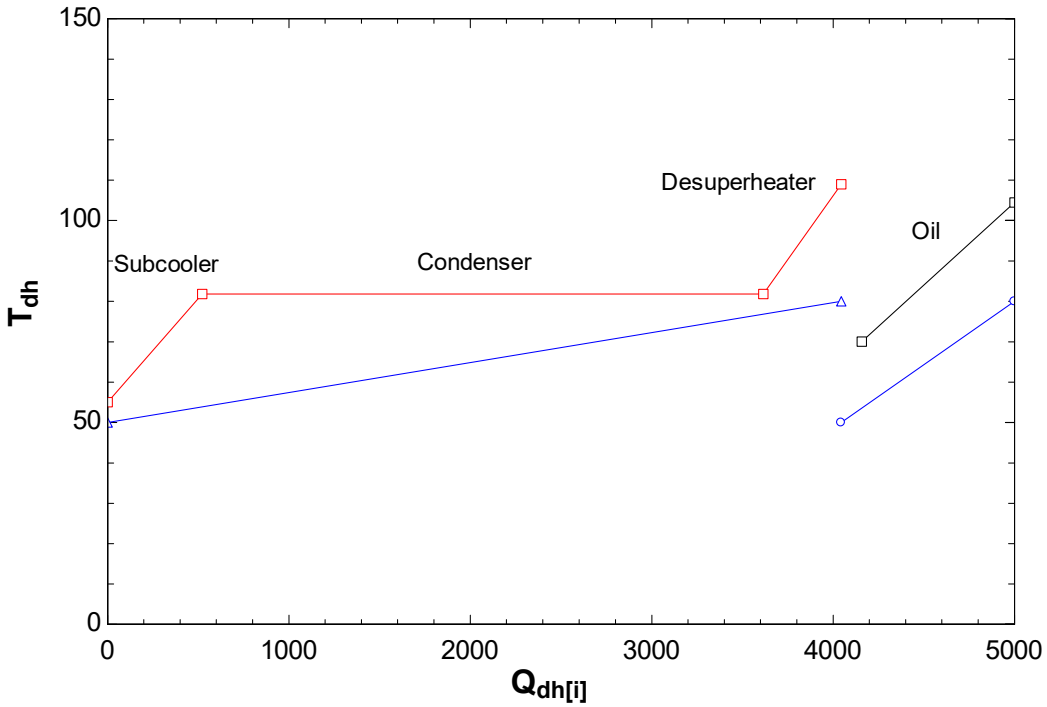

Figure 5.5– Q-T diagram for the example model.

The most important parameters of the cycle are summarized in the table.

Table 5.2 – Main parameters before the optimization

Parameter	Value	Unit
Condensing temperature $T[3]$	81.861	°C
Maximum temperature $T[2] = T_{oil_1}$	108,46	°C
Temperature after subcooling $T[5]$	55	°C
ΔT_{cond}	5	°C
ΔT_{sub}	5	°C
COP	3.69	/

The steps that are followed to build the composite curves are recapped below [33]:

- The first step is to decide the number of intervals (N) in which the temperature range of the hot streams should be divided into. Usually the initial value is N=100 but if a better accuracy is desired it can be increased to 200.
  Then the size of the intervals is found as follows:

$$\Delta T_{int} = \frac{T_{max} - T_{min}}{N - 1} \tag{5.3}$$

where T_{max} is the maximum overall temperature of the hot streams and T_{min} is the minimum temperature of the hot streams.

- Consequently an array containing all the N values of temperatures T_{hot_i} was created inside the procedure
- For each one of the m hot stream the heating capacity of the stream has been divided into the intervals included in the temperature range to which each hot stream belongs. To divide the heating capacities properly into the intervals a control loop has been created: it checks that the sum of the values in each interval is equal to the total heating capacity of the hot stream; this is necessary because a non-integer temperature difference must be divided into an integer number of intervals, so some troubles can occur when rounding the number of intervals. Further details can be found in the code in Appendix D.
- For each interval the heating capacities that are present in that interval have been summed up

$$\dot{Q}_{hot_i} = \sum_{j=1}^{m} \dot{C}P_j \tag{5.4}$$

- An array $\dot{Q}_{heat_i}$ has been created starting from the design heating capacity of 5000 kW and subtracting the sum of the values of $\dot{Q}_{hot_i}$ up to the last one before the value of $\dot{Q}_{heat_i}$

$$\dot{Q}_{heat_{i(i=1)}} = 5000 \tag{5.5}$$

$$\dot{Q}_{heat_{i(i>1)}} = 5000 - \sum_{j=1}^{i-1} \dot{Q}_{hot_j} \tag{5.6}$$

- In order to mirror the number of points of the hot composite curve with their respective horizontal distance to the cold composite curve another array has been built for the temperatures of the cold stream of DH water starting from $\dot{Q}_{heat_i}$ and using the slope of the DH water line.

$$T_{cold_i} = \left(T_{dh_{out}} - T_{dh_{in}}\right) * \frac{\dot{Q}_{heat_i}}{5000} + T_{dh_{in}} \tag{5.7}$$

- The composite curves have been plotted using the two temperatures arrays T_{cold_i} and T_{hot_i} and the array $\dot{Q}_{heat_i}$, obtaining as a result the figure below.

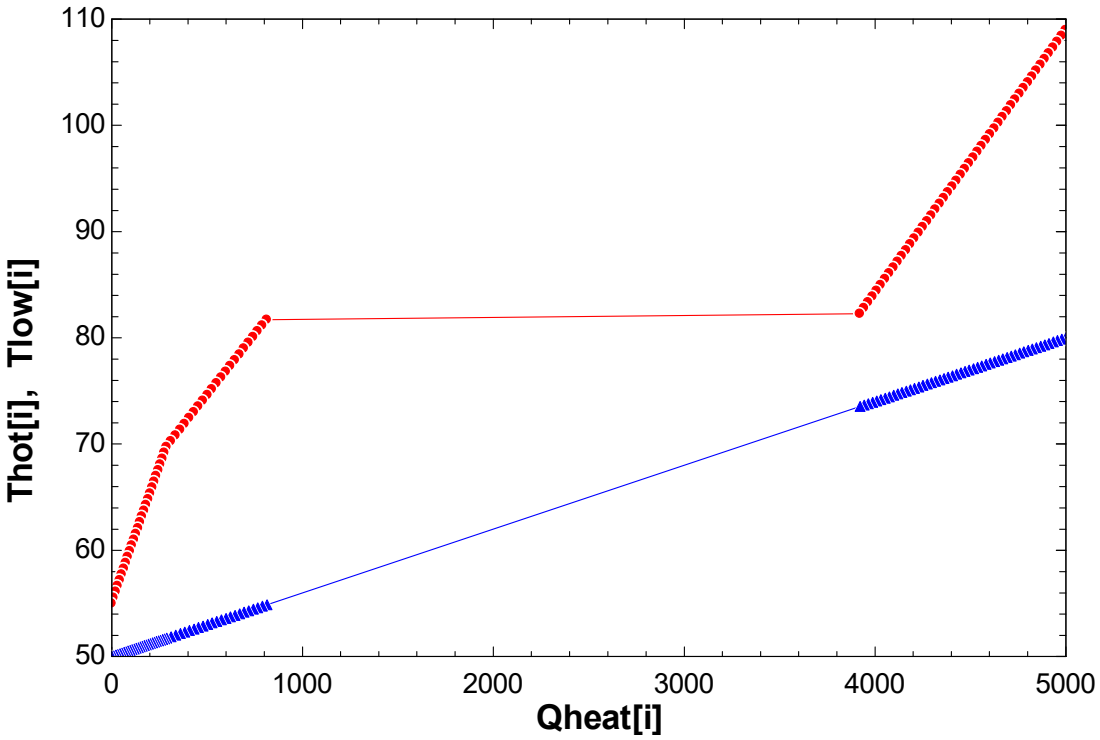

Figure 5.6– Resulting composite curves

- An array containing all the temperatures differences between the hot temperatures array and the cold temperatures array was created outside of the procedure that was used to build the composite curves.

$$\Delta T_j = T_{hotj} - T_{coldj} \tag{5.8}$$

- Having this array it was finally possible to set the lower limit of each value in the array to the desired minimum temperature difference ΔT_{min} in the window *variable info* in order to ensure that the desired minimum temperature difference is always respected.

At this point it was possible to proceed with the optimization, that was done with the following steps:

- Creating two degrees of freedom for the model by commenting the equations that were setting the minimum temperature differences at the subcooler and at the condenser ΔT_{cond} and ΔT_{sub}.
- Selecting one of the multi-dimensional optimization tools provided by EES; in this project the Variable Metric Method was used.
- In the optimization window, the function that has to be optimized must be chosen, so the choice is to maximize the COP.
- Then ΔT_{cond} and ΔT_{sub} were chosen as the two independent variables that will vary during the optimization; the lower and upper bounds for each variable were set and finally the optimization could be launched.

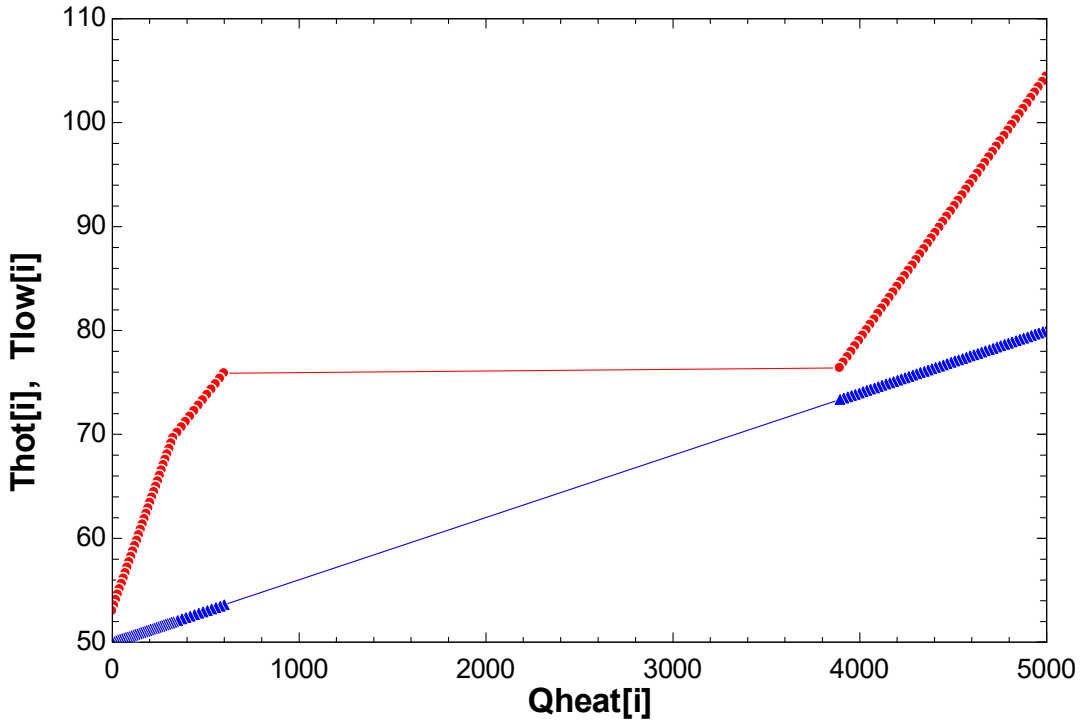

Figure 5.7– Resulting composite curves after the optimization

The result of the optimization is a new set of key temperatures that can be used to design a HEN in which in each heat exchanger the minimum temperature difference is respected.

Table 5.3 – Main parameters after the optimization

Parameter	Value	Unit
Condensing temperature $T[3]$	76.42	°C
Maximum temperature $T[2] = T_{oil_1}$	104.12	°C
Temperature after subcooling $T[5]$	53.136	°C
$\Delta T_{pp,cond}$	3.015	°C
$\Delta T_{pp,sub}$	3.136	°C
COP	3.95	/

Looking at the composite curves, the two pinch points remain at the inlet of the subcooler and at the outlet of the condenser, as expected for this simple example; the new values of ΔT_{pp} can be seen in the updated array of the temperature differences between the hot and the cold composite curves and are reported in the above table.

This implies that a HEN that is built using the new temperatures that are the result of the optimization could maintain these values of pinch point while providing the highest thermodynamically attainable COP.
In this case the suggested HEN is very simple, as the only adjustment that is required consists in splitting the oil cooler's heat at the condensing temperature, so that no heat is transferred through the pinch point and the MER criteria are respected.
The resulting HEN is presented below, and it is possible to see that the minimum temperature difference is respected at the pinch point. This configuration allows to reach the maximum COP with only one more heat exchanger.
The improvement is close to 6.5 % compared to the first configuration.

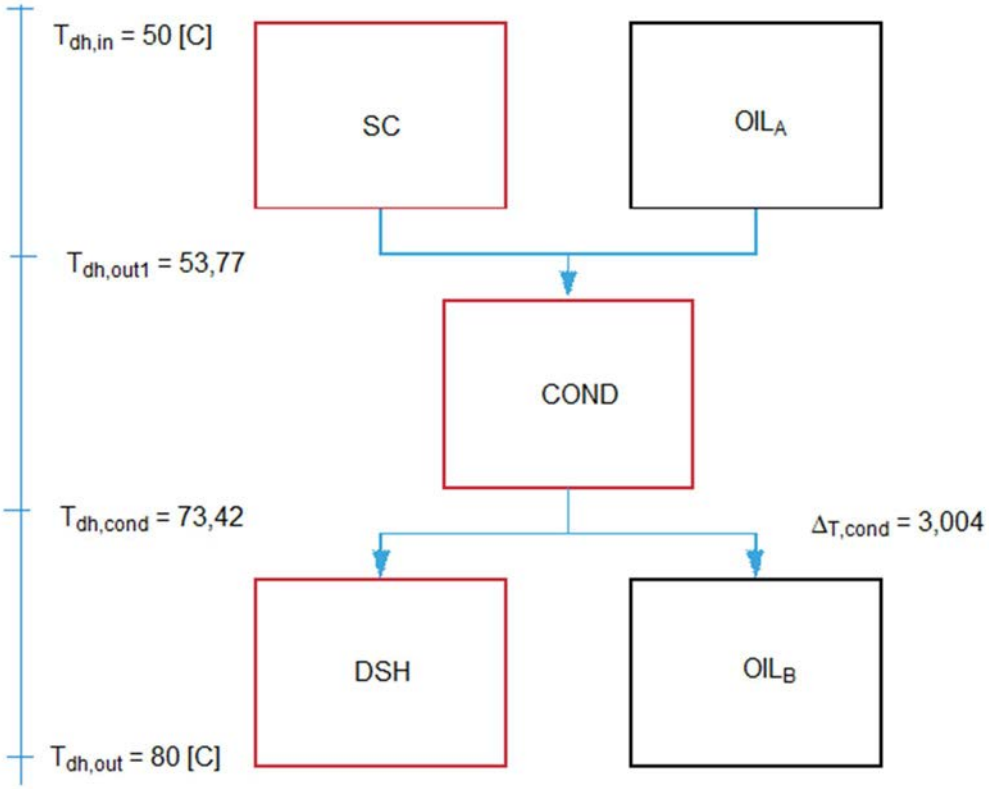

Figure 5.8– Resulting HEN with the DH water temperatures along it.

Chapter 6 Results

6.1 Introduction

In the first phase of the project the focus has been put on 1-stage configurations for some reasons:

- To get confident with the modelling of heat pump system
- To try different refrigerants in order to find the most performing one
- To see how the type of refrigerant impacts the selection of the compressor and hence the characteristics of the system
- To realize how placing the heat exchangers at different temperature levels affects the condensing temperature and the COP of the systems

Before presenting some results it´s necessary to show the assumptions that are used as hypothesis and inputs of the system:

- Design heating capacity of the system: 5 MW
- District heating water temperatures:
  - Return temperature: $T_{dh,in} = 50℃$
  - Forward temperature: $T_{dh,out} = 80℃$
- Geothermal water temperatures:
  - Extraction temperature: $T_{gw,in} = 73℃$
  - Injection temperature: $T_{gw,out} = 16℃$
- Types of compressors:
  - Screw with oil cooling
  - Piston w/o oil cooling
- Compressor isentropic efficiency and cooling oil volumetric flowrate: are found in the GEA compressors selection software RTSelect
- Oil inlet temperature: $T_{oil_{in}} = 70℃$
- Maximum allowable temperature at the compressor discharge: $T_{2max\_} = 110℃$
- Pinch temperature differences:
  - Evaporator: 2℃
  - Condenser and subcooler: 3℃
  - Other heat exchangers: 3℃
- Refrigerants:
  - R717 (Ammonia, NH_3)
  - R290 (Propane)
  - HFOs (R1234ze(E),R1234yf, R1243zf)

6.2 1-stage HP with screw compressor and oil cooling

The first model that was built is a simple 1-stage HP cycle with screw compressor and oil cooling using ammonia as the refrigerant.
This cycle is used as a reference for the developing of improved cycles.

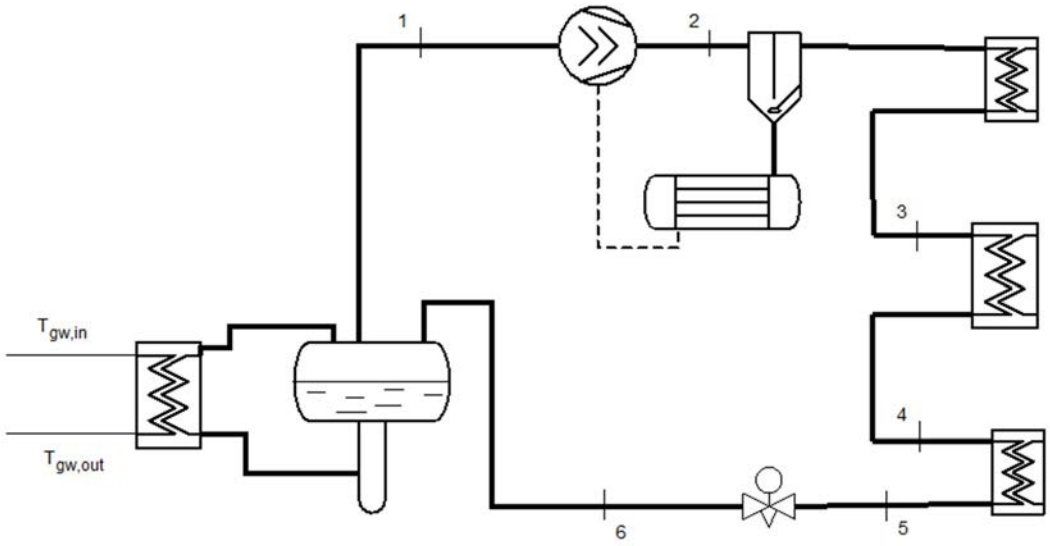

Figure 6.1– Scheme of the 1-stage model with screw compressor and oil cooling.

The most suitable compressor that was found in the GEA´s selection software is the model YR-Y2655H-52, that is sized for a total cooling capacity of 4041.5 kW and operates with an isentropic efficiency of 0.79.
One difficulty that was encountered using the RTselect is that for this application the oil cooling was not enough, so the software expected some additional refrigerant injection in the compressor.
However to simplify the problem, and considering that these 1-stage configurations are not practically interesting but are useful to understand how to improve the cycle, only oil cooling has been used in the model for the compressor. In particular, when the value of the oil volumetric flowrate was not provided directly by RTselect, it was decided to choose a value for which the temperature at the discharge of the compressor was lower than the maximum allowable temperature.
For this model the DH water was heated up in two different streams, as it can be seen in the graphs below. In order to keep the condensing temperature as low as possible the water that is heated by the oil has been let free to surpass the outlet temperature of 80 °C so that the main stream can be heated up to a lower temperature, resulting in a lower condensing temperature.

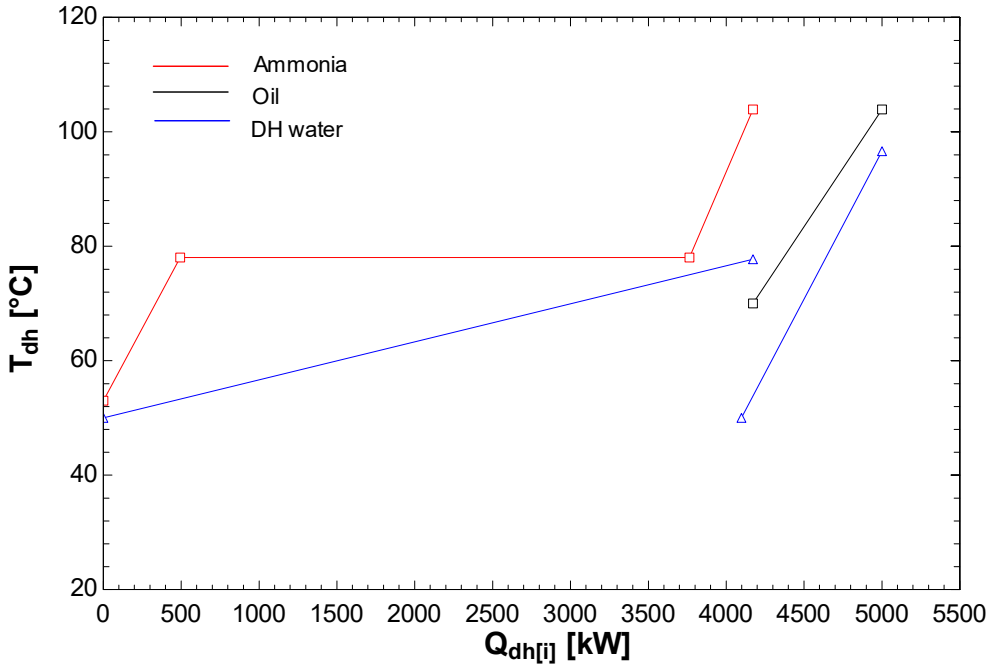

Figure 6.2– Q-T diagram for the considered cycle.

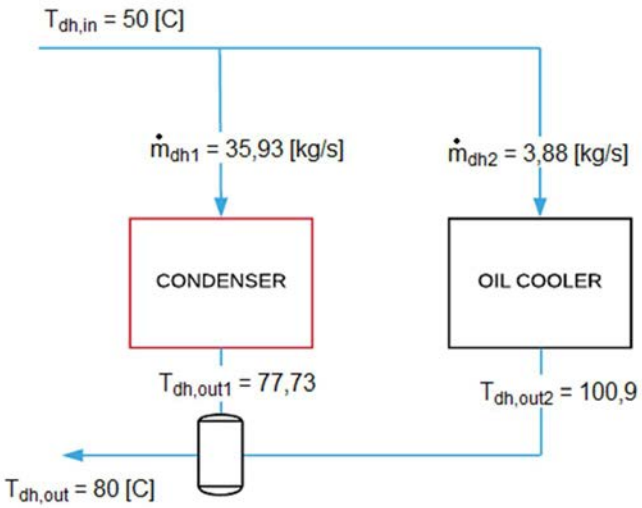

Figure 6.3– Block diagram for the 1-stage configuration.

With these assumptions the resulting COP and other parameters are listed below the diagram of the cycle.

- $COP_{tot} = 4{,}032$
- $T_{cond} = 78{,}03°C$
- $\dot{W}_{comp} = 1240kW$
- $p_{min} = 7{,}05bar$
- $p_{max} = 39{,}66bar$
- $r_p = 5{,}627$
- $\dot{V}_{refin} = 2392m^3/h$
- $\dot{V}_{refout} = 4955m^3/h$
- $v_i\,(required) = 4{,}827$
- $T_{max} = 104°C$
- $\dot{m}_{ref} = 3{,}687kg/s$
- $\eta_{is} = 0{,}79$
- $\dot{V}_{oil} = 800l/m$

The improvement related to the outlet temperature after the oil cooler has brought an improvement of around 2 %.

6.3 Ammonia configurations with direct heat exchanger

Even if the simple solution that has been presented above seems to be reasonable, it doesn´t take into account the fact that the heat source of the system (the geothermal water) arrives at the heat pump at a temperature ($T_{gw_{in}} = 73°C$), that is above the return temperature of the district heating water, giving the possibility to recover a large amount of heat before the HP cycle. Hence different solutions that include a direct heat exchanger before the HP have been analyzed in order to find the best one.
Below the results obtained with these configurations will be presented.

6.3.1 2nd configuration

This configuration is obtained by splitting the DH water in two streams, one passing through DHEX and oil cooler HEX while the main one exchanges heat with the condenser section.
With this configuration no improvement was shown by letting the outlet temperature of the oil cooler free, as a reduction in the flow through the DHEX was penalizing the COP .
Nonetheless, it can already be seen how impactful the presence of the DHEX is for the COP, as it increased of 0.8 points (+20%) compared to the basic configuration.
The compressor model that was the closer to this application is again the model YR-Y2655H-52.

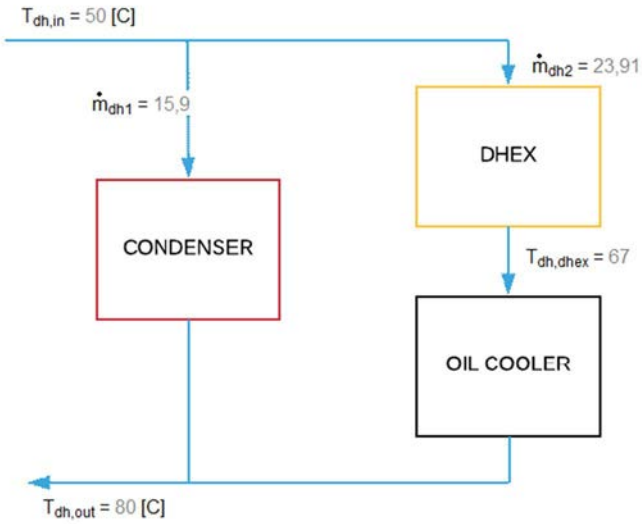

Figure 6.4– Block diagram for the 2nd configuration.

All the most relevant parameters are indicated below:

- $COP_{tot} = 4{,}81$
- $T_{cond} = 79{,}88°C$
- $\dot{W}_{comp} = 10{,}40kW$
- $p_{min} = 7{,}05bar$
- $p_{max} = 41{,}3bar$
- $r_p = 5{,}859$
- $\dot{Q}_{dhex} = 8{,}97kW$
- $T_{max} = 107{,}4°C$
- $\eta_{is} = 0{,}79$
- $\dot{V}_{oil} = 60{,}0l/min$

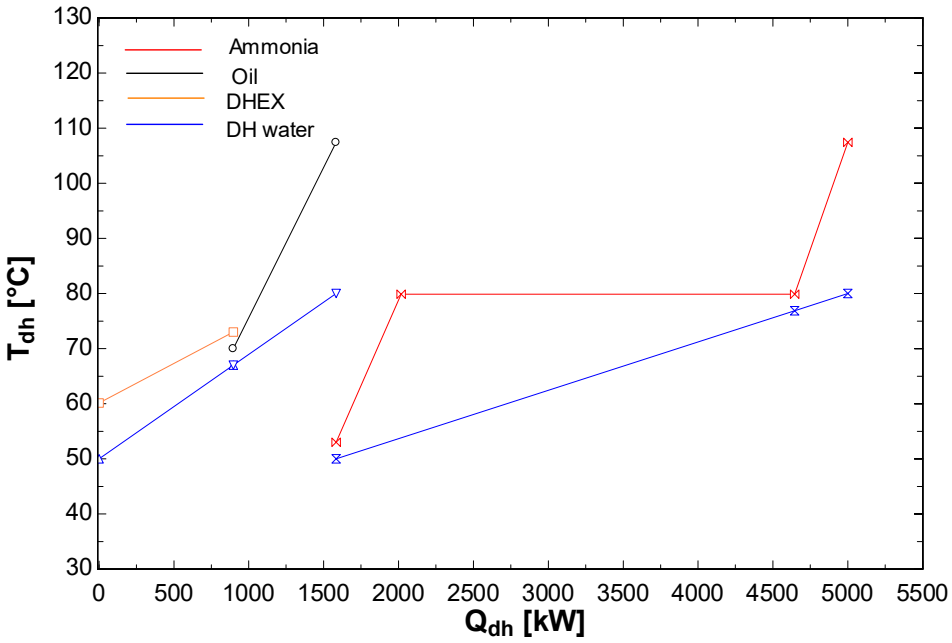

Figure 6.5– Q-T diagram for the 2nd configuration.

6.3.2 3rd configuration

This configuration is obtained by splitting the DH water in three streams, one passing through DHEX ,one through the oil cooler HEX while the main one exchanges heat with the condenser section. In this way it was possible to increase the temperature of the DH water in the oil cooler heat exchanger obtaining a significantly higher COP. The compressor model is: VR-V2655H-52.

The relevant parameters are indicated below:

- $COP_{tot} = 5{,}044$
- $COP_{hp} = 3{,}624$
- $T_{cond} = 84{,}57°C$
- $\dot{W}_{comp} = 10{,}40kW$
- $p_{min} = 7{,}05bar$
- $p_{max} = 45{,}67bar$
- $r_p = 6{,}48$
- $\dot{Q}_{dhex} = 14{,}08kW$
- $T_{max} = 105{,}5°C$
- $\eta_{is} = 0{,}751$
- $\dot{V}_{oil} = 70{,}0l/min$

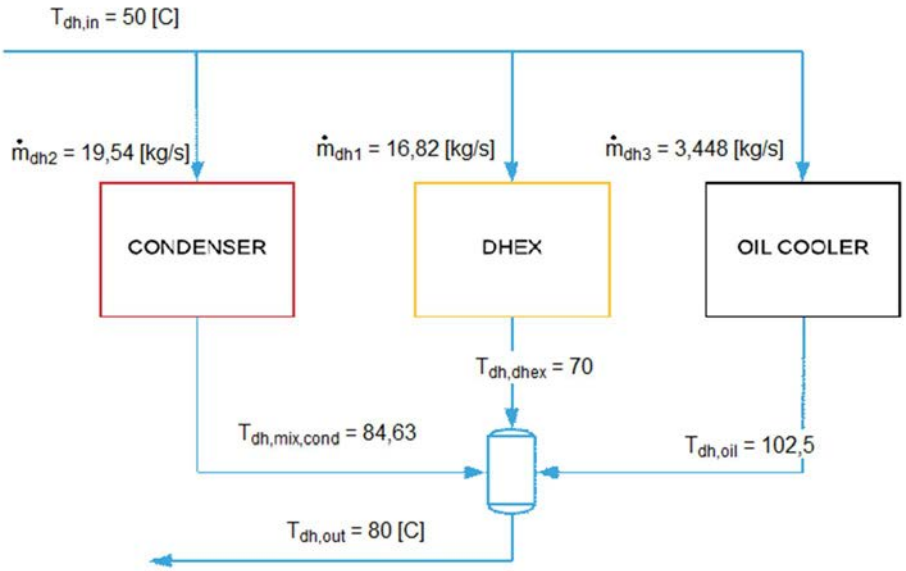

Figure 6.6– Block diagram for the 3rd configuration.

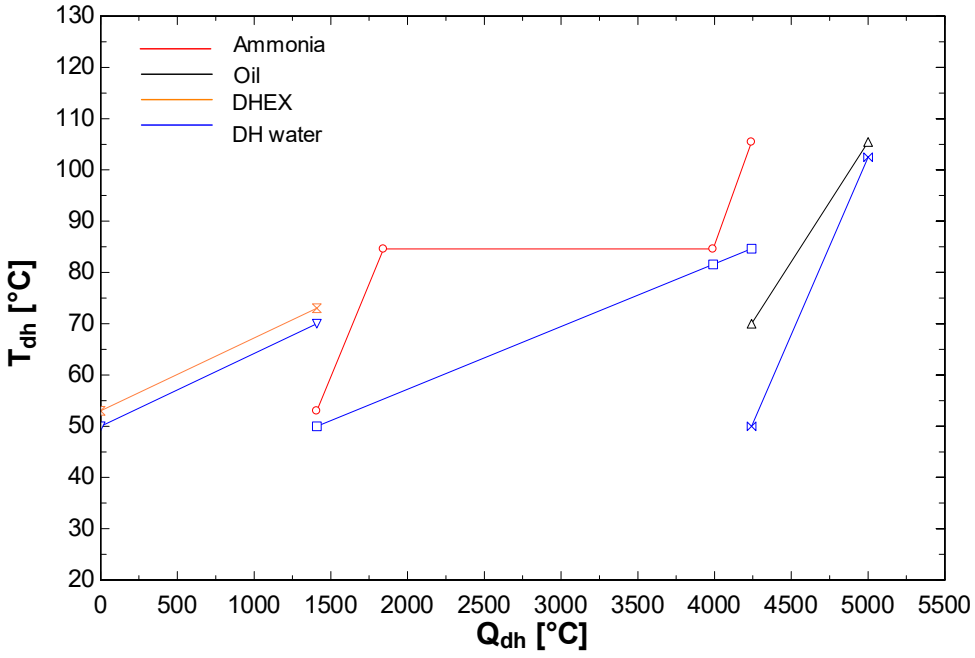

Figure 6.7– Q-T diagram for the 3rd configuration.

6.3.3 4th configuration

In this configuration a main stream of DH water passes through the succession of DHEX and condenser while a minor stream gets heated up by the oil cooler HEX.
The compressor model is: VR-V2655H-52
The main results are the following

- $COP_{tot} = 5.241$
- $COP_{hp} = 3.752$
- $T_{cond} = 79.49°C$
- $\dot{W}_{comp} = 95.39kW$
- $p_{min} = 7.05bar$
- $p_{max} = 40.95bar$
- $r_p = 5.809$
- $\dot{Q}_{dhex} = 14.21kW$
- $T_{max} = 102.1°C$
- $\eta_{is} = 0.769$
- $\dot{V}_{oil} = 70.0l/min$

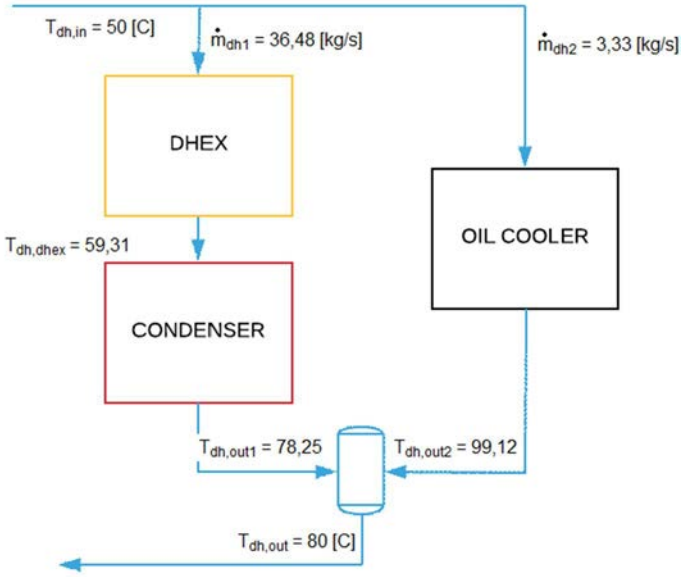

Figure 6.8– Block diagram for the 4th configuration.

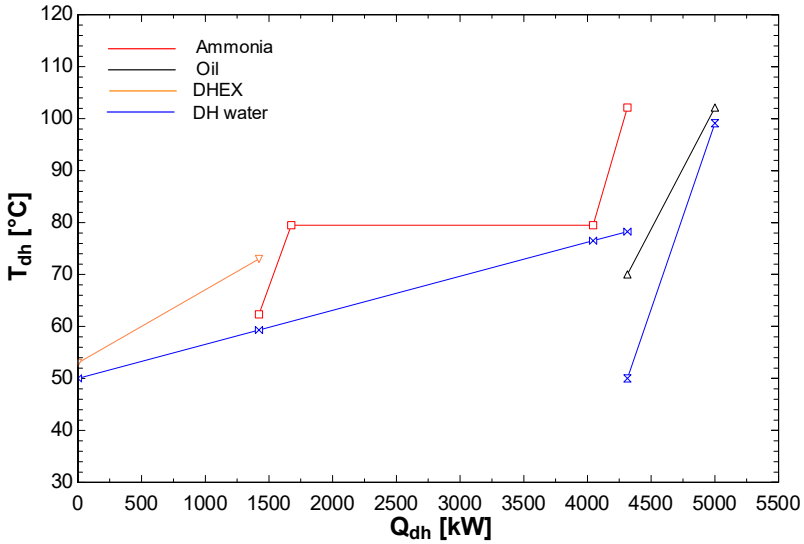

Figure 6.9– Q-T diagram for the 4th configuration.

6.3.4 5th configuration

The last and best configuration was obtained letting the whole DH water go through the DHEX in order to maximize its convenience and then splitting the stream into two and letting the stream to the oil cooler reach the maximum possible temperature in order to decrease the condensing temperature as much as possible.
The results are the following:

- $COP_{tot} = 5.275$
- $COP_{hp} = 3.774$
- $T_{cond} = 79.32°C$
- $\dot{W}_{comp} = 9.479kW$
- $p_{min} = 7.05bar$
- $p_{max} = 40.8bar$
- $r_p = 5.788$
- $\dot{Q}_{dhex} = 14.23kW$
- $T_{max} = 99.1°C$
- $\eta_{is} = 0.77$
- $\dot{V}_{oil} = 80.0l/min$

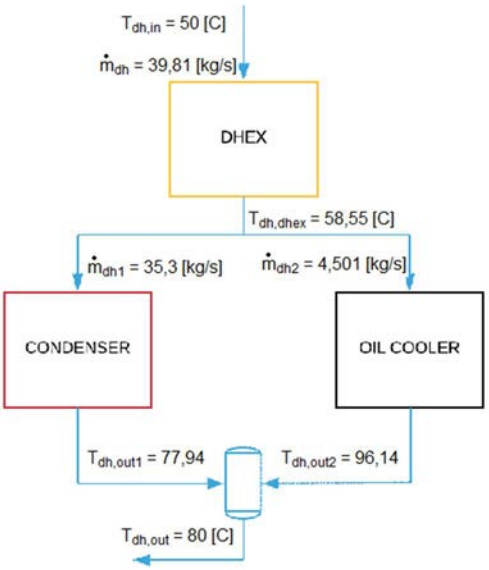

Figure 6.10– Block diagram for the 5th configuration

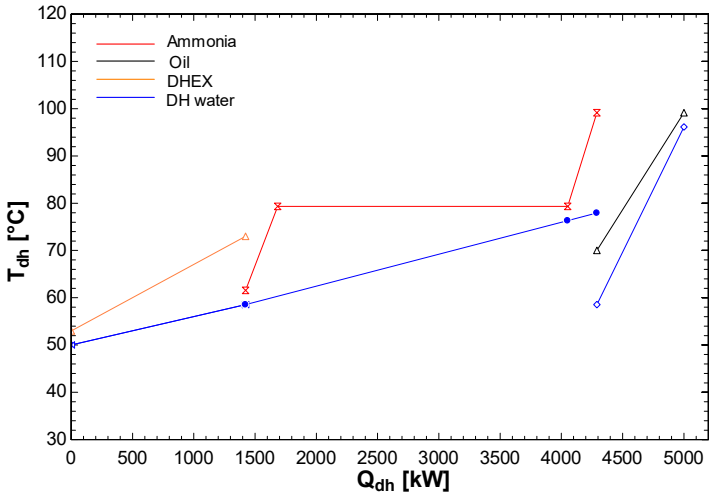

Figure 6.11– Q-T diagram for the 5th configuration

6.4 1-stage HP with piston compressor without oil cooling

A piston compressor without oil cooling can be used with refrigerants that don't reach high discharge temperature and are therefore compatible with this solution; such refrigerants, differently from ammonia, work at lower pressures and when compressed only reach limited superheated gas temperatures. In this application R-290 (propane) and different HFOs (R-134ze(E),R-1234yf,R-1243zf) were used.

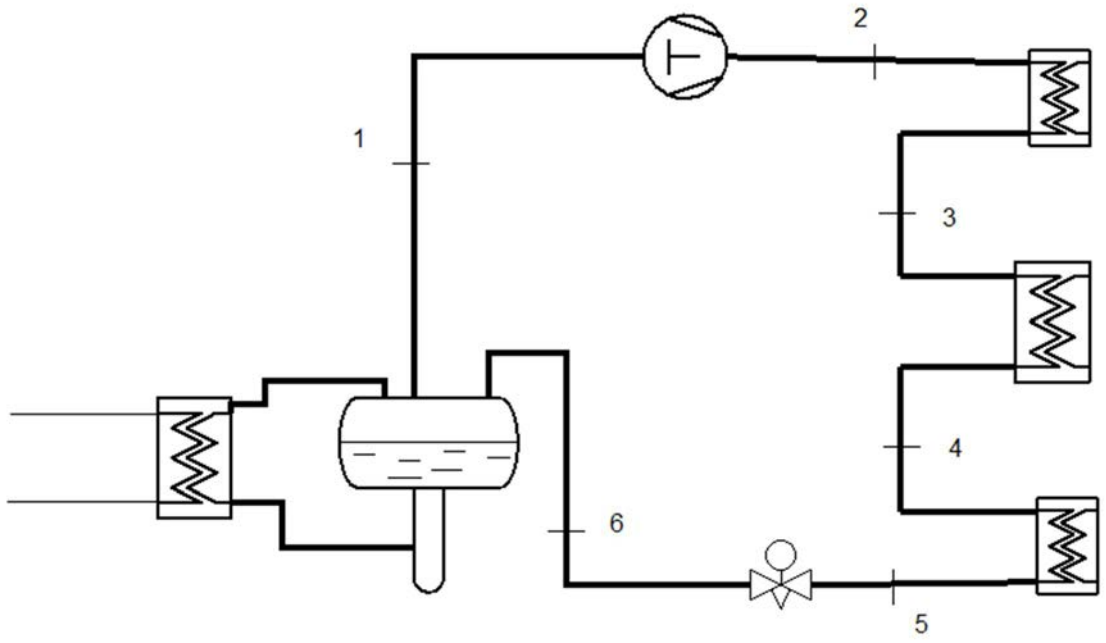

Figure 6.12– Scheme of the 1-stage model with piston compressor.

With these refrigerants it was difficult, if not impossible, to find suitable compressors for this application, so standard values of isentropic efficiency ($\eta_{is} = 0{,}75$) were used.
Initially the model was designed without direct heat exchanger, and the best solution was found using R-1234ze(E). The results are presented below.

- $COP_{hp} = 3{,}726$
- $T_{cond} = 81{,}76°C$
- $\dot{W}_{comp} = 13{,}42kW$
- $p_{min} = 3{,}54bar$
- $p_{max} = 20{,}84bar$
- $r_p = 5{,}8$
- $\eta_{is} = 0{,}75$
- $T_{max} = 85{,}13°C$
- $\dot{m}_{ref} = 3{,}131kg/s$
- $\dot{V}_{inlet} = 59{,}28m^3/h$
- $\dot{V}_{outlet} = 93{,}46m^3/$

The model provides a lower COP when compared to the basic model with the screw compressor. However, the most important difference is given by the mass and volumetric flowrate of the refrigerant. In fact, R-1234ze(E) has a smaller volumetric

capacity so a much larger amount of it is required to obtain the 5 MW design capacity of the system.
Finally, it can be said that the results with the other refrigerant are the following:

- R-1243zf → COP=3.722
- Propane → COP=3.709
- R-1234yf → COP=3.69

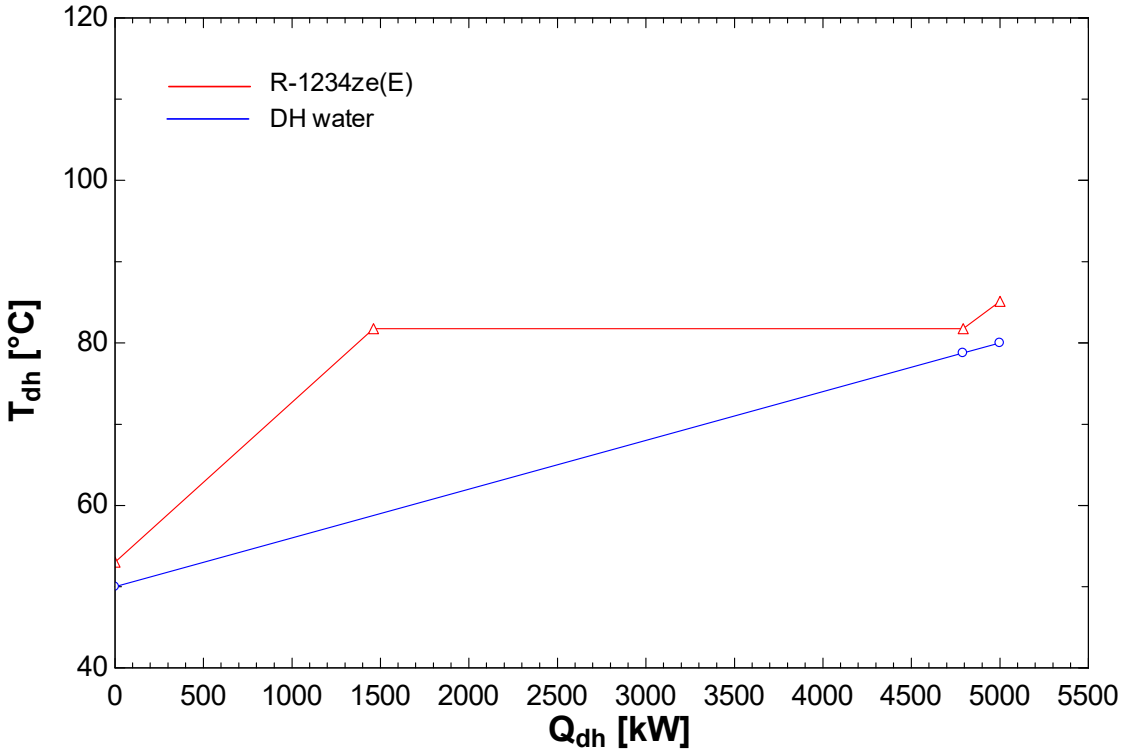

Figure 6.13– Q-T diagram for the piston configuration without DHEX

6.5 Configurations with direct heat exchanger

As it was done for the ammonia configurations, also now the direct heat exchanger will be added to the basic model, to see how much improvement it can bring.
Since no oil cooler is considered, the number of possible configurations is limited to 2, that are the series or the parallel of DHEX and condenser.

6.5.1 2nd configuration

The first configuration consists of the series of DHEX and condenser; the most performing refrigerant with this configuration is still R-1234ze(E).

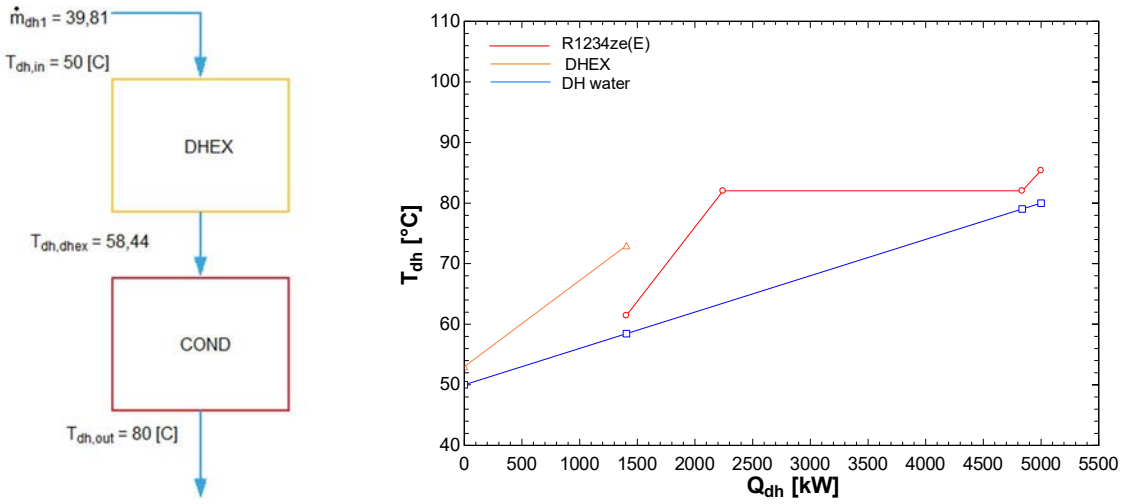

Figure 6.14– Block diagram and Q-T diagram for the 2nd configuration

The results are the following:

- $COP_{tot} = 4755$
- $COP_{hp} = 36$
- $T_{cond} = 8202°C$
- $\dot{W}_{comp} = 1051kW$
- $p_{min} = 354bar$
- $p_{max} = 2096bar$
- $r_p = 5916$
- $\eta_{is} = 075$
- $T_{max} = 8513°C$
- $\dot{m}_{ref} = 2447kg/s$
- $\dot{V}_{inlet} = 4632m^3/h$
- $\dot{V}_{outlet} = 7254m^3/h$
- $Q_{dhex} = 1405kW$

As expected, the overall COP increased of around 0.8 points, allowing a 30% reduction in refrigerant charge and so a much better usage of the heat source.

6.5.2 3rd configuration

The second and best configuration consists of the parallel of DHEX and the condenser, where the temperature after the condenser has to be higher than 80 °C to obtain the right temperature after the mixing with the stream that goes through the DHEX. Nonetheless, the COP is quite higher compared to the previous configuration, as shown below in the results.
This is probably due to the fact that this configuration allows the best utilization of the DHEX.

The best refrigerant in this situation is R-1243zf, but the performances of R-1234ze(E) (COP=4.958) and propane (COP=4.952) are very close, almost identical.

- $COP_{tot} = 496$
- $COP_{hp} = 3738$
- $T_{cond} = 8643°C$
- $\dot{W}_{comp} = 1008kW$
- $p_{min} = 42bar$
- $p_{max} = 2512bar$
- $r_p = 5982$
- $\eta_{is} = 075$
- $T_{max} = 8513°C$
- $\dot{m}_{ref} = 1994kg/s$
- $\dot{V}_{inlet} = 3736m^3/h$
- $\dot{V}_{outlet} = 5848m^3/h$
- $Q_{dhex} = 1420kW$

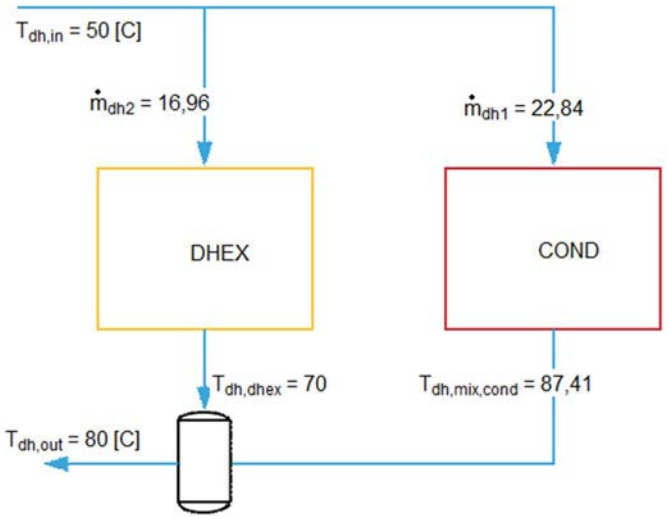

Figure 6.15– Block diagram for the 3rd configuration

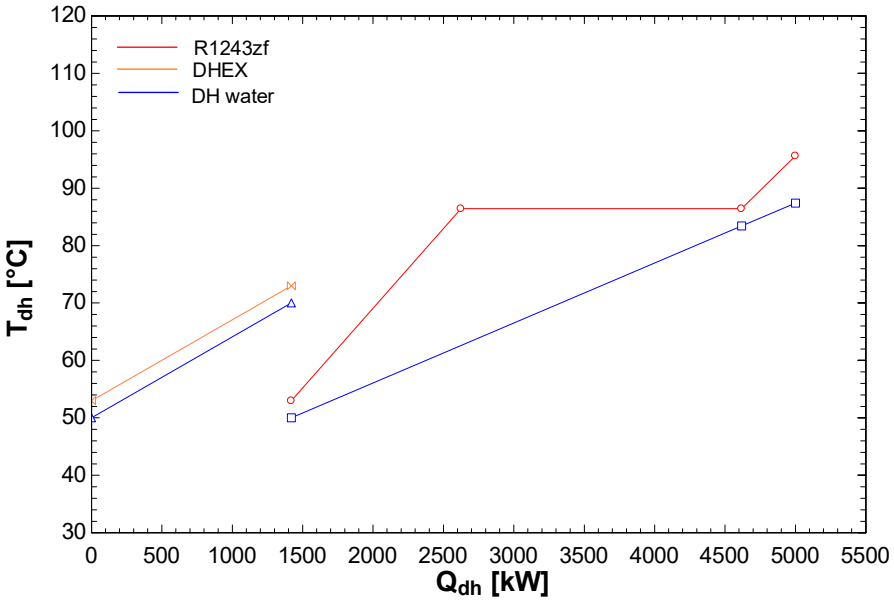

Figure 6.16– Q-T diagram for the 3rd configuration

6.6 Resume

The performances of the different 1-stage configurations are summarised in the bar graph below.
What emerges clearly from the graph is the impact of the DHEX for all the considered refrigerants; its presence gives an increase from 20% to 30% to the COP compared to the simple cycle without the direct heat exchanger.
Another important point is that the best configuration with ammonia provides a better COP than the best configuration with HFO's refrigerants.

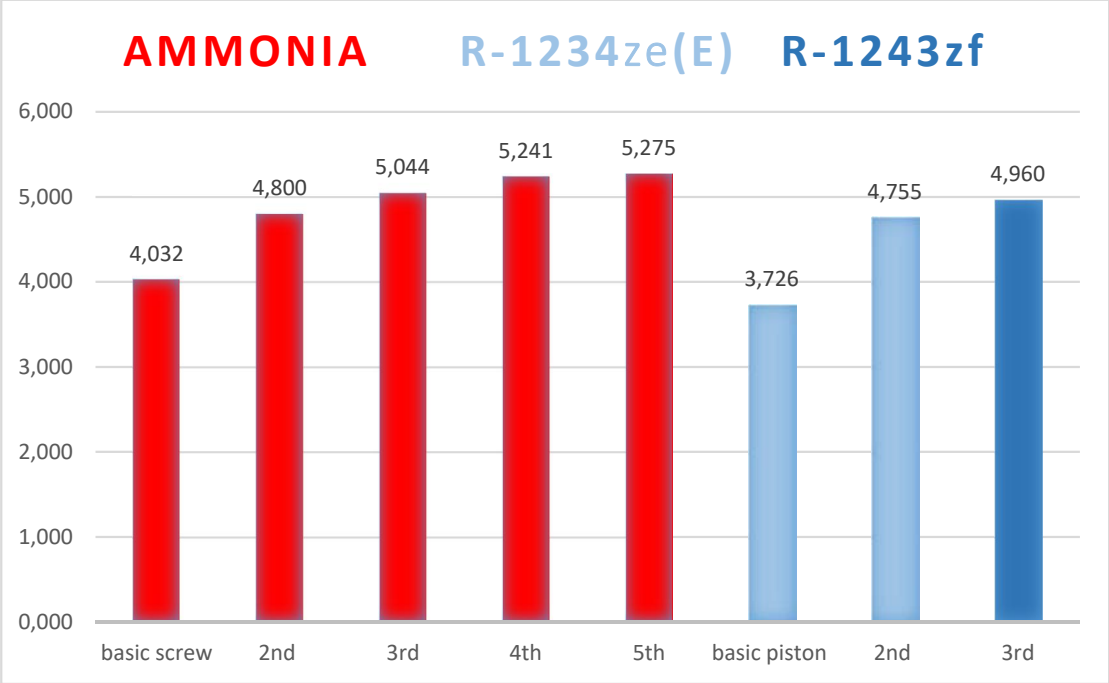

Figure 6.17– Performances of the different 1-stage configurations.

6.7 2-stage configurations

At this point all the 1-stage configurations that have been studied up to now were adjusted as 2-stage cycles, to verify the improvement that can be obtained by dividing the compression work into two steps.
The 2-stage cycle configurations differ from the 1-stage for the presence of an intermediate pressure between the two stages of compression.
For the screw compressors with oil cooling the scheme of the cycle that is used as a reference is the one presented in the figure 2.4 (paragraph 2.4), in which an open intercooler separates the two stages and a low-stage desuperheater uses the heat available after the first compressor.
For the piston compressors applications the cycle is similar to the one shown below, where the presence of the low stage desuperheater is not necessary due to the low temperatures reached by the refrigerant gas after the compression.

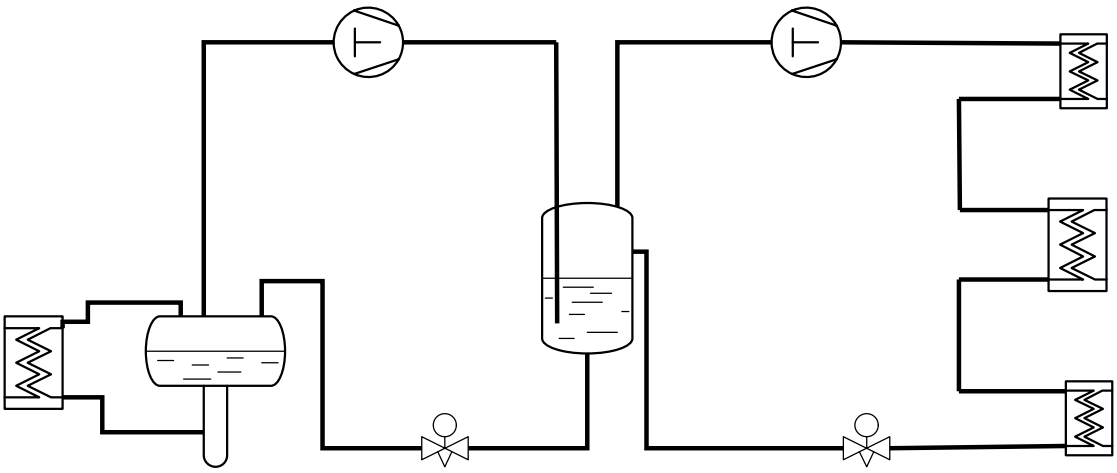

Figure 6.18– Scheme of a 2-stage piston cycle.

The configurations of the 2-stages cycle are exactly the same as shown before in this chapter, so only the main results will be reported, to highlight the overall improvement that was achieved with this solution.
One last consideration regarding the choice of the intermediate pressure has to be made before presenting the results; in a 2-stage cycle with ideal compression processes the optimal pressure is given by the equation:

$$p_{opt} = \sqrt{p_{ev} * p_{cond}} \tag{6.1}$$

However, when modelling real cycles it can be noticed that the intermediate pressure (and the consequent temperature) that gives the best overall COP is usually slightly higher; nonetheless, when choosing the right compressor for the high-pressure stage, it was observed that when increasing the intermediate temperature, the isentropic efficiency of the selected compressor was decreasing significantly.

So finally, a compromise was made to choose the right intermediate temperature, as the temperature for which the COP is higher and the isentropic efficiency of the compressor is high enough not to penalize the overall COP.
This considerations can be found explicitly in the table with the results that is presented below.

Table 6.1 – Main results from the 2-stage configurations

Configuration	Compressor Efficiency: Low-stage High-stage	Pressure ratio: Low-stage High-stage	Condensing Temperature [°C]	Intermediate Temperature (optimal)	Overall COP (improvement)
Basic screw (ammonia)	$\eta_{is1} = 0,83$ $\eta_{is2} = 0,72$	$r_{p1} = 2,6$ $r_{p2} = 2,2$	$T_{con} = 795$	$T_{int} = 46$ $(T_{int} = 43)$	4,189 (+3.9 %)
2nd ammonia configuration	0,815 0,7	2.6 2.7	89	46 (47)	5.197(+8.3%)
3rd ammonia configuration	0,815 0,7	2.73 2.51	87,4	48 (46)	5.318(+5.4%)
4th ammonia configuration	0,815 0,68	2.73 2.2	81	48 (44)	5.5(+4.9 %)
5th ammonia configuration	0,825 0,7	2.74 2.2	81	48 (44)	5.61(+6.3%)
Basic piston (R1234-ze(E))	0,75 0,75	1.85 3.1	82	35 (57)	3.91(+4.9%)
2nd R1234-ze(E) configuration	0,75 0,75	2 2.9	82	38 (58)	5.194(+9.2%)
3rd R1234-ze(E) configuration	0,75 0,75	2.285 2.9	88	42 (63)	5.132(+3.5%)

Significant improvements emerge both for ammonia and R-1234ze(E) configurations, with an average increase of 4.8% for the natural refrigerant and 5.8% for the HFO.
For the ammonia configurations is important to point out the relevance of the isentropic efficiency of the high pressure stage compressor: its low value impact the COP far more than the variation of the intermediate temperature. If compressors with higher efficiency were available, the improvements obtained with the 2-stages cycles would be way more relevant.
For the configurations with R-1234ze(E) the most relevant result that emerges from the table above is the great disparity between the intermediate temperature predicted by the expression mentioned above and the actual temperature that provides the highest COP for each configuration.
This can be explained with the particular shape of the pressure-enthalpy diagrams of the HFOs substances, which differ a lot compared to ammonia or other more common substances.
In fact if the intermediate temperature was as high as predicted by the above expression, the refrigerant after the high-stage expansion device would be still at liquid phase,

meaning that at the exit of the low-stage expansion valve the refrigerant would be at a much higher quality.
Therefore more refrigerant would be necessary to extract the same heat at the evaporator, with a relevant increase in the compressors power.

6.8 Multiple 2-stage HPs configurations without DHEX

Considering the size of the system, a very large quantity of heat is transferred at constant temperature at the condenser of the cycle; this means that the heat exchange profiles will stay quite separated for a major portion of the total heating capacity.
A way to make the profiles closer to each other is designing a system with two HPs in series at two different temperature levels, so that the heat at the condenser is transferred at two different condensing temperature, each one being closer to the temperature of the district heating water.
In this first case the DHEX won't be used, to compare the improvement of this design to the basic configurations studied before. Then the results will give a more clear idea about the impact of the DHEX and adjustments will be done accordingly.
The reference cycle scheme is presented below.

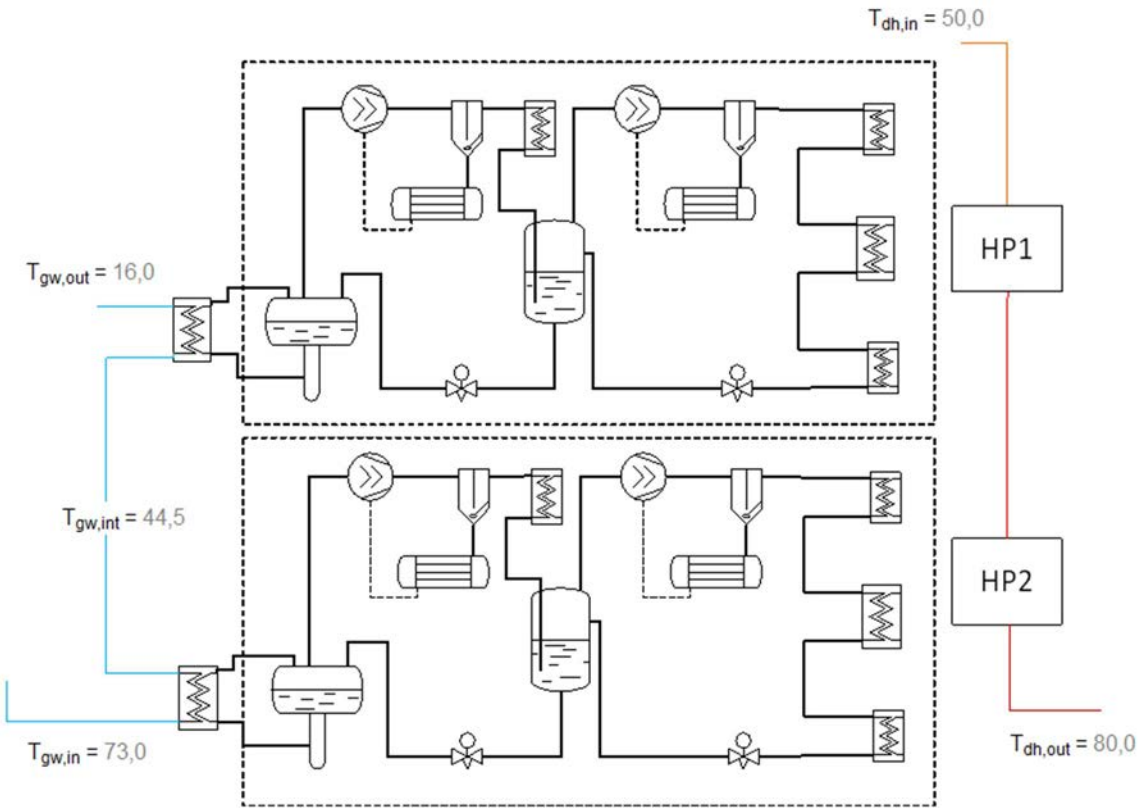

Figure 6.19– Scheme of a system of 2 HPs connected in series.

6.8.1 Ammonia 2 serially connected HPs configuration

This ammonia configuration consists of two HPs with the evaporators connected in series and both with the same capacity. The low-temperature HP works with an evaporating temperature $T_{ev} = 14°C$ $(p_{ev} = 7.05bar)$, a condensing temperature $T_{cond} = 69°C$ $(p_{cond} = 32.4bar)$ and an intermediate temperature $T_{int} = 42°C$ $(p_{int} = 16.4bar)$; its COP is equal to 4.7.
The high temperature one operates between an evaporating temperature $T_{ev} = 42.5°C$ $(p_{ev} = 16.7bar)$, a condensing temperature $T_{cond} = 82°C$ $(p_{cond} = 43.23bar)$ and an intermediate temperature $T_{int} = 55°C$ $(p_{int} = 23.1bar)$; its COP is equal to 5.84.
The heat exchangers have been placed so that the subcoolers and the low stage desuperheaters are used for heating the first part of the DH water, in order to use all the possible heat at lower temperature. The configuration then appears as presented below.

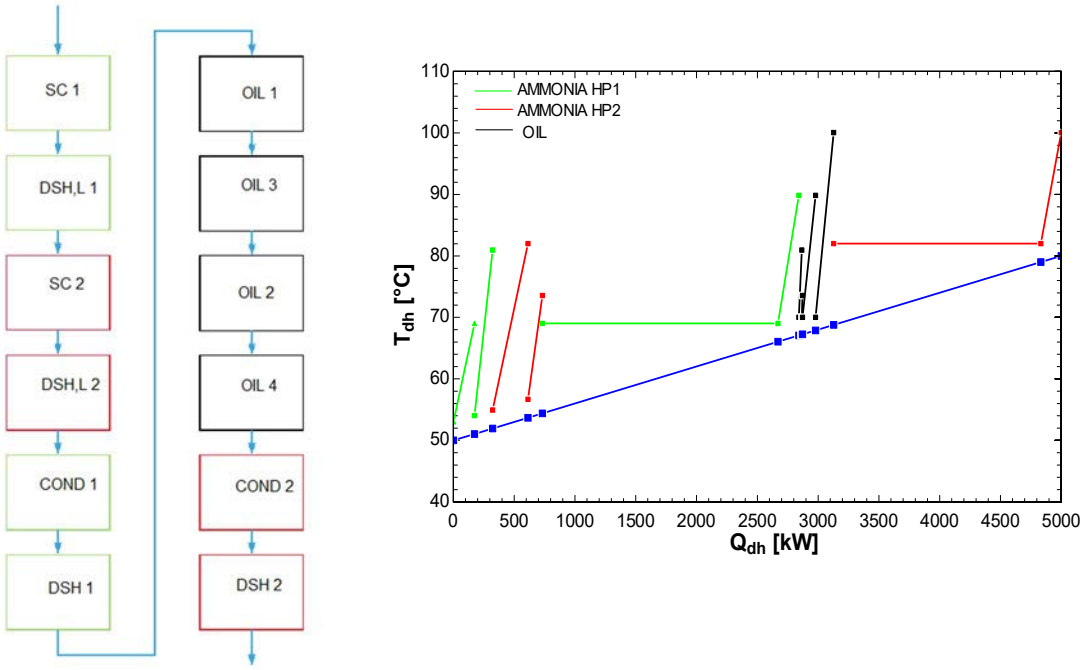

Figure 6.20 Block diagram and Q-T diagram for the 2 HPs configuration

The model for the HP working at high temperature presented some issues about the compressor selection; in fact the unusual operating conditions forced to select compressors working with a very low isentropic efficiency (below 0.65) and this element constituted a relevant penalization for the overall COP. However the resulting COP (5.195) is quite high considering the absence of the DHEX and compared to the basic 2-stage single HP configuration (COP=4.189). This results confirmed what was already expected, that the DHEX is necessary, but that a single HP is probably not efficient enough compared to this multiple HPs solution.

6.8.2 R1234ze(E) 2 serially connected HPs configuration

For the HFOs the reference cycle is the same represented above but with piston compressors without oil cooling and no low-stage desuperheaters. The heat exchanger network (that can be seen in the diagrams below) is built around the same concept, with one DH water stream passing through the series of heat exchangers and getting heated up from 50 to 80°C. The isentropic efficiency of the four compressors is fixed at the standard value of 0.75.

The first HP operates between an evaporating temperature $T_{ev} = 14°C$ (corresponding to a pressure $p_{ev} = 3.5 bar$) and a condensing temperature $T_{cond} = 72.2°C$ ($p_{cond} = 16.95 bar$) with an intermediate temperature $T_{int} = 34°C$ ($p_{int} = 6.5 bar$). Its COP is equal to 4.3.

The second HP works between an evaporating temperature $T_{ev} = 4.25°C$ ($p_{ev} = 8.2 bar$) and a condensing temperature $T_{cond} = 82.6°C$ ($p_{cond} = 21.2 bar$) with an intermediate temperature $T_{int} = 57°C$ ($p_{int} = 11.9 bar$). Its COP is 6.65.

The overall COP is 5.172, significantly higher than 3.91, which was the COP of the basic 2-stage piston configuration. The main differences with the ammonia configuration are the reduced maximum working pressures (21.2 vs 43 bar), the lower maximum temperatures of the cycle (82 vs 100°C) and the much larger volumetric flowrate of the refrigerant at the inlet of the low stage compressor (2600 m^3/h vs 1200 m^3/h).

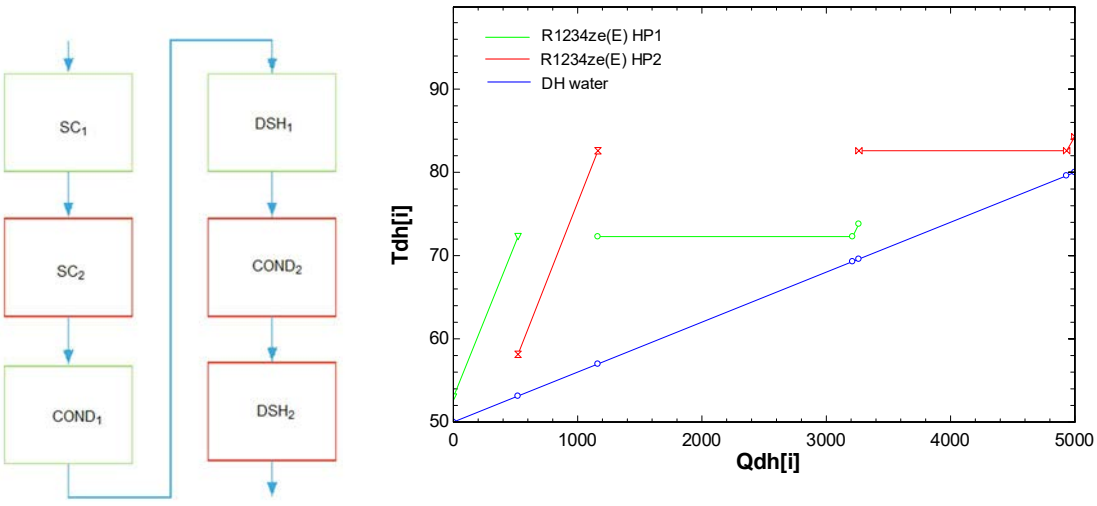

Figure 6.21– Block diagram and Q-T diagram for the 2 HPs configuration using R1234ze(E)

6.9 2 HPs connected in series with DHEX

What emerged from the last results is that even if a solution with two heat pumps shows great improvements over the single HP configurations, the absence of the DHEX is a significant drawback, since the best 1-stage solution with DHEX provides a higher COP compared to the configuration with ammonia using 2 HPs (5.61 vs 5.195).
As a consequence of that, the possibility of having multiple heat pumps combined with the direct heat exchanger has been considered, and in these paragraphs this solution will be presented both for ammonia and for R1234ze(E).
When this solution will be proved to be the most efficient one, it will also be optimized using the pinch method, to obtain the best thermodynamically achievable performance of the system.

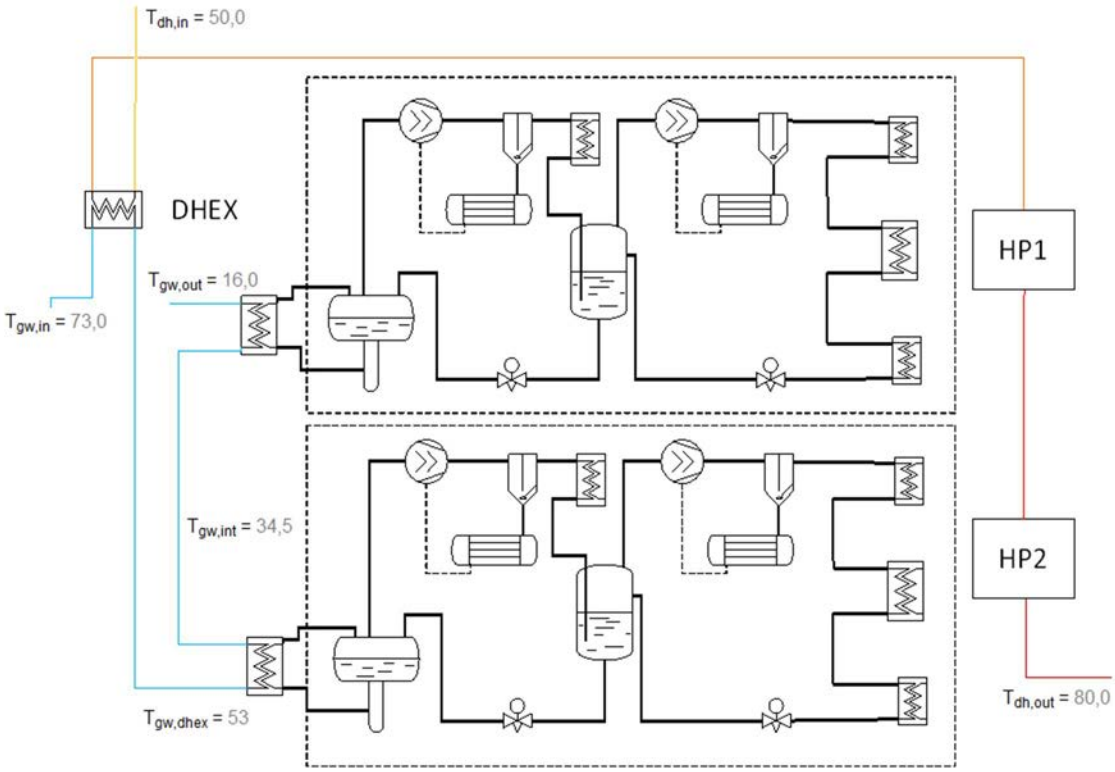

Figure 6.22– Scheme of the DHEX and 2 HPs configuration

6.9.1 Ammonia configuration with 2 HPs and direct heat exchanger

In this configuration, the direct heat exchanger is placed at the beginning of the series of heat exchangers, so that it transfers heat to the first portion of the DH water stream. The cycles of the 2 HPs are represented in the following p-h diagram.

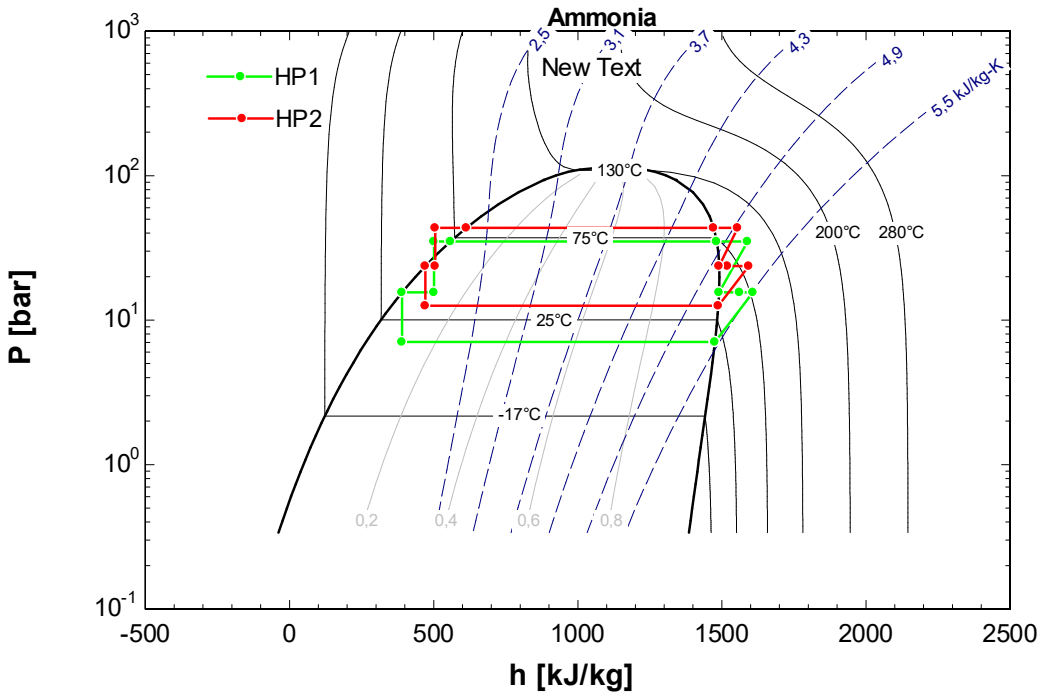

Figure 6.23– p-h diagram for the double HP ammonia configuration

Except for the presence of the DHEX, the configuration of the HEN is built as in the previous case, and as it is shown in the two diagrams below.

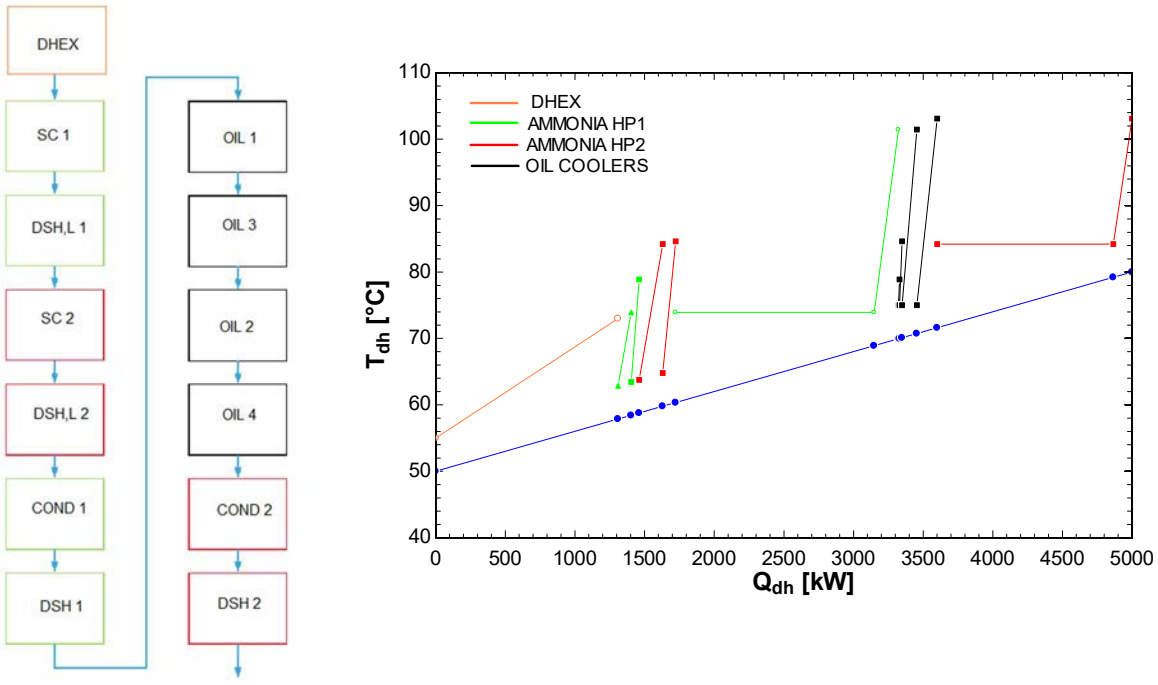

Figure 6.24– Block diagram and Q-T diagram for the considered configuration

For this configuration a temperature difference equal to 5 °C was kept for all the seven heat exchangers for which a minimum temperature difference was set (DHEX, subcoolers, low-stage desuperheaters, condensers).

The reason for this is that when the pinch method will be used to optimize the cycle, this temperature differences will be optimized starting from the value of 5 °C, but the new optimized temperature differences will be the best possible scenario, also compared to the case in which they are equal to 3 °C. The resulting COP is 5.8371, which is higher than any configuration using a 3 °C temperature difference that has been analysed so far. This result is quite promising, considering that with all the hot streams present in the system, there should be a huge potential of improvement using the pinch method. The operating condition of the two HPs are presented below.

Table 6.2 – Operating conditions for the 2HPs plus DHEX ammonia configuration

	PARAMETER	NOTATION	VALUE	UNITS
HP1	Coefficient of Performance	COP	4.18	/
	Evap. temperature	T_{ev}	14	°C
	Evap. pressure	p_{ev}	7	bar
	Int. temp. (opt.)	T_{int}	40(41)	°C
	Int. pressure (opt)	p_{int}	15.5 (15.9)	bar
	Cond. temperature	T_{cond}	73.9	°C
	Cond. pressure	p_{cond}	36.2	bar
HP2	Coefficient of Performance	COP	4.45	/
	Evap. temperature	T_{ev}	33.5	°C
	Evap. pressure	p_{ev}	12.9	bar
	Int. temp. (opt.)	T_{int}	56 (57)	°C
	Int. pressure (opt)	p_{int}	23.7 (24.21)	bar
	Cond. temperature	T_{cond}	84	°C
	Cond. Pressure.	p_{cond}	45.3	bar
OVERALL	Coefficient of Performance	COP	5.837	/

The heat obtained at the DHEX is $\dot{Q}_{dhex} = 1310kW$.
The streams passing through the oil coolers are placed after the first condenser, and the temperature of the DH water at that point is already quite high, so the inlet temperature of the oil in the compressors has been adjusted to 75 °C.

Some data regarding the compressors operating conditions are now presented in the following table. The most critical component is the high pressure compressor of the second heat pump, that operates with very low isentropic efficiency.
These data were obtained from GEA's selection software RTselect.

Table 6.3 – Compressor models and data for the configuration with DHEX and serially connected HPs

Compressor function	**Selected model**	**Isentropic efficiency**	**Pressure ratio**	**Outlet pressure [bar]**	**Oil volumetric flowrate [l/min]**	**Discharge temperature [°C]**
Low-stage HP1	PR-P1830S-28	0.795	2.2	15.5	58	78.9
High-stage HP1	MMR-H17T-52	0.7	2.33	36.2	130	101.4
Low-stage HP2	MMR-H13T-52	0.715	1.83	23.7	66	84.6
High-stage HP2	ER-D13T-52	0.535	1.91	45.3	170	103.1

6.9.2 Pinch optimization for the ammonia configuration

The model that has just been presented has been optimized using the pinch method, as explained in the previous chapter. The function that has been maximized is the overall COP, whilst the variables that have been let free to vary are shown in the following table. The minimum temperature difference limit for the composite curves was set to 3 °C. The global COP changed from 5.8371 to 6.39 (+ 9.46%).
However, compared to the configuration with 3 °C for each heat exchanger the increase is 2.4% (6.24 vs 6.39). The heat flux at the DHEX is $\dot{Q}_{dhex} = 1481kW$.
The number of intervals N was set to 200.

Table 6.4 – Key temperatures and associated pinch temperature differences.

Key temperatures	**Associated variable**	**Variable meaning**	**Value before the optimization**	**Value after the optimization**
$\boldsymbol{T_{cond1}}$	ΔT_{cond1}	Temperature difference at the first condenser outlet	5	1.46
$\boldsymbol{T_{cond2}}$	ΔT_{cond2}	Temperature difference at the second condenser outlet	5	1.38
$\boldsymbol{T_{subcooler1}}$	$\Delta T_{subcooler1}$	Temperature difference at the first subcooler inlet	5	3.91
$\boldsymbol{T_{subcooler2}}$	$\Delta T_{subcooler2}$	Temperature difference at the second subcooler inlet	5	3.95
$\boldsymbol{T_{dsh1}}$	ΔT_{lsdsh1}	Temperature difference at the first low-stage desuperheater inlet	5	3.95
$\boldsymbol{T_{dsh2}}$	ΔT_{lsdsh2}	Temperature difference at the second low-stage desuperheater inlet	5	3.96
$\boldsymbol{T_{dhex}}$	ΔT_{dhex}	Temperature difference at the DHEX inlet	5	3.001
$\boldsymbol{T_{int1}}$	T_{int1}	Intermediate temperature HP1	40	40.132
$\boldsymbol{T_{int2}}$	T_{int2}	Intermediate temperature HP1	56	56.156

Observing the composite curves it is possible to appreciate the variation of the temperature profiles given by the optimization in the Q-T diagram.

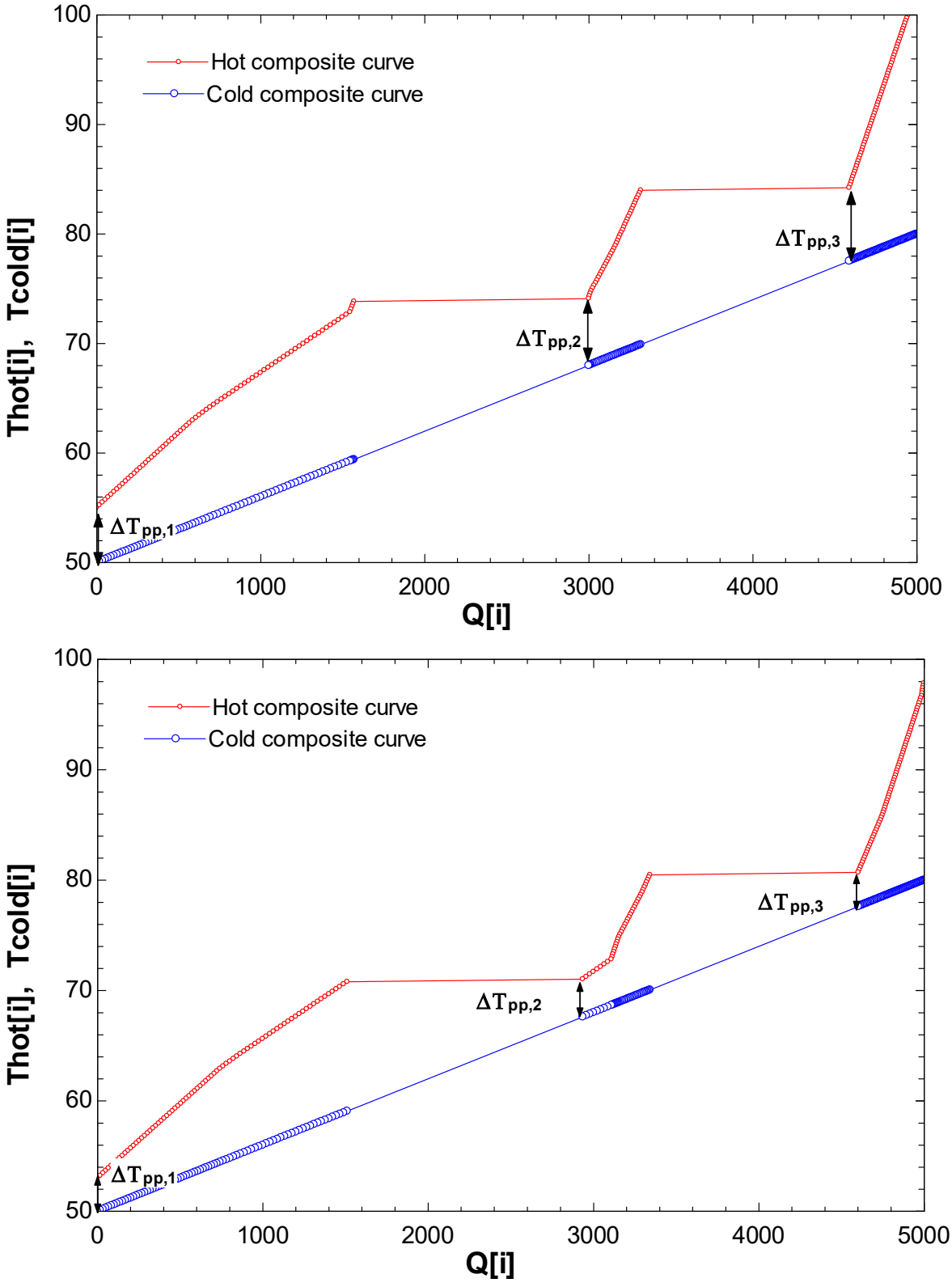

Figure 6.25– Comparison of the composite curves before (above) and after (below) the optimization

One thing must be noticed regarding the optimization; to obtain the final result the starting value of the independent variables had to be modified "by hand" to allow the optimization method to find the best solution. In fact if the guess values are kept equal to 5 the optimization doesn't work in the same way as when the guess values are modified to values closer to the final outcome; this is an aspect of the method that is difficult to explain but is probably due to the mathematical approach of the Variable Metric Method itself.
The optimization modifies the values of the key temperatures shown in the table and simultaneously check the values of the array containing all the temperature differences between hot and composite curves' points, in order to move the two curves closer to each other while keeping a minimum temperature difference equal to 3 °C between the curves. After the optimization was performed, three new pinch points are created, and their values are the following:

$$\Delta T_{pp1} = 3001°C$$
$$\Delta T_{pp2} = 3407\ 9°C \quad (6.2)$$
$$\Delta T_{pp3} = 3088\ 9°C$$

The other aspect that emerges from the composite curves is the decrease of the condensing temperatures that of course is the primary cause of the increase in the overall COP.
Not only the condensing temperatures are modified, but also all the other key temperatures related to the variables that were mentioned above.
The new values of the key temperatures are presented below:

$T_{cond1} = 739°C \rightarrow 709°C$

$T_{cond2} = 84°C \rightarrow 807°C$

$T_{sub1} = 6343°C \rightarrow 628°C$

$T_{sub2} = 6377°C \rightarrow 6358°C$

$T_{dshl1} = 6343°C \rightarrow 63251°C$

$T_{dshl2} = 6479°C \rightarrow 6441°C$

$T_{gwdhex} = 53°C \rightarrow 53001°C$

$T_{int1} = 40°C \rightarrow 40132°C$

$T_{int2} = 56°C \rightarrow 56156°C$

The consequence of this is that with the new set of key temperatures obtained from the pinch optimization it is possible to build a HEN that respects the new values of the pinch points temperature differences and that realizes the optimal COP.
This HEN was built splitting the streams that were crossing the two pinch points at the two temperatures related to the condensing processes.

In this way all the streams that are placed before the first condenser will have the same outlet temperature and so will have the DH water streams to which they are related. The same happens for the streams before the second condenser.
The HEN consists of 22 heat exchangers compared to the 13 of the not-optimized configuration.
The resulting HEN is here presented in a block diagram that shows also the temperatures of the DH water stream along the heat exchangers and the temperature differences obtained at the three pinch points, respectively at the inlet of the DHEX, at the outlet of the first and at the outlet of the second condenser.

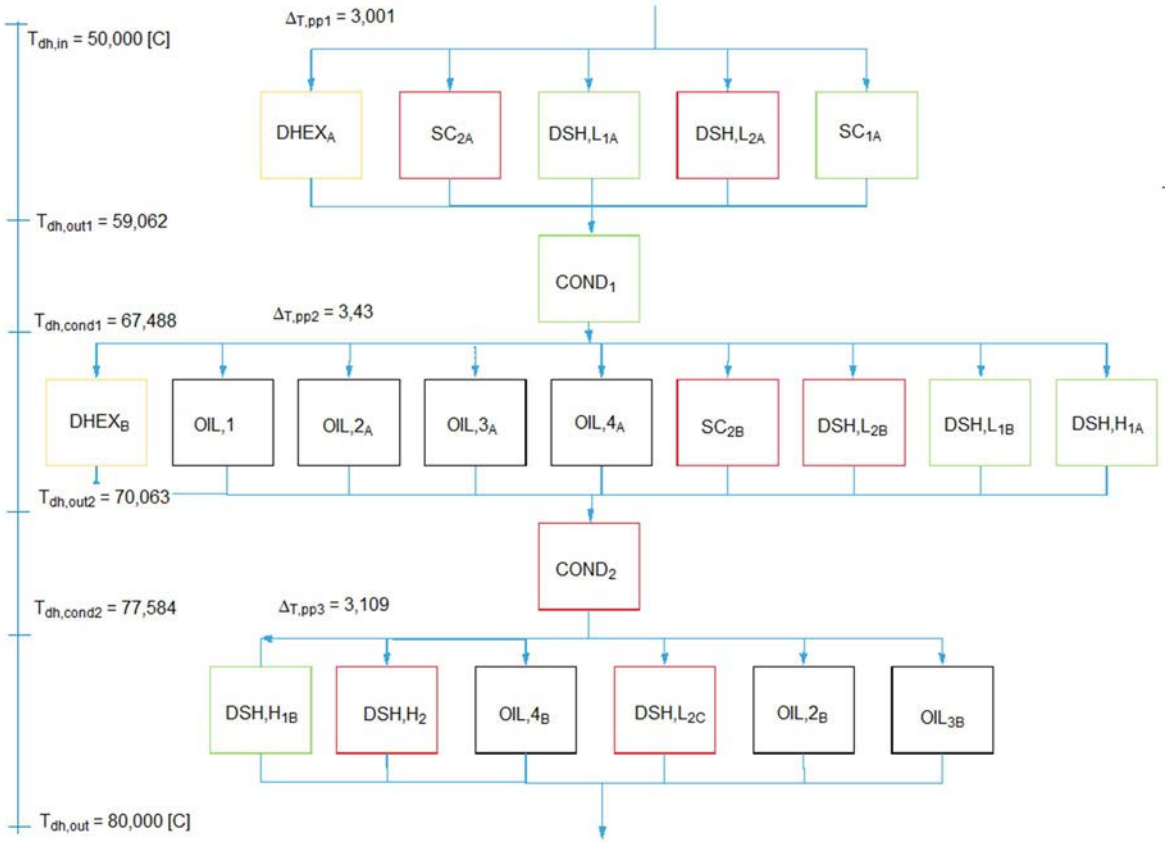

Figure 6.26– Resulting HEN with the DH water temperatures along it.

The three values are in accordance to what was obtained from the optimization:

$$\Delta T_{pp1,HEN} = 3001°C$$

$$\Delta T_{pp2,HEN} = 343°C$$

$$\Delta T_{pp3,HEN} = 3109°C$$

The fact that they are slightly higher is an expected result as the precision that is obtained with the ideal optimization is not achievable with the real HEN design.

The Q-T diagram for this HEN is presented below, together with the table containing all the temperature differences in every HEX and the related heat flux.

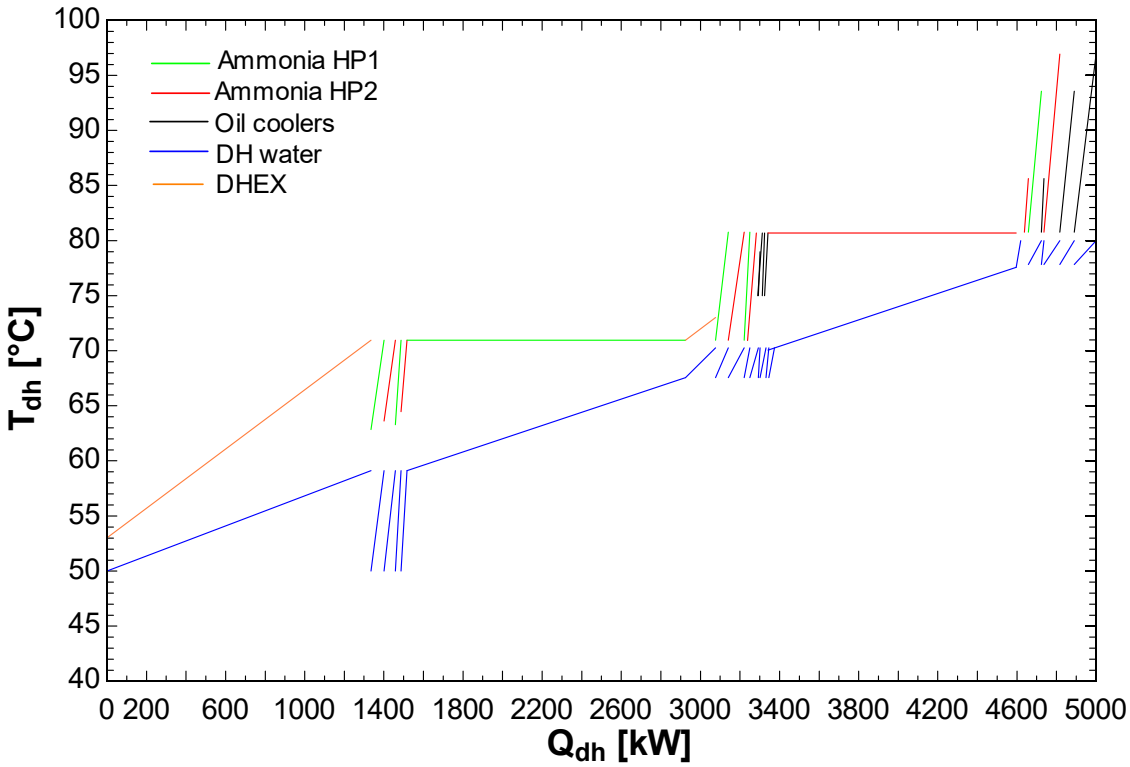

Figure 6.27– Q-T diagram for the 22 HEX of the considered HEN.

This diagram is useful to understand how the optimized composite curves are practically realized with the heat exchanger network and gives an idea about the distribution of the DH flows in the HEN.

In the following table is possible to explicitly see the heat load of every HEX and the operating temperature differences at the outlets and inlets of them.

Table 6.5 – Temperature differences and heat flux for every HEX

HEX cycle 1	ΔT_{inlet}	ΔT_{outlet}	$\dot{Q}[kW]$	HEX cycle 2	ΔT_{inlet}	ΔT_{outlet}	$\dot{Q}[kW]$
SC_{1A}	12.81	11.86	65.8	SC_{2A}	13.58	11.86	56.64
$DSHL_{1A}$	13.25	11.86	28.028	$DSHL_{2A}$	14.4	11.86	31.13
$DHEX_A$	3.001	11.86	1326.7	$DSHL_{2B}$	3.43	10.63	43.7
$COND_1$	11.86	3.43	1403.7	SC_{2B}	3.43	10.63	79.5
$DSHL_{1B}$	3.43	8.988	28.08	OIL_{3_A}	3.43	10.63	11.38
DSH_{1A}	3.43	10.63	64.432	OIL_{4_A}	3.43	10.63	17.43
OIL_{1_A}	3.43	8.98	7.08	$COND_2$	10.63	3.109	1254.6
OIL_{2_A}	3.43	10.63	22.53	$DSHL_{2C}$	3.109	5.977	22.5
$DHEX_B$	3.43	2.937	154.35	DSH_2	3.109	23.27	145.54
DSH_{1B}	3.109	16.9	91.42	OIL_{3_B}	3.109	5.977	10.56
OIL_{2_B}	3.109	16.9	64.27	OIL_{4_B}	3.109	23.27	69.15

The main results for the operating conditions of the optimized configuration are presented below.

Table 6.6 – Main results for the optimized configuration

HP 1			**HP 2**		
T_{ev}	14	$°C$	T_{ev}	32.5	$°C$
T_{int}	40.13	$°C$	T_{int}	56.15	$°C$
T_{cond}	70.9	$°C$	T_{cond}	80.7	$°C$
p_{ev}	7.05	bar	p_{ev}	12.56	bar
p_{int}	15.6	bar	p_{int}	23.8	bar
p_{cond}	33.8	bar	p_{cond}	42	bar
$r_{p,lowstage}$	2.21	-	$r_{p,lowstage}$	1.89	-
$r_{p,highstage}$	2.16	-	$r_{p,highstage}$	1.77	-
$\dot{m}_{ref,lowstage}$	1.26	kg/s	$\dot{m}_{ref,lowstage}$	1.35	kg/s
$\dot{m}_{ref,highstage}$	1.5	kg/s	$\dot{m}_{ref,highstage}$	1.44	kg/s
$\dot{V}_{ref,lowstage,inlet}$	818.7	m^3/h	$\dot{V}_{ref,lowstage,inlet}$	498.4	m^3/h
$\dot{V}_{ref,highstage,inlet}$	448.4	m^3/h	$\dot{V}_{ref,highstage,inlet}$	280.2	m^3/h
$\dot{Q}_{evap}$	1368.2	kW	$\dot{Q}_{evap}$	1368.2	kW
$\dot{Q}_{cond}$	1625.3	kW	$\dot{Q}_{cond}$	1505.2	kW
$\dot{Q}_{oil1}$	7.1	kW	$\dot{Q}_{oil1}$	21.9	kW
$\dot{Q}_{oil2}$	86.8	kW	$\dot{Q}_{oil2}$	118.4	kW
$\dot{Q}_{lsdsh}$	56.8	kW	$\dot{Q}_{lsdsh}$	97.27	kW
$\dot{W}_{comp1}$	175.1	kW	$\dot{W}_{comp1}$	166.1	kW
$\dot{W}_{comp2}$	232.7	kW	$\dot{W}_{comp2}$	208.5	kW
COP	4.35	-	**COP**	4.65	-

6.9.3 HFOs configuration with 2 HPs and direct heat exchanger

The same configuration that has been proved to be the best one for ammonia has been studied with R1234ze(E) to compare the performances of the two refrigerants.

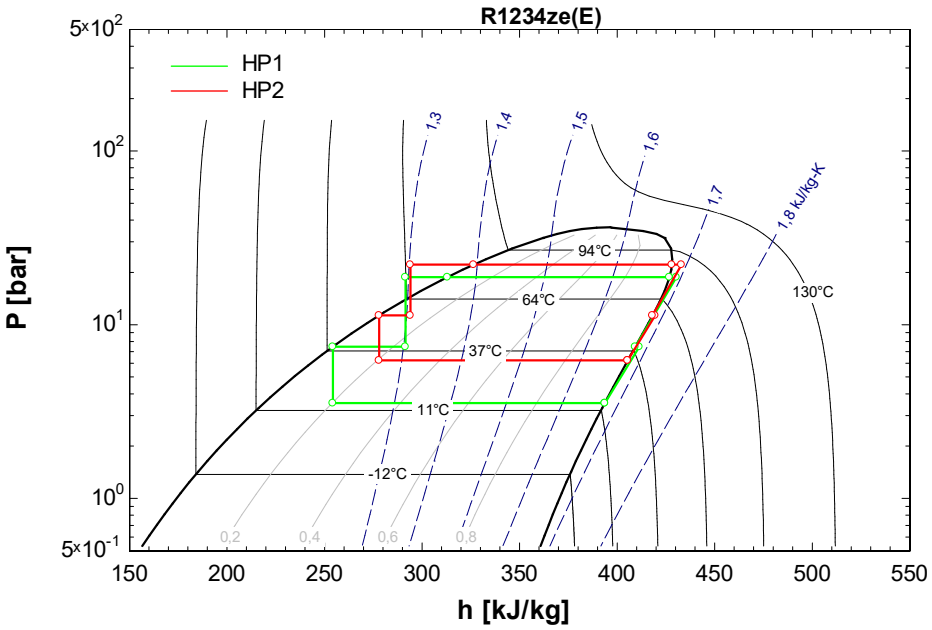

Figure 6.28– p-h diagram for the double HP R1234ze(E) configuration

The configuration of the system is presented in the two following graphs: a block diagram explaining the sequence of the heat exchangers and the Q-T diagram of the system.

A 5 °C temperature difference was used to define the key temperatures of the cycle, at the inlet of the DHEX, of the subcoolers and at the end of the condensers.

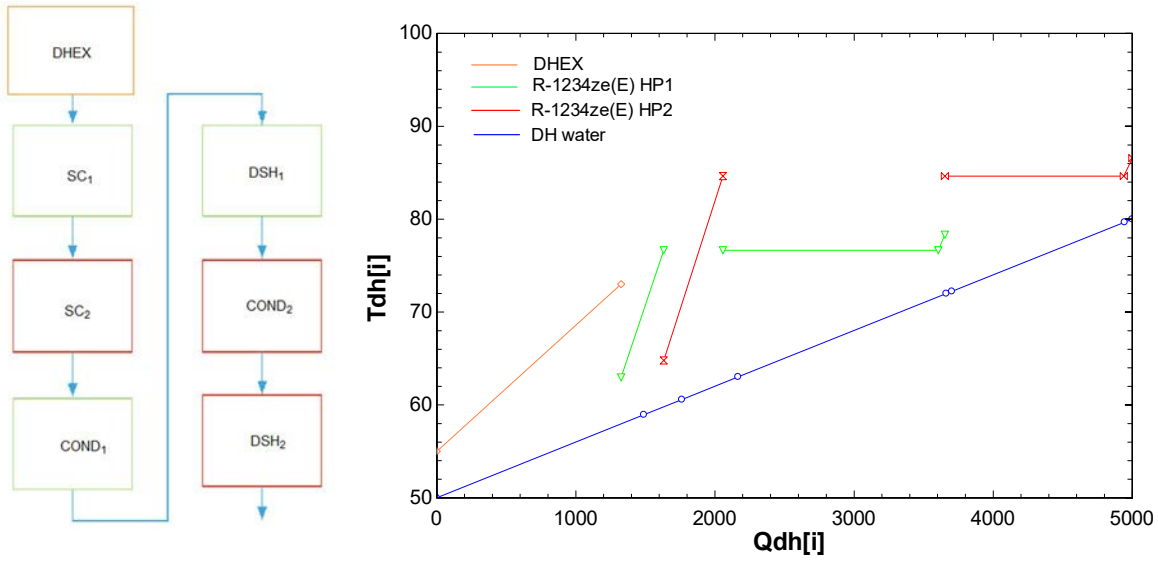

Figure 6.29– Block diagram and Q-T diagram for the considered configuration

This configuration provided a COP equal to 5.888, higher than the same configuration with ammonia (5.831). The heat from the direct heat exchanger is $Q_{dhex} = 1325kW$. The main parameters for the 2 HPs are presented in the following table.

Table 6.7 – Main results for the optimized configuration

	PARAMETER	NOTATION	VALUE	UNITS
HP1	Coefficient of Performance	COP	3.872	/
	Evap. temperature	T_{ev}	14	°C
	Evap. pressure	p_{ev}	3.5	bar
	Int. temp. (opt.)	T_{int}	39 (42.1)	°C
	Int. pressure (opt)	p_{int}	7.4 (8.1)	bar
	Cond. temperature	T_{cond}	76.6	°C
	Cond. pressure	p_{cond}	18.7	bar
HP2	Coefficient of Performance	COP	4.951	/
	Evap. temperature	T_{ev}	33.5	°C
	Evap. pressure	p_{ev}	6.4	bar
	Int. temp. (opt.)	T_{int}	57 (57.1)	°C
	Int pressure (opt)	p_{int}	11.8 (11.91)	bar
	Cond. temperature	T_{cond}	84.6	°C
	Cond. Pressure.	p_{cond}	22.1	bar
OVERALL	Coefficient of Performance	COP	5.888	/

What emerges from the table is that at higher temperatures the heat pump for the HFO works better compared to the ammonia configuration. This result is clearly affected by the isentropic efficiencies for the screw compressors at high temperatures, where they drop; for this application instead they remain constant (equal to 0.75), making it easier to reach high efficiencies in the second HP. One consideration that can be made looking at the Q-T diagram is that there are not many streams that cross potential pinch points

in the system. This can help predicting that probably the pinch analysis could be less impactful in this application because the streams are naturally already quite integrated.

6.9.4 Pinch optimization for the HFO configuration

A problem was encountered when applying the pinch method to the configuration using R1234ze(E); in fact because of the overlapping of the saturated vapour curve to the constant entropy lines, some errors were found during the optimization because the varying condensing temperature was getting to some points in which the thermodynamic functions were not converging. For this reason another refrigerant with similar properties, the R1243zf, was used for the optimization. With this refrigerant these kinds of errors were avoided.
Before explaining the results of the optimization, it´s important to compare the performances of the two refrigerants for the same application with 5 and 3 °C as temperature differences to show how close they are. That emerges from the next table but also from the similarities between the p-h diagrams for the two refrigerants, as it is shown below.

Table 6.8 – Comparison of the performances between R1234ze(E) and R1243zf

	Overall COP ($\Delta T = 5°C$)	Overall COP ($\Delta T = 3°C$)
R1234ze(E)	5.888	6.276
R1243zf	5.86	6.245

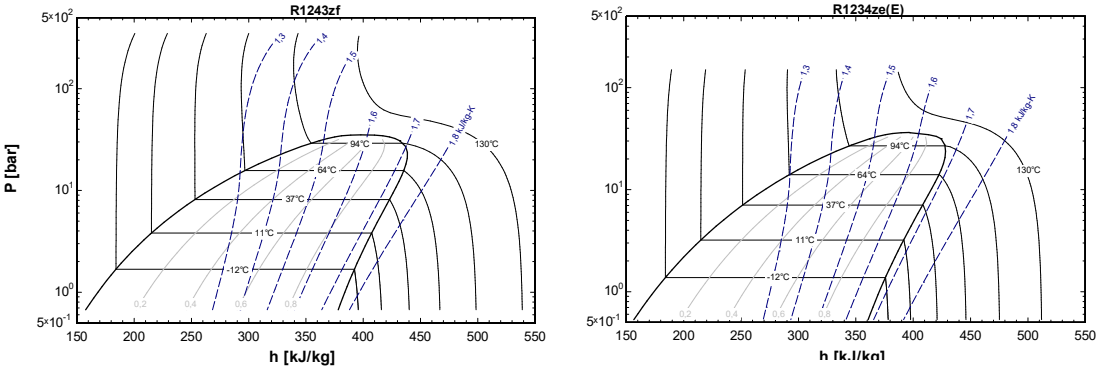

Figure 6.30– Comparison between the saturation curves of R-1243zf and R-1234ze(E)

The optimization has been done with the same procedure as before, giving a certain number of degrees of freedom to the system and maximizing the objective function that is the COP. In this case the low-stage desuperheaters are not present, so the number of degrees of freedom is 7. The resulting COP is 6.287, meaning an improvement of 7.2 % compared to the case with 5°C as temperature difference and 0.67 % compared to

the case with 3°C as temperature difference in the heat exchangers. As expected the pinch method is not as effective as in the ammonia case, because the hot streams of the system don't have many pinch crossing points, and so the process integration is less impactful. The heat load of the DHEX is $\dot{Q}_{dhex} = 1490kW$.
In the next table the free variables of the system are shown together with the related change obtained from the optimization.

Table 6.9 – Key temperatures and associated pinch temperature differences.

Key temperatures	**Variable name**	**Variable meaning**	**Value before the optimization**	**Value after the optimization**
$\boldsymbol{T_{cond1}}$	ΔT_{cond1}	Temperature difference at the first condenser outlet	5	1.856
$\boldsymbol{T_{cond2}}$	ΔT_{cond2}	Temperature difference at the second condenser outlet	5	3.17
$\boldsymbol{T_{subcooler1}}$	$\Delta T_{subcooler1}$	Temperature difference at the first subcooler inlet	5	3.23
$\boldsymbol{T_{subcooler2}}$	$\Delta T_{subcooler2}$	Temperature difference at the second subcooler inlet	5	3.25
$\boldsymbol{T_{dhex}}$	ΔT_{dhex}	Temperature difference at the DHEX inlet	5	3.0195
$\boldsymbol{T_{int1}}$	T_{int1}	Intermediate temperature HP1	39	38.998
$\boldsymbol{T_{int2}}$	T_{int2}	Intermediate temperature HP1	50	49.99

After the optimization, three pinch points were found as it can be seen in the graphs of the composite curves; their values are:

$$\Delta T_{pp1} = 3019\ 5°C$$
$$\Delta T_{pp2} = 3001\ °C \quad (6.3)$$

$$\Delta T_{pp3} = 31.74\,°C$$

The new set of key temperatures is presented as follows.

$T_{cond1} = 76.29°C \rightarrow 73.47°C$

$T_{cond2} = 84.27°C \rightarrow 82.53°C$

$T_{sub1} = 62.95°C \rightarrow 62.17°C$

$T_{sub2} = 64.76°C \rightarrow 63.64°C$

$T_{gwdhex} = 53°C \rightarrow 53.019\,5°C$

$T_{int1} = 39°C \rightarrow 38.998°C$

$T_{int2} = 50°C \rightarrow 49.99°C$

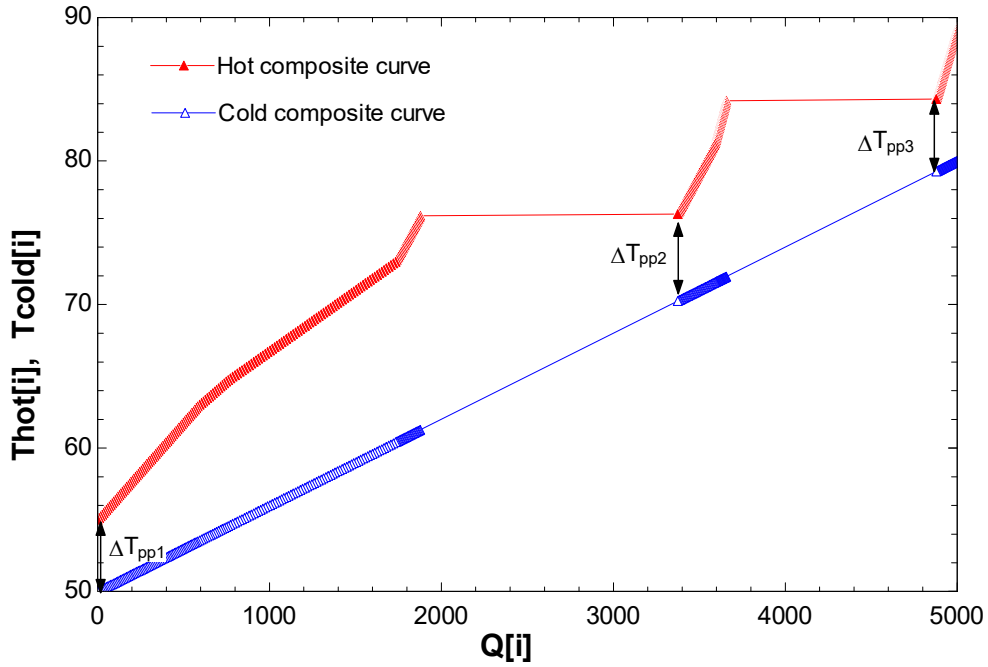

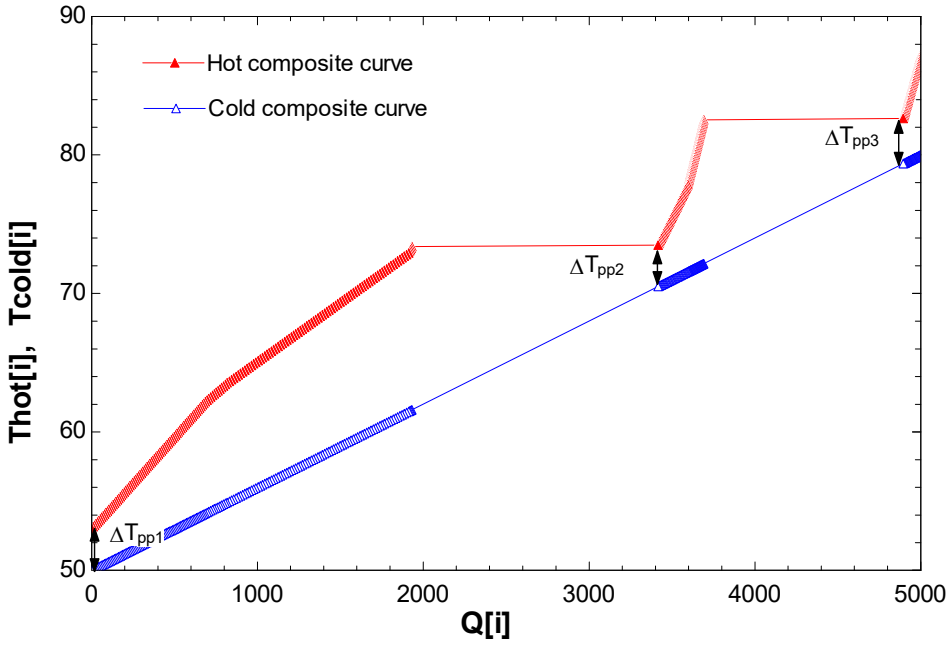

Figure 6.31– Comparison of the composite curves before (previous page) and after (above) the optimization

Using the new set of key temperatures a HEN was built by splitting the hot stream related to the second heat pump subcooler, that was the only stream crossing a pinch point.

So the HEN consists of just one more heat exchanger compared to the initial configuration, and yet it provides the best achievable COP while respecting the three temperature differences at the pinch points that were found in the optimization. The only disparity is on the third pinch point, for which the HEN provides a temperature difference that is lower than the one found in the optimization; this is probably due to the mismatch between the condensing temperature and the final point of the composite curve that is not necessarily at that temperature.

$$\begin{aligned} \Delta T_{pp1,HEN} &= 3.02\,°C \\ \Delta T_{pp2,HEN} &= 3.039\,°C \\ \Delta T_{pp3,HEN} &= 3.169\,°C \end{aligned} \tag{6.4}$$

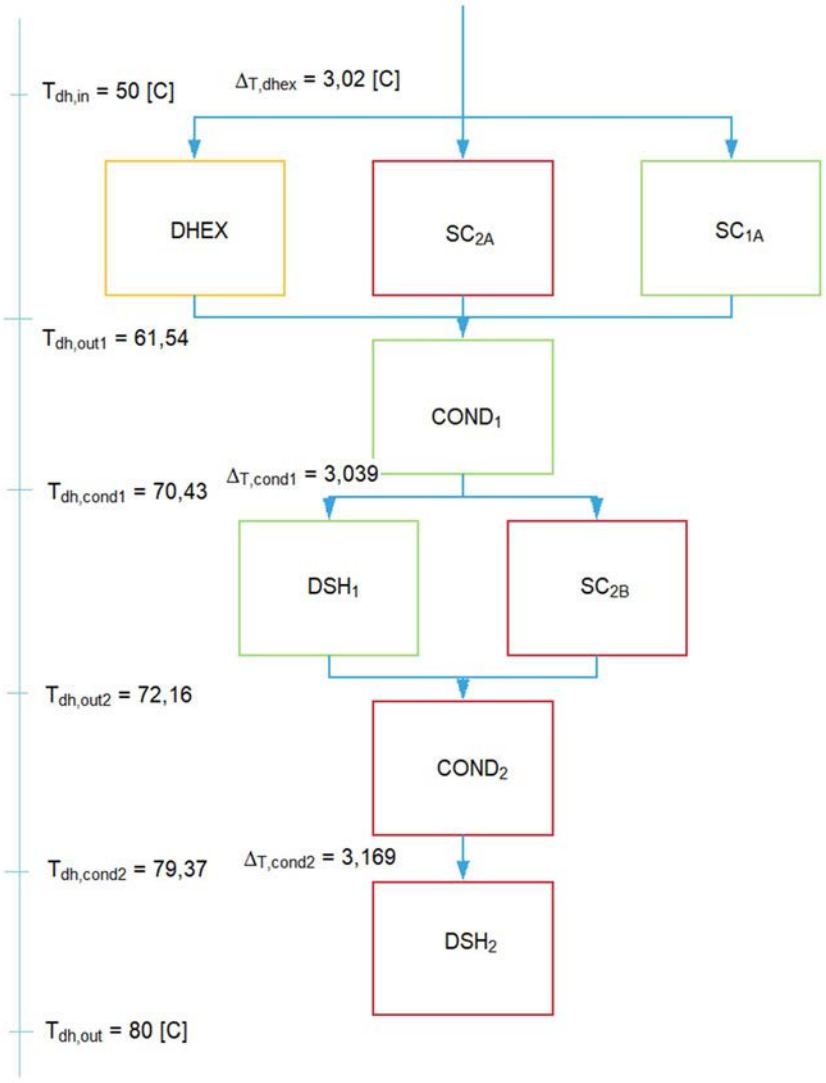

Figure 6.32– Resulting HEN with the DH water temperatures along

The Q-T diagram of the HEN for this configuration is presented below, followed by the table with all the temperatures differences for every HEX and their relative heat flux.

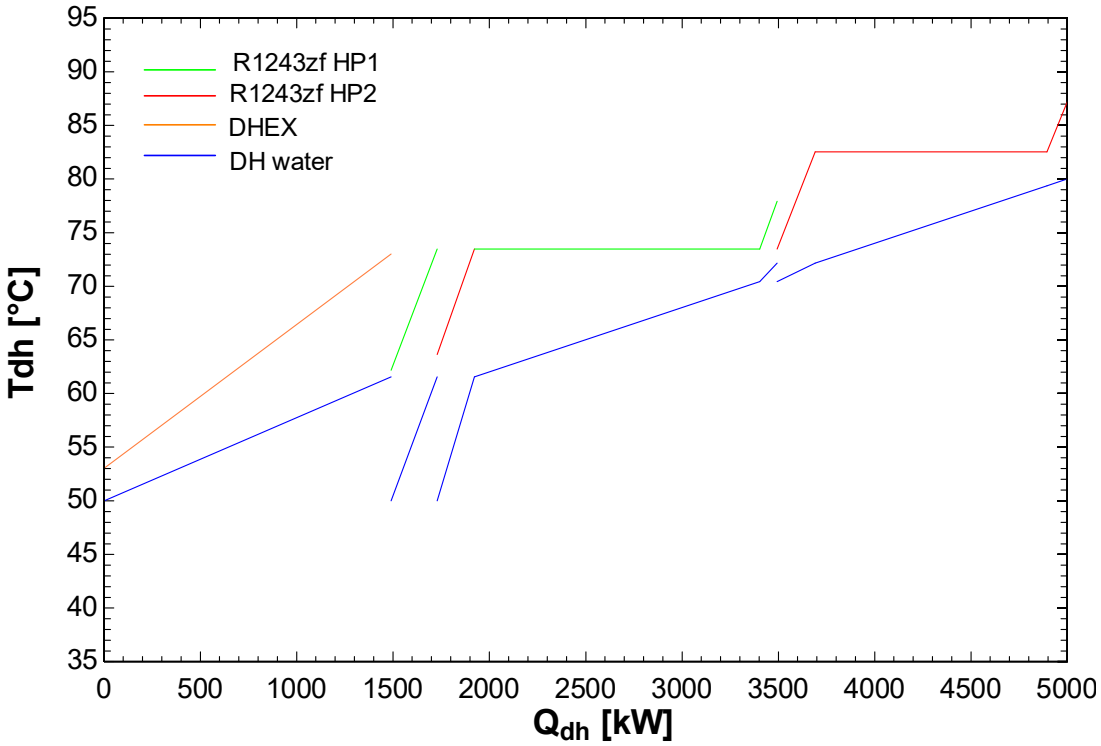

Figure 6.33– Q-T diagram for the 8 HEX of the considered HEN

Table 6.10 – Temperature differences and heat flux for every HEX.

HEX cycle 1	ΔT_{inlet}	ΔT_{outlet}	$\dot{Q}[kW]$	HEX cycle 2	ΔT_{inlet}	ΔT_{outlet}	$\dot{Q}[kW]$
SC	12.18	11.93	240.1	SC_{2A}	13.64	11.93	192.5
$DHEX$	3.02	11.93	1489	SC_{2B}	3.039	10.38	197.2
$COND_1$	11.93	3.039	1482	$COND_2$	10.38	3.169	1204
DSH_1	3.039	5.77	89.88	DSH_2	3.169	7.216	105.5

The summary results for the described configuration are presented in the table below.

Table 6.11 – Main results for the considered configuration

HP 1			**HP 2**		
T_{ev}	14	$°C$	T_{ev}	32.5	$°C$
T_{int}	39	$°C$	T_{int}	50	$°C$
T_{cond}	73.47	$°C$	T_{cond}	82.5	$°C$
p_{ev}	4.2	bar	p_{ev}	7.2	bar
p_{int}	8.56	bar	p_{int}	11.3	bar
p_{cond}	19.2	bar	p_{cond}	23	bar
$r_{p,lowstage}$	2.05	-	$r_{p,lowstage}$	1.57	-
$r_{p,highstage}$	2.24	-	$r_{p,highstage}$	2.05	-
$\dot{m}_{ref,lowstage}$	9	kg/s	$\dot{m}_{ref,lowstage}$	9,37	kg/s
$\dot{m}_{ref,highstage}$	12	kg/s	$\dot{m}_{ref,highstage}$	11.1	kg/s
$\dot{V}_{ref,lowstage,inlet}$	1686	m^3/h	$\dot{V}_{ref,lowstage,inlet}$	1020	m^3/h
$\dot{V}_{ref,highstage,inlet}$	1082	m^3/h	$\dot{V}_{ref,highstage,inlet}$	752.5	m^3/h
$\dot{Q}_{evap}$	1377	kW	$\dot{Q}_{evap}$	1377	kW
$\dot{Q}_{cond}$	1811	kW	$\dot{Q}_{cond}$	1698	kW
$\dot{W}_{comp1}$	188.2	kW	$\dot{W}_{comp1}$	121.7	kW
$\dot{W}_{comp2}$	268.6	kW	$\dot{W}_{comp2}$	216,5	kW
COP	3.965	-	**COP**	5.02	-

Chapter 7 Conclusion

7.1 Discussion of the results

The last results related to the multiple HPs configurations with the direct heat exchanger represent the final outcome of the optimization process that was realized in this project. The most performing ammonia configuration provided a COP equal to 6.39, while the best configuration using a HFO refrigerant (R-1243zf) reached at
6.29.
The progression that brought to these results is shown in the bar graphs below.

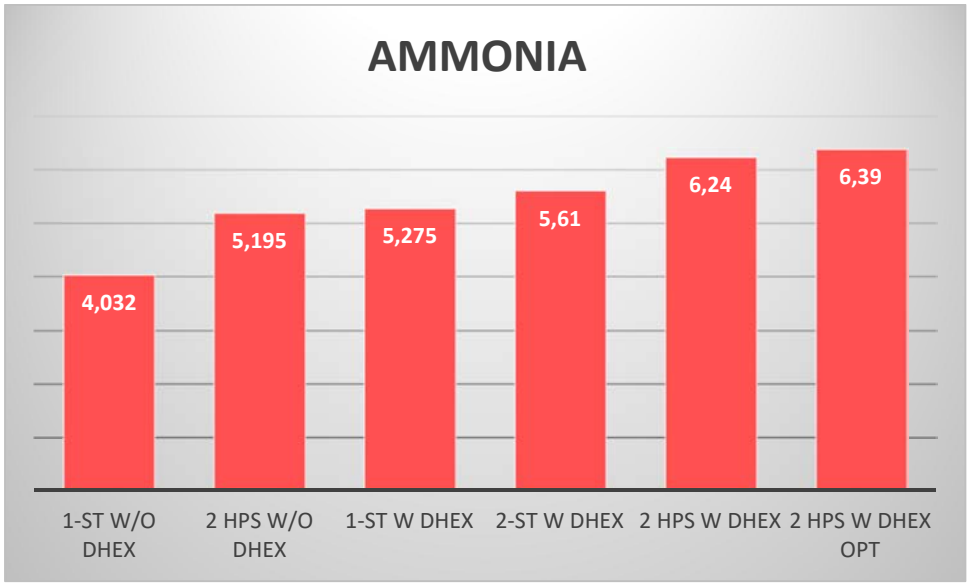

Figure 7.1– COP progression for ammonia configurations.

For ammonia configurations the COP saw a total increase of 58.5 % compared to the basic 1-stage configuration without the direct heat exchanger.
The total increase in the COP can be seen as the sum of different small improvements, as it can be seen in the pie graph below. The graph was made taking the average improvement given by each solution.

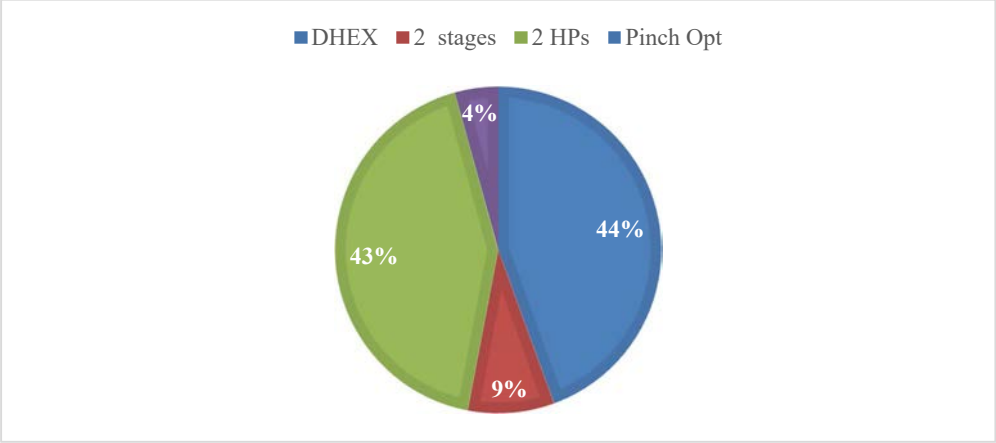

Figure 7.2– Contributions to the total improvement for ammonia configurations.

For HFO's configurations the total increase was of 68.8%, even if two different refrigerants are involved, but it should be reminded that their performance are quite similar when comparing the performances. The distribution of the improvements is similar to the one for ammonia, but the pinch method is less impactful for what has already been said in chapter 6.

The difference between ammonia and HFO's performances is very narrow in absolute values, but when discussing the assumptions on which these results are based, the margin increase for different reasons.

In the case of R1234ze(E) and R1243zf standard values of the isentropic efficiencies ($\eta_{is} = 075$) were used for the piston compressors in the model; but in reality it's quite probable that for the high-temperature stages the isentropic efficiency decreases like in the real cases with screw compressors, and that would bring the COP down in a relevant way.

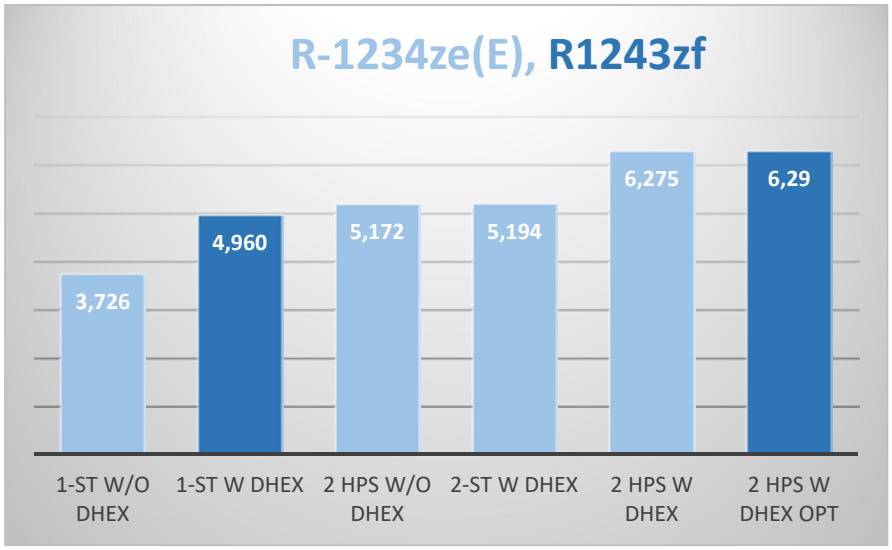

Figure 7.3– COP progression for HFOs configurations

For example to show the impact of the isentropic efficiency for the HFO's best configuration, the last optimization has been run again with the two low-stages

compressors having isentropic efficiency equal to 0.75 and the two high-stages having isentropic efficiency equal to 0.70.
The results show that the COP decreased from 6.29 to 6.13 (-2.5%). Let's remember that for the high-pressure stage compressor in the ammonia configuration the isentropic efficiency is down to 0.535.
This inaccuracy related to the piston compressors for the R1243zf and R1234ze(E) cases brings to light another factor that represents a downside for HFO's: the lack of components in the market.
In fact I did not manage to find piston compressors for HFO's refrigerants suitable for the size of this application.
The reasons for that are multiple:

Table 7.1 – Comparison between the volumetric flowrates for Ammonia and R1234ze(E)

- These refrigerants are quite new and some of them are still in the development phase
- The volumetric capacity of these refrigerants is very low, which means that for high heating or cooling capacities the volumetric flowrate is very large and it makes it difficult to have piston compressors large enough to fulfill this requirement.

This last aspect is highlighted in the table below, where the volumetric capacity of the two refrigerants (ammonia and R1234ze(E)) is reported for the non-optimized cycles. It can be seen that for the HFO the volumetric flowrate is nearly always more than double the one for ammonia.

Compressor	**Port**	**Volumetric flowrate $\dot{V}[m^3/h]$**	
		Ammonia	R-1234ze(E)
1st HP low-stage	Inlet	814.5	1869
	Outlet	453.6	906.7
1st HP high stage	Inlet	444.8	1149
	Outlet	227.7	450
2nd HP low stage	Inlet	495.8	1193
	Outlet	309	620
2nd HP high stage	Inlet	278.2	659,2
	Outlet	165.5	343

This gives a clear idea on how the size of possible compressors for HFO's would be quite bigger than what would be necessary for ammonia.
The downside of this is that ammonia works at higher pressures compared to HFO's, so the components need to be able to resist to these operating conditions.
Eventually, for these reasons ammonia seems to be the best option and at the end of this project it can be viewed as the winner refrigerant for this application.

The most performing ammonia configuration derives from the pinch optimization and it consists of 22 HEX for a COP equal to 6.39, compared to the 13 of the non-optimized solution that provides a COP of 6.24.
This improvement given by the pinch method is quite small, and even if a higher COP reduces the operating costs, it's questionable if the better performance justifies the higher investment costs related to the higher number of HEX.
What emerged clearly is that the DHEX is necessary for this application, and the improvement given by the two HPs in series compared to the single HP with 2-stages seems to assess that also the multiple HPs solution should be considered the winning configuration.
Some final considerations can be made regarding the pinch method applied to HPs in EES; it has shown to be quite effective and reliable but some limitations are present; as explained before, the optimizations had to be adjusted with targeted guess values to reach the actual optimized result, and only the Variable Metric Method has shown valid results with the optimization.
Nonetheless, the concepts of the Pinch analysis and their application resulted to be a great tool to better comprehend and integrate complex energy systems so I can say that this project was a great opportunity to develop a better knowledge of advanced energy systems and process integration.

7.2 Further development

Due to lack of time, many interesting aspects related to this project could not be developed enough and they leave some space for further study and development.
In particular an economic assessment could be the next step to verify the convenience of the thermodynamically optimized configuration compared to the other configurations; another point of interest is the dimensioning of components like the evaporators and condensers and a consequent economic evaluation for the cost of all the components of the system.

For what regards other components, it would be interesting to search the market for dry compressors suitable for HFOs refrigerants, as it is not clear if they already exist or not.

The pinch method also leaves some space for a deeper analysis; for example the case in which the DH water stream is splitted into different streams and not all of them are getting to the same temperature of 80 °C has been encountered. With the pinch optimization it was possible to obtain an increase in the overall COP but it was suggested that if the method can be adjusted to include the possibility of having different cold composite curves the increase could be higher. Some attempts have been made on this regard but fractional and not convincing results were obtained.

References

[1] HOFOR, “https://www.hofor.dk/wp-content/uploads/2016/09/district_heating_in_cph.pdf,” 09 2016. [Online].

[2] RAMBOLL, “https://ramboll.com/projects/group/district-heating-system-in-the-copenhagen-region,” [Online].

[3] S. O. GREEN, “https://stateofgreen.com/en/partners/ramboll/solutions/district-heating-in-the-copenhagen-region/,” [Online].

[4] D. FJERNVARME, “http://geotermi.dk/english/geothermal-plants/amager,” [Online].

[5] D. T. INSTITUTE, “https://www.dti.dk/projects/project-experimental-development-of-electric-heat-pumps-in-the-greater-copenhagen-dh-system-phase-2/37419,” [Online].

[6] “Final report Experimental development of electric heat pumps in the Greater Copenhagen DH system-Phase 1,” *64014-0127,* 2016.

[7] T. Ommen, P. Jørgensen, J. Jonas, M. Wiebke and E. Brian, “Design considerations for integration of two 5 MW vapour compression HPs in the Greater Copenhagen DH system,” DTU Mechanical Engineering, 2017.

[8] “https://en.wikipedia.org/wiki/Second_law_of_thermodynamics,” [Online].

[9] D. Del Col, “Heat pumps, Refrigeration and Heat pump technology,” Universitá degli studi di Padova.

[10] “http://wallpaper.istriku.site/what-causes-my-truck-ac-to-freeze-up/,” [Online].

[11] E. Granryd and K. T. h. I. f. energiteknik., Refrigerating engineering, Stockholm: Royal institute of technology KTH,Department of Energy Technology, Division of Applied Thermodynamics and Refrigeration, 2005.

[12] D. Del Col, “Cycle improvement, Refrigeration and Heat Pump technology,” Universitá degli Studi di Padova.

[13] D. Del Col, “Refrigerants; Refrigeration technology,” Universitá degli Studi di Padova.

[14] A. Cavallini, “Past, Present and Future of Refrigerant,” Universitá degli Studi di Padova.

[15] “https://en.wikipedia.org/wiki/Montreal_Protocol,” [Online].

[16] “https://www.slideshare.net/omairfarooq/refrigerant-environment-and-legislative-update-the-future-of-refrigerants-customer-presentation,” [Online].

[17] P. Makhnatch, D. o. E. Technology and KTH, “https://www.kth.se/en/itm/inst/energiteknik/forskning/ett/projekt/koldmedier-med-lag-gwp/low-gwp-news/laga-gwp-alternativa-koldmedier-i-varmepumpar-1.426276,” [Online].

[18] “http://industrialheatpumps.nl/en/how_it_works/refrigerants/,” [Online].

[19] “https://www.kth.se/en/itm/inst/energiteknik/forskning/ett/projekt/koldmedier-med-lag-gwp/low-gwp-news/nagot-om-hfo-koldmedier-1.602602,” [Online].

[20] “https://www.researchgate.net/figure/Comparison-of-the-saturation-curves-of-HFO-HCFO-refrigerants-collected-in-a-p-h-graph_fig2_327065959,” [Online].

[21] D. Del Col, “Reciprocating Compressors, Refrigerating Technology,” Universitá degli Studi di Padova.

[22] “https://berg-group.com/engineered-solutions/the-science-behind-refrigeration/,” [Online].

[23] “https://tractionmech8.wordpress.com/2014/04/18/131/,” [Online].

[24] D. Del Col, “Condensers, Refrigeration technology,” Universitá degli Studi di Padova.

[25] “https://en.wikipedia.org/wiki/Shell_and_tube_heat_exchanger,” [Online].

[26] “https://nptel.ac.in/courses/112105129/pdf/R&AC%20Lecture%2024.pdf,” [Online].

[27] “https://www.swep.net/refrigerant-handbook/4.-expansion-valves/adf1/,” [Online].

[28] “https://www.swep.net/refrigerant-handbook/6.-evaporators/asas2/,” [Online].

[29] “https://en.wikipedia.org/wiki/Pinch_analysis,” [Online].

[30] B. Elmegaard, “An algorithm for pinch analysis,” March 8, 2006.

[31] I. C. Kemp, Pinch Analysis and Process Integration A user guide on Process Integration for the Efficient Use of Energy, Butterworth-Einemann.

[32] “https://www.researchgate.net/figure/Hot-and-cold-composite-curves-of-a-generic-process_fig1_267862056,” [Online].

[33] P. H. Jørgensen, T. S. Ommen, W. B. Markussen, E. D. Rothuizen, K. Hoffman and B. Elmegaard, “Design and optimization of the heat exchanger network for

district heating ammonia heat pumps connected in series," Technical University of Denmark, 2018.

[34] "http://orbit.dtu.dk/files/141909127/SVAF_4DH_1.pdf," [Online].

[35] "https://www.danfoss.com/en/about-danfoss/our-businesses/cooling/refrigerants-and-energy-efficiency/refrigerants-for-lowering-the-gwp/ammonia-nh3/," [Online].

[36] "https://www.danfoss.com/en/about-danfoss/our-businesses/cooling/refrigerants-and-energy-efficiency/refrigerants-for-lowering-the-gwp/r32/," [Online].

Appendix A

Propane results

Together with R-717 (Ammonia) and HFOs also R-290 (propane) was considered as a possible refrigerant. Propane is an hydrocarbon so it has the advantage of a low GWP and no ODP; the downside is that is very flammable and explosive, so it needs to be treated with caution.

It was used in cycles with piston compressors without oil cooling, because it does not reach high discharge temperatures, that is an advantage compared to ammonia; however, the performances are lower compared to both ammonia and HFO's; for this reason I did not consider it a valuable solution. The results reported in the bar graph are related to the configurations that were presented also for R1234ze(E), with the difference that the pinch optimization was not applied to this case, mainly because the optimization did not provide convincing results, as the higher COP could not surpass the value 6.135, obtained with all the minimum temperature differences for the HEX equal to 3 °C.

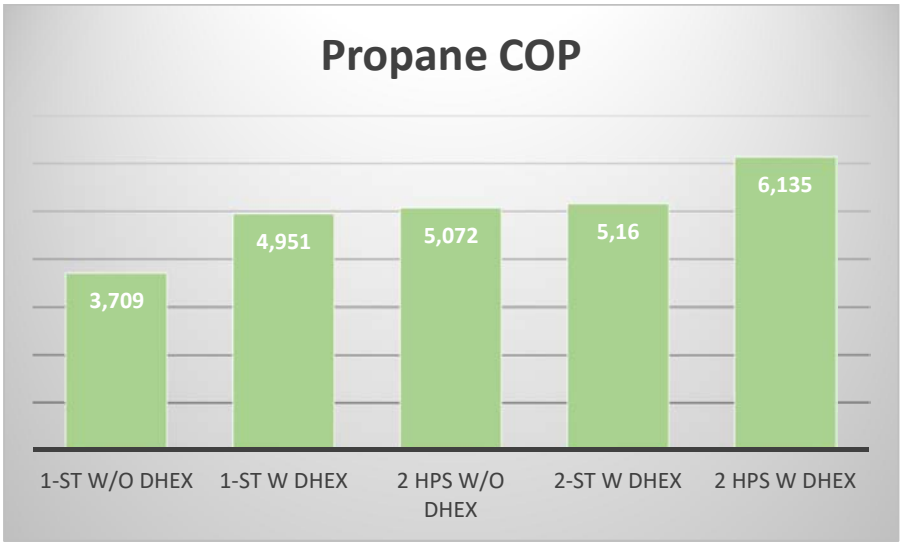

Fig. A.1 Propane COP for the different configurations.

The most significant results related to the best propane configuration are presented in the table below.

Tab A.2 – Temperature differences and heat flux for every HEX

HP 1			**HP 2**		
T_{ev}	14	$°C$	T_{ev}	32.5	$°C$
T_{int}	38	$°C$	T_{int}	51.2	$°C$
T_{cond}	74.4	$°C$	T_{cond}	81.9	$°C$
p_{ev}	7.1	bar	p_{ev}	11.4	bar
p_{int}	13.07	bar	p_{int}	16.4	bar
p_{cond}	28.18	bar	p_{cond}	32.5	bar
$r_{plowstage}$	1.836	-	$r_{plowstage}$	1.1.43	-
$r_{phighstage}$	2.15	-	$r_{phighstage}$	1.98	-
$\dot{m}_{reflowstage}$	4.76	kg/s	$\dot{m}_{reflowstage}$	4.96	kg/s
$\dot{m}_{refhighstage}$	6.45	kg/s	$\dot{m}_{refhighstage}$	6.09	kg/s
$\dot{V}_{reflowstageinlet}$	1113	m^3/h	$\dot{V}_{reflowstageinlet}$	714	m^3/h
$\dot{V}_{refhighstageinlet}$	808.5	m^3/h	$\dot{V}_{refhighstageinlet}$	595.6	m^3/h
$\dot{Q}_{evap}$	1371	kW	$\dot{Q}_{evap}$	1371	kW
$\dot{Q}_{cond}$	1818	kW	$\dot{Q}_{cond}$	1698	kW
$\dot{W}_{comp1}$	179.2	kW	$\dot{W}_{comp1}$	107.8	kW
$\dot{W}_{comp2}$	291.2	kW	$\dot{W}_{comp2}$	236.9	kW
COP	3.86	-	**COP**	4.93	-

Appendix B

Considerations on the HPs sizing

In this section some considerations will be made regarding the sizing of the HPs in the configurations with two HPs connected in series and DHEX. In particular both for ammonia and R1243zf the total evaporator capacity was splitted in half, so that the two HPs received the same heat flux from the geothermal water.
This choice will be now explained and discussed in detail to understand why different possibilities were not considered.

Ammonia

For the double HP configuration with DHEX a parametric table was created to see the variation of the total COP with the variation of heat load for the two evaporators; in particular the changing variable is $h_{gw,int}$, which is the intermediate enthalpy of the geothermal water between the enthalpy at the outlet of the DHEX $h_{gw,dhex}$ and the lower enthalpy at the exit temperature $h_{gw,out}$.
Its default value is given by:

$$h_{gw,int} = \frac{(h_{gw,dhex} + h_{gw,out})}{2} = 1446{,}3$$

Other parameters that are inserted in the table are the COPs of the 2 HPs, the optimal intermediate temperatures of the cycle, the evaporating capacities and their ratio f_Q, defined as:

$$f_Q = \frac{Q_{evap1}}{Q_{evap2}}$$

The configuration that is chosen to run the parametric table is the one with the temperature differences equal to 3 °C.
From the parametric table it emerges that the case with f_Q=1 is not the case that provides the higher COP; in fact the best performance is obtained for f_Q=1.33, with the heat loads at the evaporators being respectively $Q_{evap1} = 1556kW$ and $Q_{evap2} = 1170kW$.

Tab B.1 – Temperature differences and heat flux for every HEX

1..10	COP	COP1	COP2	$h_{gw;int}$	f_q	$\dot{Q}_{evap1}$ [kW]	$\dot{Q}_{evap2}$ [kW]	T_{opt1}	T_{opt2}
Run 1	6,213	4,299	4,461	140,0	0,8874	1280	1442	40,21	54,8
Run 2	6,228	4,286	4,497	142,2	0,94	1320	1404	40,29	55,13
Run 3	6,240	4,274	4,534	144,4	0,9956	1359	1365	40,37	55,45
Run 4	6,249	4,263	4,571	146,7	1,055	1399	1326	40,46	55,77
Run 5	6,257	4,251	4,609	148,9	1,117	1438	1287	40,54	56,1
Run 6	6,262	4,239	4,648	151,1	1,183	1478	1249	40,63	56,42
Run 7	6,265	4,227	4,687	153,3	1,254	1517	1209	40,71	56,74
Run 8	6,266	4,216	4,726	155,6	1,33	1556	1170	40,79	57,06
Run 9	6,265	4,204	4,766	157,8	1,41	1595	1131	40,88	57,38
Run 10	6,261	4,193	4,807	160,0	1,497	1634	1092	40,96	57,7

In particular the increase compared to the basic case is from 6.240 to 6.266 (+0.33%). Even if the variation is quite small, I tried to perform the pinch optimization for this case, but eventually the resulting COP was smaller than the COP that was obtained with the default case: the case with equal capacity for the two evaporators provided an optimized COP equal to 6.39 while the case with f_Q=1.33 just resulted in a COP of 6.31. The explanation that I give for this is that the pinch method is more efficient when the condensing heat streams at constant temperature are of a similar size, because in that case the composite curves are more flexible to variations and integrations among the heat streams. Also the role played by the oil coolers becomes less relevant because the inlet temperature of the oil must be increased to 77 °C to respect the minimum temperature differences.

R-1243zf

The same procedure was followed for the case with R1243zf.
From the table it emerges clearly that the highest COP is obtained for the two evaporating capacities very close to each other, so the choice that has been made can be confirmed without relevant doubts.

Tab B.2 – Temperature differences and heat flux for every HEX

1..10	COP	COP1	COP2	$h_{gw;int}$	T_{opt}	T_{opt2}	$\dot{Q}_{evap1}$	$\dot{Q}_{evap2}$	f_Q
Run 1	6,241	3,95	4,859	138	40,95	54,62	1258	1493	0,8425
Run 2	6,244	3,944	4,89	139,3	41,01	54,81	1281	1469	0,8722
Run 3	6,245	3,939	4,922	140,7	41,06	55	1305	1445	0,9029
Run 4	6,246	3,933	4,955	142	41,12	55,19	1329	1422	0,9346
Run 5	6,246	3,927	4,988	143,3	41,17	55,38	1353	1398	0,9674
Run 6	6,245	3,922	5,021	144,7	41,23	55,57	1376	1374	1,001
Run 7	6,242	3,916	5,054	146	41,28	55,77	1400	1351	1,037
Run 8	6,24	3,911	5,088	147,3	41,33	55,96	1423	1327	1,073
Run 9	6,236	3,906	5,122	148,7	41,39	56,15	1447	1303	1,111
Run 10	6,231	3,9	5,157	150	41,44	56,34	1470	1279	1,15

Appendix C

Not optimized configurations with 3°C as temperature difference results

In this section the main results for the configurations with 2 HPs and DHEX (using a 3°C temperature difference in every heat exchanger) are reported both for ammonia and R1243zf.
In fact in the main report the results are given for the configurations with 5 °C temperature difference and then for the optimized configurations, but for the intermediate step only the overall COP has been mentioned. Here more complete results are summarized, to take into account also these configurations.

Ammonia

For ammonia the overall COP obtained with this configuration is 6.24. The heat load on the DHEX is $\dot{Q}_{dhex} = 1475kW$.

Tab C.1 – Main result for the non optimized ammonia configuration

HP 1			**HP 2**		
T_{ev}	14	$°C$	T_{ev}	32.5	$°C$
T_{int}	40	$°C$	T_{int}	56	$°C$
T_{cond}	72.48	$°C$	T_{cond}	82.3	$°C$
p_{ev}	7.1	bar	p_{ev}	12.5	bar
p_{int}	15.55	bar	p_{int}	23.7	bar
p_{cond}	35.05	bar	p_{cond}	43.5	bar
$r_{plowstage}$	2.2	-	$r_{plowstage}$	1.88	-
$r_{phighstage}$	2.25	-	$r_{phighstage}$	1.84	-
$\dot{m}_{reflowstage}$	1.25	kg/s	$\dot{m}_{reflowstage}$	1.341	kg/s

$\dot{m}_{ref,highstage}$	1.48	kg/s	$\dot{m}_{ref,highstage}$	1.428	kg/s
$\dot{V}_{ref,lowstage,inlet}$	814	m^3/h	$\dot{V}_{ref,lowstage,inlet}$	495.8	m^3/h
$\dot{V}_{ref,highstage,inlet}$	444.9	m^3/h	$\dot{V}_{ref,highstage,inlet}$	278.2	m^3/h
$\dot{Q}_{evap}$	1362	kW	$\dot{Q}_{evap}$	1362	kW
$\dot{Q}_{cond}$	1373	kW	$\dot{Q}_{cond}$	1225	kW
$\dot{W}_{comp1}$	173.3	kW	$\dot{W}_{comp1}$	164.2	kW
$\dot{W}_{comp2}$	242.8	kW	$\dot{W}_{comp2}$	220.9	kW
COP	4.27	-	**COP**	4.53	-

R1234ze(E)

For R1234ze(E) the overall COP obtained with this configuration is 6.276.The heat load on the DHEX is $\dot{Q}_{dhex} = 1490kW$.

Tab C.2 – Temperature differences and heat flux for every HEX

HP 1			**HP 2**		
T_{ev}	14	$°C$	T_{ev}	32.5	$°C$
T_{int}	38	$°C$	T_{int}	57	$°C$
T_{cond}	74.9	$°C$	T_{cond}	82.7	$°C$
p_{ev}	3.54	bar	p_{ev}	6.228	bar
p_{int}	7.26	bar	p_{int}	11.87	bar
p_{cond}	17.9	bar	p_{cond}	21.2	bar
$r_{p,lowstage}$	2.05	-	$r_{p,lowstage}$	1.9	-
$r_{p,highstage}$	2.47	-	$r_{p,highstage}$	1.791	-
$\dot{m}_{ref,lowstage}$	9.77	kg/s	$\dot{m}_{ref,lowstage}$	11.07	kg/s
$\dot{m}_{ref,highstage}$	12.84	kg/s	$\dot{m}_{ref,highstage}$	12.04	kg/s

$\dot{V}_{ref,lowstage,inlet}$	1850	m^3/h	$\dot{V}_{ref,lowstage,inlet}$	1193	m^3/h
$\dot{V}_{ref,highstage,inlet}$	1181	m^3/h	$\dot{V}_{ref,highstage,inlet}$	659.2	m^3/h
$\dot{Q}_{evap}$	1377	kW	$\dot{Q}_{evap}$	1377	kW
$\dot{Q}_{cond}$	1498	kW	$\dot{Q}_{cond}$	1263	kW
$\dot{W}_{comp1}$	175.8	kW	$\dot{W}_{comp1}$	176.8	kW
$\dot{W}_{comp2}$	280.5	kW	$\dot{W}_{comp2}$	163.6	kW
COP	3.97	-	**COP**	4.99	-

R1243zf

For R1234zf the overall COP obtained with this configuration is 6.245. The heat load on the DHEX is $\dot{Q}_{dhex} = 1489kW$.

Table C.3 – Temperature differences and heat flux for every HEX

HP 1			**HP 2**		
T_{ev}	14	$°C$	T_{ev}	32.5	$°C$
T_{int}	38	$°C$	T_{int}	52	$°C$
T_{cond}	74.6	$°C$	T_{cond}	82.4	$°C$
p_{ev}	4.2	bar	p_{ev}	7.2	bar
p_{int}	8.4	bar	p_{int}	11.9	bar
p_{cond}	19.7	bar	p_{cond}	23.16	bar
$r_{p,lowstage}$	1.99	-	$r_{p,lowstage}$	1.65	-
$r_{p,highstage}$	2.35	-	$r_{p,highstage}$	1.95	-
$\dot{m}_{ref,lowstage}$	8.89	kg/s	$\dot{m}_{ref,lowstage}$	9.6	kg/s
$\dot{m}_{ref,highstage}$	11.8	kg/s	$\dot{m}_{ref,highstage}$	11.12	kg/s
$\dot{V}_{ref,lowstage,inlet}$	1667	m^3/h	$\dot{V}_{ref,lowstage,inlet}$	1042	m^3/h

$\dot{V}_{ref,high\,stage,inlet}$	1105	m^3/h	$\dot{V}_{ref,high\,stage,inlet}$	714	m^3/h
$\dot{Q}_{evap}$	1375	kW	$\dot{Q}_{evap}$	1375	kW
$\dot{Q}_{cond}$	1451	kW	$\dot{Q}_{cond}$	1207	kW
$\dot{W}_{comp1}$	179.3	kW	$\dot{W}_{comp1}$	137.5	kW
$\dot{W}_{comp2}$	283.4	kW	$\dot{W}_{comp2}$	200.5	kW
COP	3.922	-	**COP**	5.019	-

Appendix D

EES MODEL

The EES model for the best ammonia configuration is here attached.

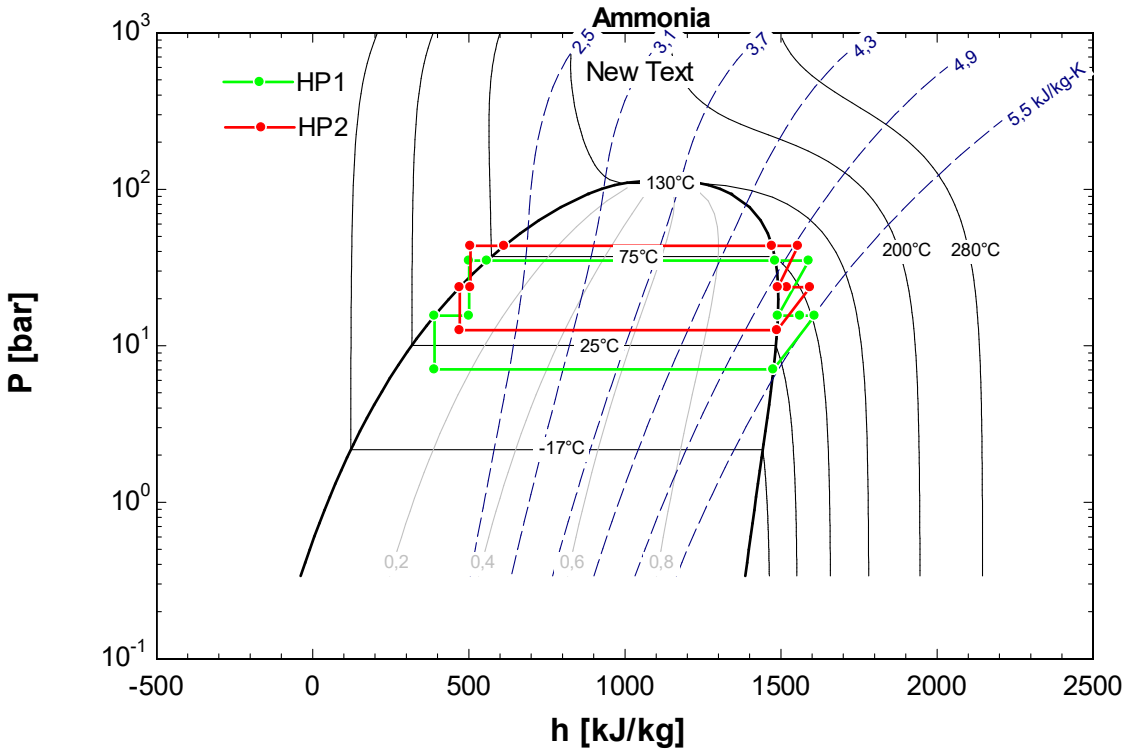

Fig. C.1 p-h diagram for the ammonia configuration with 2 HPs and DHEX

```
$defaultarraysize 200
Procedure thigh(T_max;T_min;DELTA_T;N:Thot[1..N];Tcold[1..N])
$Arrays On
$common
T_max;T_min;DELTA_T_int;T_dh_out;T_dh_in;N;Q_dot_cond1;Q_dot_cond2;Q_dot_oil1;Q_
dot_oil2;Q_dot_oil3;Q_dot_oil4;T_oil_in;T_oil_2;T_oil_3;T_oil_4;T_oil_1;T_cond2a;T_cond2b;
T_cond1a;T_cond1b;Q_dot_sc;
Q_dot_sc2;Q_dot_dsh2;Q_dot_dsh1;Q_dot_dsh1_l;Q_dot_dsh2_l;T[3];T2[3];T[2];T2[2];T[8];T
2[8];T[5];T2[5];T_gw_dhex;T_gw_in;Q_dot_dhex;
 "This procedures creates the temperature arrays for the hot and cold streams to calculate the
temperature differences between the composite curves"
"Hot streams temperature intervals definition"
Thot[1]:=T_max
i:=1
```

```
Repeat
Tlow[i]:=Thot[i]-DELTA_T_int
Thot[i+1]:=Thot[i]-DELTA_T_INT
i:=i+1
Until Thot[i]=T_gw_dhex
thig=Thot[i]

"Subcooling HP1 hot stream "
i:=1
Repeat
If (Thot[i]>T_cond1b) or (Thot[i]<T[8]) Then
Chot[i;1]=0
Else
p1=ceil(((T_COND1B-T[8]))/(DELTA_T_INT))
Chot[i;1]=Q_dot_sc/p1
C1tot=sum(Chot[1..i;1])
Endif
i=i+1
Until i=N

If C1tot<>Q_DOT_SC Then
i:=1
 Repeat
If (Thot[i]>T_cond1b) or (Thot[i]<T[8]) Then
Chot[i;1]=0
Else
p2=floor(((T_COND1B-T[8]))/(DELTA_T_INT))
Chot[i;1]=Q_dot_sc/p2
C1tot=sum(Chot[1..i;1])
Endif
i=i+1
Until i=N
Endif

"Desuperheating low stage HP1 hot stream"
i:=1
Repeat
If (Thot[i]<T[3]) or (Thot[i]>T[2])   Then
Chot[i;2]=0
Else
d1=ceil((T[2]-T[3])/(DELTA_T_INT))
Chot[i;2]=Q_dot_dsh1_l/d1
C2tot=sum(Chot[1..i;2])
Endif
i=i+1
Until i=N

 If C2tot<>Q_DOT_DSH1_L Then
i:=1
Repeat
If (Thot[i]<T[3]) or (Thot[i]>T[2])    Then
Chot[i;2]=0
Else
d2=floor((T[2]-T[3])/(DELTA_T_INT))
Chot[i;2]=Q_dot_dsh1_l/d2
C2tot=sum(Chot[1..i;2])
Endif
i=i+1
```

```
Until i=N
Endif

"Subcooling HP2 hot stream"
i:=1
Repeat
If (Thot[i]>T_cond2b) or (Thot[i]<T2[8]) Then
Chot[i;3]=0
Else
p3=ceil(((T_COND2B-T2[8]))/(DELTA_T_INT))
Chot[i;3]=Q_dot_sc2/p3
C3tot=sum(Chot[1..i;3])
Endif
i=i+1
Until i=N

If C3tot<>Q_DOT_SC2 Then
i:=1
 Repeat
If (Thot[i]>T_cond2b) or (Thot[i]<T2[8]) Then
Chot[i;3]=0
Else
p4=floor(((T_COND2B-T2[8]))/(DELTA_T_INT))
Chot[i;3]=Q_dot_sc2/p4
C3tot=sum(Chot[1..i;3])
Endif
i=i+1
Until i=N
Endif


"Desuperheating  low stage HP2 hot stream"
i:=1
Repeat
If (Thot[i]<T2[3]) or (Thot[i]>T2[2])   Then
Chot[i;4]=0
Else
d7=ceil((T2[2]-T2[3])/(DELTA_T_INT))
Chot[i;4]=Q_dot_dsh2_l/d7
C4tot=sum(Chot[1..i;4])
Endif
i=i+1
Until i=N

 If C4tot<>Q_DOT_DSH2_L Then
i:=1
Repeat
If (Thot[i]<T2[3]) or (Thot[i]>T2[2]) Then
Chot[i;4]=0
Else
d8=floor((T2[2]-T2[3])/(DELTA_T_INT))
Chot[i;4]=Q_dot_dsh2_l/d8
C4tot=sum(Chot[1..i;4])
Endif
i=i+1
Until i=N
Endif
```

```
"Condenser HP1 hot stream "
i:=1
Repeat
If (Thot[i]>T_cond1a+DELTA_T_int) or (Thot[i]<T_COND1b) Then
Chot[i;5]=0
Else
Chot[i;5]=Q_dot_cond1
C5tot=sum(Chot[1..i;5])
Endif
i=i+1
Until i=N

If C5tot<>Q_DOT_COND1 Then
i:=1
 Repeat
If (Thot[i]>T_cond1a+DELTA_T_int) or (Thot[i]<T_COND1b) Then
Chot[i;5]=0
Else
Chot[i;5]=Q_dot_cond1/2
C5tot=sum(Chot[1..i;5])
Endif
i=i+1
Until i=N
 Endif

"Desuperheating HP1 hot stream"
i:=1
Repeat
If (Thot[i]<T_cond1a+DELTA_T_int) or  (Thot[i]>T[5]) Then
Chot[i;6]=0
Else
d3=ceil((T[5]-(T_COND1A+DELTA_T_INT))/(DELTA_T_INT))
Chot[i;6]=Q_dot_dsh1/d3
C6tot=sum(Chot[1..i;6])
Endif
i=i+1
Until i=N

 If C6tot<>Q_DOT_DSH1 Then
i:=1
Repeat
If (Thot[i]<T_cond1a+DELTA_T_int) or  (Thot[i]>T[5])  Then
Chot[i;6]=0
Else
d4=floor((T[5]-(T_COND1A+DELTA_T_INT))/(DELTA_T_INT))
Chot[i;6]=Q_dot_dsh1/d4
C6tot=sum(Chot[1..i;6])
Endif
i=i+1
Until i=N
Endif

"Oil cooling low stage HP1 hot stream "
i:=1
Repeat
If (Thot[i]<T_oil_in) or  (Thot[i]>T_oil_1) Then
Chot[i;7]=0
Else
```

```
m1=floor((T_OIL_1-T_OIL_IN)/(DELTA_T_INT))
Chot[i;7]=Q_dot_oil1/m1
C7tot=sum(Chot[1..i;7])
Endif
i=i+1
Until i=N

 If C7tot<>Q_DOT_OIL1 Then   "to check that the hot stream is divided between the intervals in the right way"
i:=1
 Repeat
If (Thot[i]<T_oil_in) or  (Thot[i]>T_oil_1) Then
Chot[i;7]=0
Else
m2=ceil((T_OIL_1-T_OIL_IN)/(DELTA_T_INT))
Chot[i;7]=Q_dot_oil1/m2
C7tot=sum(Chot[1..i;7])
Endif
i=i+1
Until i=N
Endif


"Oil cooling low stage HP2 hot stream "
i:=1
Repeat
If (Thot[i]<T_oil_in) or  (Thot[i]>T_oil_3) Then
Chot[i;8]=0
Else
m3=floor((T_OIL_3-T_OIL_IN)/(DELTA_T_INT))
Chot[i;8]=Q_dot_oil3/m3
C8tot=sum(Chot[1..i;8])
Endif
i=i+1
Until i=N

 If C8tot<>Q_DOT_OIL3 Then   "to check that the hot stream is divided between the intervals in the right way"
i:=1
 Repeat
If (Thot[i]<T_oil_in) or  (Thot[i]>T_oil_3) Then
Chot[i;8]=0
Else
m4=ceil((T_OIL_3-T_OIL_IN)/(DELTA_T_INT))
Chot[i;8]=Q_dot_oil3/m4
C8tot=sum(Chot[1..i;8])
Endif
i=i+1
Until i=N
Endif


"Oil cooling high stage HP1 hot stream"
i:=1
Repeat
If (Thot[i]<T_oil_in) or  (Thot[i]>T_oil_2) Then
Chot[i;9]=0
Else
```

```
m5=floor((T_OIL_2-T_OIL_IN)/(DELTA_T_INT))
Chot[i;9]=Q_dot_oil2/m5
C9tot=sum(Chot[1..i;9])
Endif
i=i+1
Until i=N

 If C9tot<>Q_DOT_OIL2 Then   "to check that the hot stream is divided between the intervals in the right way"
i:=1
 Repeat
If (Thot[i]<T_oil_in) or  (Thot[i]>T_oil_2) Then
Chot[i;9]=0
Else
m6=ceil((T_OIL_2-T_OIL_IN)/(DELTA_T_INT))
Chot[i;9]=Q_dot_oil2/m6
C9tot=sum(Chot[1..i;9])
Endif
i=i+1
Until i=N
Endif


"Oil cooling high stage HP2 hot stream"
i:=1
Repeat
If (Thot[i]<T_oil_in) or  (Thot[i]>T_oil_4) Then
Chot[i;10]=0
Else
m10=ceil((T_OIL_4-T_OIL_IN)/(DELTA_T_INT))
Chot[i;10]=Q_dot_oil4/m10
C10tot=sum(Chot[1..i;10])
Endif
i=i+1
Until i=N

If C10tot<>Q_DOT_OIL4 Then   "to check that the hot stream is divided between the intervals in the right way"
i:=1
 Repeat
If (Thot[i]<T_oil_in) or  (Thot[i]<T_oil_4) Then
Chot[i;10]=0
Else
m11=floor((T_OIL_4-T_OIL_IN)/(DELTA_T_INT))
Chot[i;10]=Q_dot_oil4/m11
C10tot=sum(Chot[1..i;10])
Endif
i=i+1
Until i=N
Endif


"Condenser HP2 hot stream "
i:=1
Repeat
If (Thot[i]>T_cond2a+DELTA_T_int) or (Thot[i]<T_COND2b) Then
Chot[i;11]=0
Else
```

```
Chot[i;11]=Q_dot_cond2
C11tot=sum(Chot[1..i;11])
Endif
i=i+1
Until i=N

If C11tot<>Q_DOT_COND2 Then
i:=1
 Repeat
If (Thot[i]>T_cond2a+DELTA_T_int) or (Thot[i]<T_COND2b) Then
Chot[i;11]=0
Else
Chot[i;11]=Q_dot_cond2/2
C11tot=sum(Chot[1..i;11])
Endif
i=i+1
Until i=N
 Endif

"Desuperheating HP2 hot stream"
i:=1
Repeat
If (Thot[i]<T_cond2a+DELTA_T_int)   Then
Chot[i;12]=0
Else
d5=ceil((T_max-T_COND2A)/(DELTA_T_INT))
Chot[i;12]=Q_dot_dsh2/d5
C12tot=sum(Chot[1..i;12])
Endif
i=i+1
Until i=N

 If C12tot<>Q_DOT_DSH2 Then
i:=1
Repeat
If (Thot[i]<T_cond2a+DELTA_T_int)   Then
Chot[i;12]=0
Else
d6=floor((T_max-T_COND2A)/(DELTA_T_INT))
Chot[i;12]=Q_dot_dsh2/d6
C12tot=sum(Chot[1..i;12])
Endif
i=i+1
Until i=N
Endif

"DHEX"
i:=1
Repeat
If (Thot[i]<T_gw_dhex) or  (Thot[i]>T_gw_in) Then
Chot[i;13]=0
Else
f2=ceil((T_GW_IN-T_GW_DHEX)/(DELTA_T_INT))
Chot[i;13]=Q_dot_dhex/f2
C13tot=sum(Chot[1..i;13])
Endif
i=i+1
Until i=N
```

```
If C13tot<>Q_DOT_DHEX Then
i:=1
Repeat
If (Thot[i]<T_gw_dhex) or  (Thot[i]>T_gw_in) Then
Chot[i;13]=0
Else
f3=floor((T_GW_IN-T_GW_DHEX)/(DELTA_T_INT))
Chot[i;13]=Q_dot_dhex/f3
C13ot=sum(Chot[1..i;13])
Endif
i=i+1
Until i=N

Endif

"Total hot stream for every temperature interval"
i:=1
Repeat
CThot[i]=Chot[i;1]+Chot[i;2]+Chot[i;3]+Chot[i;4]+Chot[i;5]+Chot[i;6]+Chot[i;7]+Chot[i;8]+
Chot[i;9]+Chot[i;10]+Chot[i;11]+Chot[i;12]+Chot[i;13]
i=i+1
Until i=N

i:=1
Repeat
Qsum=sum(CThot[1..13])
i=i+1
Until i=N


"Sum of hot streams for plotting"
 i:=1
j:=1
Repeat
If  i=1 Then
Qheat[i]=5000
Else
Qheat[i]=5000-sum(CThot[1..j])
Endif
i=i+1
j=i-1
Until i=N+1

"Cold stream temperature intervals definition"
i:=1
Repeat
Tcold[i]=30*Qheat[i]/5000 +50
i:=i+1
Until i=N+1

End

T_cond1a=T[7]
T_cond1b=T[7]
T_cond2a=T2[7]
T_cond2b=T2[7]
T_max=T2[5]
```

```
T_min=T_dh_in

DELTA_T_int= (T_max-T_gw_dhex)/ (N-1)
N=200



" Call thigh(T_max;T_min;DELTA_T_int;N:deltaT[1..N])"
 Call thigh(T_max;T_min;DELTA_T_int;N:Thot[1..N];Tcold[1..N])
"Temperature difference between hot streams and cold one"
Duplicate j=1;N
deltaT[j]=Thot[j]-Tcold[j]
End

DELTA_T_pinch1=min(deltaT[1..N])
DELTA_T_min=3


"geothermal water "
T_gw_in=73 [C]
T_gw_out=16 [C]
P_atm=1 [bar]

"pinch temperature differences"

DELTA_T_ev=2 [C]
DELTA_T_cond1=3
DELTA_T_cond2=3
DELTA_T_pinch_dshl1=3 [C]
DELTA_T_pinch_dshl2=3 [C]
DELTA_T_pinch_sc1=3 [C]
DELTA_T_pinch_sc2=3 [C]
 DELTA_T_dhex=3 [C]

"intermediate temperatures and optimal intermediate temperatures and pressures"
T[10]=40
T2[10]=56

p_opt1=sqrt(p[1]*p[6])
T_opt1=temperature(ref$;P=p_opt1;x=0)

p_opt2=sqrt(p2[1]*p2[6])
T_opt2=temperature(ref$;P=p_opt2;x=0)


"screw compressors isentropic efficiencies"
eta_is1=0,795 "model PR-P1830S-28"
eta_is2=0,7  "model MMR-H17T-52"
eta_is3=0,715 "model MMR-H13T-52"
eta_is4=0,535  "model ER-D13T-52"

"Oil inlet temperature"
T_oil_in=75 [C]

"screw compressors volumetric flowrates"
V_dot_oil1=58*convert(l/min;(m^3)/s)
V_dot_oil2=130*convert(l/min;(m^3)/s)
V_dot_oil3=66*convert(l/min;(m^3)/s)
```

```
V_dot_oil4=170*convert(l/min;(m^3)/s)


"district heating water"
T_dh_out=80 [C]
T_dh_in=50 [C]
p_dh=5 [bar]
Q_dot_dh= 5000   "design heating capacity (5000 kW) provided to the DH"
Q_dot_cond+Q_dot_oil+Q_dot_dsh1_l+Q_dot_cond_2+Q_dot_dsh2_l+Q_dot_dhex=Q_dot_
dh
h_dh_out=enthalpy(Water;T=T_dh_out;P=p_dh)
h_dh_in=enthalpy(Water;T=T_dh_in;P=p_dh)
Q_dot_oil=Q_dot_oil1+Q_dot_oil2+Q_dot_oil3+Q_dot_oil4

"Refrigerant"
ref$='ammonia'


 "DHEX"
T_gw_dhex=T_dh_in+DELTA_T_dhex
Q_dot_dhex=m_dot_gw*(h_gw_in-h_gw_dhex)
Q_dot_dhex=m_dot_dh*(h_dh_dhex- h_dh_in)
h_gw_dhex=enthalpy(Water;T=T_gw_dhex;P=P_atm)
h_dh_dhex=enthalpy(Water;T=T_dh_dhex;P=p_dh)

"Low stage DSH HP1"
Q_dot_dsh1_l=m_dot_dh*(h_dh_dsh1_l-h_dh_sc)
Q_dot_dsh1_l=m_dot_ref_l*(h[2]-h[3])
h[3]=enthalpy(ref$;T=T[3];P=p[3])
h_dh_dsh1_l=enthalpy(Water;T=T_dh_dsh1_l;P=p_dh)
T[3]=T_dh_sc+DELTA_T_pinch_dshl1


"CONDENSER HP1"
"T[6]=67" "assumption on the condensing temperature"
"3 sections of condenser"
Q_dot_cond=Q_dot_dsh1+Q_dot_cond1+Q_dot_sc
Q_dot_cond1+Q_dot_dsh1=m_dot_dh*(h_dh_out1-h_dh_dsh2_l)
h_dh_out1=enthalpy(Water;T=T_dh_out1;P=p_dh)
Q_dot_dsh1=m_dot_ref_h*(h[5]-h[6])
h[6]=enthalpy(ref$;T=T[6];x=1)
s[6]=entropy(ref$;T=T[6];h=h[7])
p[6]=pressure(ref$;T=T[6];x=1)
T[6]=T[7]

"2) condensing section of the heat exchanger"
Q_dot_cond1=m_dot_ref_h*(h[6]-h[7])
h[7]=enthalpy(ref$;T=T[7];x=0)
s[7]=entropy(ref$;T=T[7];x=0)
p[7]=p[6]
Q_dot_cond1=m_dot_dh*(h_dh_cond-h_dh_dsh2_l)
h_dh_cond=enthalpy(Water;T=T_dh_cond;P=p_dh)
T_dh_cond=T[7]-DELTA_T_cond1

"3) subcooling section of the heat exchanger"
T[8]=T_dh_dhex+DELTA_T_pinch_sc1 "assumption on the temperature of ammonia after
subcooling"
Q_dot_sc=m_dot_ref_h*(h[7]-h[8])
```

```
Q_dot_sc=m_dot_dh*(h_dh_sc-h_dh_dhex)
h_dh_sc=enthalpy(Water;T=T_dh_sc;P=p_dh)
h[8]=enthalpy(ref$;T=T[8];P=p[7])
s[8]=entropy(ref$;T=T[8];P=p[7])
p[8]=p[7]


"Evaporator HP1"
h_gw_in=enthalpy(Water;T=T_gw_in;P=1)
h_gw_out=enthalpy(Water;T=T_gw_out;P=1)
h_gw_int=(h_gw_dhex+h_gw_out)/2
T_gw_int=temperature(Water;h=h_gw_int;P=p_atm)
Q_dot_evap1=m_dot_gw*(h_gw_int-h_gw_out)
T[1]=T_gw_out-DELTA_T_ev "ammonia temperature at the inlet of the evaporator"
P_amm=pressure(ref$;T=T[1];x=0)
Q_dot_evap1=m_dot_ref_l * (h[1]-h[11])
h[1]=enthalpy (ref$;T=T[1];x=1) "Point 1 is after evaporation"
s[1]=entropy(ref$;h=h[1];T=T[1])
p[1]=pressure(ref$;T=T[1];h=h[1])

"low stage compressor HP1"
p[2]=p[3] "point 2 after compression"
s[2]=s[1]
h_is=enthalpy(ref$;P=p[2];s=s[2])

h[2;1]=(h_is-h[1])/eta_is1+h[1]
W_dot_comp1=m_dot_ref_l*(h[2;1]-h[1]) "compressor power"
T[2;1]=temperature(ref$;h=h[2;1];P=p[2])
T[2]=T_oil_1
T_avg1=(T_oil_in+T_oil_1)/2
h[2]=enthalpy(ref$;T=T_oil_1;P=p[2])
rho_avg1=density(Engine_oil_10W;T=T_avg1)
cp_avg1=specheat(Engine_oil_10W;T=T_avg1)

Q_dot_oil1=rho_avg1*cp_avg1*V_dot_oil1*(T_oil_1-T_oil_in)
Q_dot_oil1=m_dot_dh*(h_dh_oil1_1-h_dh_out1)
Q_dot_oil1=m_dot_ref_l*(h[2;1]-h[2])
h_dh_oil1_1=enthalpy(Water;T=T_dh_oil1_1;P=p_dh)


"point 9 after 1st expansion device"
h[9]=h[8]
p[9]=p[2]
T[9]=T[4]
T[9]=T[10]

"point 10 after intercooler"
h[10]=enthalpy(ref$;T=T[10];x=0)
s[10]=entropy(ref$;T=T[10];x=0)
p[10]=p[2]
p[4]=p[2]

"point 11 after 2nd expansion device"
h[11]=h[10]
s[11]=entropy(ref$;T=T[1];h=h[11])
p[11]=p[1]
T[11]=T[1]
```

```
"point 12 equal to point 1"
h[12]=h[1]
p[12]=p[1]

"high stage compressor HP1"
p[5]=p[7]
s[5]=s[4]
h_is2=enthalpy(ref$;P=p[5];s=s[4])

h[5;1]=(h_is2-h[4])/eta_is2+h[4]
W_dot_comp2=m_dot_ref_h*(h[5;1]-h[4]) "compressor power"
T[5;1]=temperature(ref$;h=h[5;1];P=p[5])
T[5]=T_oil_2
T_avg2=(T_oil_in+T_oil_2)/2
h[5]=enthalpy(ref$;T=T_oil_2;P=p[5])
rho_avg2=density(Engine_oil_10W;T=T_avg2)
cp_avg2=specheat(Engine_oil_10W;T=T_avg2)

Q_dot_oil2=rho_avg2*cp_avg2*V_dot_oil2*(T_oil_2-T_oil_in)
Q_dot_oil2=m_dot_dh*(h_dh_oil1_2-h_dh_oil2_1)
h_dh_oil1_2=enthalpy(Water;T=T_dh_oil1_2;P=p_dh)
Q_dot_oil2=m_dot_ref_h*(h[5;1]-h[5])
h[4]=enthalpy(ref$;P=p[2];x=1)
T[4]=temperature(ref$;P=p[2];x=1)
s[4]=entropy(ref$;P=p[2];x=1)

"Energy balance at the 1st intercooler"
m_dot_ref_l*h[3]+m_dot_ref_h*h[9]=m_dot_ref_l*h[10]+m_dot_ref_h*h[4]

"Volumes flowrates and pressure ratio 1 HP1"
rho_ref1_in=density(ref$;T=T[1];x=1)
V1_dot_ref1_in=m_dot_ref_l/rho_ref1_in*3600
rho_ref1_out=density(ref$;T=T[2];P=p[2])
V1_dot_ref1_out=m_dot_ref_l/rho_ref1_out*3600
v_i1=V1_dot_ref1_in/V1_dot_ref1_out
r_p1=p[2]/p[1]

"Volumes flowrates and pressure ratio 2 HP2"
rho_ref2_in=density(ref$;T=T[4];x=1)
V1_dot_ref2_in=m_dot_ref_h/rho_ref2_in*3600
rho_ref2_out=density(ref$;T=T[5];P=p[7])
V1_dot_ref2_out=m_dot_ref_h/rho_ref2_out*3600
v_i2=V1_dot_ref2_in/V1_dot_ref2_out
r_p2=p[5]/p[2]

 "!SECOND HEAT PUMP"

 "Low stage DSH HP2"
Q_dot_dsh2_l=m_dot_dh*(h_dh_dsh2_l-h_dh_sc2)
Q_dot_dsh2_l=m_dot_ref_2l*(h2[2]-h2[3])
h2[3]=enthalpy(ref$;T=T2[3];P=p2[4])
h_dh_dsh2_l=enthalpy(Water;T=T_dh_dsh2_l;P=p_dh)
T2[3]=max(T2[4];T_dh_sc2+DELTA_T_pinch_dshl2)
p2[4]=pressure(ref$;T=T2[4];x=0)

"CONDENSER"
"T2[6]=85" "assumption on the condensing temperature"
"3 sections of condenser"
```

Q_dot_cond_2=Q_dot_dsh2+Q_dot_cond2+Q_dot_sc2
Q_dot_cond2+Q_dot_dsh2=m_dot_dh*(h_dh_out-h_dh_oil2_2)
Q_dot_dsh2=m_dot_ref_2h*(h2[5]-h2[6])
h2[6]=**enthalpy**(ref$;***T***=T2[6];***x***=1)
s2[6]=**entropy**(ref$;***T***=T2[6];***h***=h2[6])
p2[6]=**pressure**(ref$;***T***=T2[6];***x***=1)
T2[6]=T2[7]

"2) condensing section of the heat exchanger"
Q_dot_cond2=m_dot_ref_2h*(h2[6]-h2[7])
h2[7]=**enthalpy**(ref$;***T***=T2[7];***x***=0)
s2[7]=**entropy**(ref$;***T***=T2[7];***x***=0)
p2[7]=p2[6]
Q_dot_cond2=m_dot_dh*(h_dh_cond2-h_dh_oil2_2)
h_dh_cond2=**enthalpy**(***Water***;***T***=T_dh_cond2;***P***=p_dh)
T_dh_cond2=T2[7]-DELTA_T_cond2

"3) subcooling section of the heat exchanger"
T2[8]=T_dh_dsh1_l+DELTA_T_pinch_sc2 "assumption on the temperature of ammonia after subcooling"
Q_dot_sc2=m_dot_ref_2h*(h2[7]-h2[8])
Q_dot_sc2=m_dot_dh*(h_dh_sc2-h_dh_dsh1_l)
h_dh_sc2=**enthalpy**(***Water***;***T***=T_dh_sc2;***P***=p_dh)
h2[8]=**enthalpy**(ref$;***T***=T2[8];***P***=p2[6])
s2[8]=**entropy**(ref$;***T***=T2[8];***P***=p2[7])
p2[8]=p2[7]

"Evaporator 2"
Q_dot_evap2=m_dot_gw*(h_gw_dhex-h_gw_int)
T2[1]=T_gw_int-DELTA_T_ev
P_amm2=**pressure**(ref$;***T***=T2[1];***x***=0)
Q_dot_evap2=m_dot_ref_2l * (h2[1]-h2[11])
h2[1]=enthalpy (ref$;***T***=T2[1];***x***=1) "Point 1 is after evaporation"
s2[1]=**entropy**(ref$;***h***=h2[1];***T***=T2[1])
p2[1]=**pressure**(ref$;***T***=T2[1];***h***=h2[1])

"Low stage compressor HP2"
p2[2]=p2[3]
s2[2]=s2[1]
h_is3=**enthalpy**(ref$;***P***=p2[2];***s***=s2[2])

h2[2;1]=(h_is3-h2[1])/eta_is3+h2[1]
W_dot_comp3=m_dot_ref_2l*(h2[2;1]-h2[1]) "compressor power"
T2[2;1]=**temperature**(ref$;***h***=h2[2;1];***P***=p2[2])
T2[2]=T_oil_3
T_avg3=(T_oil_in+T_oil_3)/2
h2[2]=**enthalpy**(ref$;***T***=T_oil_3;***P***=p2[2])
rho_avg3=**density**(Engine_oil_10W;***T***=T_avg3)
cp_avg3=**specheat**(Engine_oil_10W;***T***=T_avg3)

Q_dot_oil3=rho_avg3*cp_avg3*V_dot_oil3*(T_oil_3-T_oil_in)
Q_dot_oil3=m_dot_dh*(h_dh_oil2_1-h_dh_oil1_1)
Q_dot_oil3=m_dot_ref_2l*(h2[2;1]-h2[2])
h_dh_oil2_1=**enthalpy**(***Water***;***T***=T_dh_oil2_1;***P***=p_dh)

"Point 9 after 1st expansion device"
h2[9]=h2[8]

```
p2[9]=p2[2]
T2[9]=T2[4]
T2[9]=T2[10]

"Point 10 after second intercooler"

h2[10]=enthalpy(ref$;T=T2[10];x=0)
s2[10]=entropy(ref$;T=T2[10];x=0)
p2[10]=p2[2]

 "point 11 after 1st expansion device"
h2[11]=h2[10]
s2[11]=entropy(ref$;T=T2[1];h=h2[11])
p2[11]=p2[1]
T2[11]=T2[1]

"point 12 equal to point 1"
h2[12]=h2[1]
p2[12]=p2[1]

"High stage compressor HP2"
p2[5]=p2[7]
s2[5]=s2[4]
h_is4=enthalpy(ref$;P=p2[5];s=s2[4])

h2[5;1]=(h_is4-h2[4])/eta_is4+h2[4]
W_dot_comp4=m_dot_ref_2h*(h2[5;1]-h2[4])
T2[5;1]=temperature(ref$;h=h2[5;1];P=p2[5])
T2[5]=T_oil_4
T_avg4=(T_oil_in+T_oil_4)/2
h2[5]=enthalpy(ref$;T=T_oil_4;P=p2[5])
rho_avg4=density(Engine_oil_10W;T=T_avg4)
cp_avg4=specheat(Engine_oil_10W;T=T_avg4)

Q_dot_oil4=rho_avg4*cp_avg4*V_dot_oil4*(T_oil_4-T_oil_in)
Q_dot_oil4=m_dot_dh*(h_dh_oil2_2-h_dh_oil1_2)
Q_dot_oil4=m_dot_ref_2h*(h2[5;1]-h2[5])
h_dh_oil2_2=enthalpy(Water;T=T_dh_oil2_2;P=p_dh)

h2[4]=enthalpy(ref$;P=p2[2];x=1)
T2[4]=temperature(ref$;P=p2[2];x=1)
s2[4]=entropy(ref$;P=p2[2];x=1)

"Energy balance at the 2nd intercooler"
m_dot_ref_2l*h2[3]+m_dot_ref_2h*h2[9]=m_dot_ref_2l*h2[10]+m_dot_ref_2h*h2[4]

"Volumes flowrates and volume ratio 1 HP1"
rho2_ref1_in=density(ref$;T=T2[1];x=1)
V2_dot_ref1_in=m_dot_ref_2l/rho2_ref1_in*3600
rho2_ref1_out=density(ref$;T=T2[2];P=p2[2])
V2_dot_ref1_out=m_dot_ref_2l/rho2_ref1_out*3600
v_2i1=V2_dot_ref1_in/V2_dot_ref1_out
r_2p1=p2[2]/p2[1]

"Volumes flowrates and volume ratio 2 HP2"
rho2_ref2_in=density(ref$;T=T2[4];x=1)
V2_dot_ref2_in=m_dot_ref_2h/rho2_ref2_in*3600
rho2_ref2_out=density(ref$;T=T2[5];P=p2[5])
```

```
V2_dot_ref2_out=m_dot_ref_2h/rho2_ref2_out*3600
v_2i2=V2_dot_ref2_in/V2_dot_ref2_out
r_2p2=p2[6]/p2[2]

 "COP HP"
COP1=(Q_dot_cond+Q_dot_dsh1_l+Q_dot_oil1+Q_dot_oil2)/(W_dot_comp1+W_dot_comp2)
COP2=(Q_dot_cond_2+
Q_dot_dsh2_l+Q_dot_oil3+Q_dot_oil4)/(W_dot_comp3+W_dot_comp4)


"COP calculation"
COP=(Q_dot_dh)/(W_dot_comp1+W_dot_comp2+W_dot_comp3+W_dot_comp4)

"Q-T plots"

Qdh[1]=0
Qdh[2]=Q_dot_dhex
Qdh[3]=Qdh[2]+Q_dot_sc
Qdh[4]=Qdh[3]+Q_dot_dsh1_l
Qdh[5]=Qdh[4]+Q_dot_sc2
Qdh[6]=Qdh[5]+Q_dot_dsh2_l
Qdh[7]=Qdh[6]+Q_dot_cond1
Qdh[8]=Qdh[7]+Q_dot_dsh1
Qdh[9]=Qdh[8]+Q_dot_oil1
Qdh[10]=Qdh[9]+Q_dot_oil3
Qdh[11]=Qdh[10]+Q_dot_oil2
Qdh[12]=Qdh[11]+Q_dot_oil4
Qdh[13]=Qdh[12]+Q_dot_cond2
Qdh[14]=Qdh[13]+Q_dot_dsh2

Tdh[1]=T_dh_in
Tdh[2]=T_dh_dhex
Tdh[3]=T_dh_sc
Tdh[4]=T_dh_dsh1_l
Tdh[5]=T_dh_sc2
Tdh[6]=T_dh_dsh2_l
Tdh[7]=T_dh_cond
Tdh[8]=T_dh_out1
Tdh[9]=T_dh_oil1_1
Tdh[10]=T_dh_oil2_1
Tdh[11]=T_dh_oil1_2
Tdh[12]=T_dh_oil2_2
Tdh[13]=T_dh_cond2
Tdh[14]=T_dh_out

 Tdhex[1]=T_gw_dhex
Tdhex[2]=T_gw_in

Qdhex[1]=0
Qdhex[2]=Q_dot_dhex



Tsc[1]=T[8]
Tsc[2]=T[7]

Qsc[1]=Q_dot_dhex
```

```
Qsc[2]=Q_dot_sc+Q_dot_dhex

Tdsh[1]=T[3]
Tdsh[2]=T[2]

Qdsh[1]=Qsc[2]
Qdsh[2]=Qsc[2]+Q_dot_dsh1_l


Tsc2[1]=T2[8]
Tsc2[2]=T2[7]

Qsc2[1]=Qdsh[2]
Qsc2[2]=Qsc2[1]+Q_dot_sc2

Tdsh2[1]=T2[3]
Tdsh2[2]=T2[2]

 Qdsh2[1]=Qsc2[2]
Qdsh2[2]=Qsc2[2]+Q_dot_dsh2_l

Tcond1[1]=T[7]
Tcond1[2]=T[6]
Tcond1[3]=T[5]

Qcond1[1]=Qdsh2[2]
Qcond1[2]=Qcond1[1]+Q_dot_cond1
Qcond1[3]=Qcond1[2]+Q_dot_dsh1

Toil1[1]=T_oil_in
Toil1[2]=T_oil_1

Qoil1[1]=Qcond1[3]
Qoil1[2]=Qoil1[1]+Q_dot_oil1

Toil2[1]=T_oil_in
Toil2[2]=T_oil_3

Qoil2[1]=Qoil1[2]
Qoil2[2]=Qoil2[1]+Q_dot_oil3

Toil3[1]=T_oil_in
Toil3[2]=T_oil_2

Qoil3[1]=Qoil2[2]
Qoil3[2]=Qoil3[1]+Q_dot_oil2

Toil4[1]=T_oil_in
Toil4[2]=T_oil_4

Qoil4[1]=Qoil3[2]
Qoil4[2]=Qoil3[2]+Q_dot_oil4

Tcond2[1]=T2[7]
Tcond2[2]=T2[6]
Tcond2[3]=T2[5]

Qcond2[1]=Qoil4[2]
```

```
Qcond2[2]=Qcond2[1]+Q_dot_cond2
Qcond2[3]=Qcond2[2]+Q_dot_dsh2
```